Responses to Reviewers comments, "Estimates of Exceedances of Critical Loads for Acidifying Deposition in Alberta and Saskatchewan"

Original reviewer comments are in normal font text, and the responses are in *italics.*

Anonymous Referee #1
Received and published: 31 May 2018

General Comments:

This manuscript by Makar et al. entitled "Estimates of Exceedances of Critical Loads for Acidifying Deposition in Alberta and Saskatchewan," is a comprehensive assessment of atmospheric deposition of nitrogen (Ndep), sulfur (Sdep), and base cations (BCdep) for Alberta and Saskatchewan, and how that relates to critical loads of acidification for terrestrial and aquatic systems. They explore many different improvements to base datalayers using climatic adjustment, and improved source emissions from aircraft estimates. These improvements move the field forward in our understanding of this environmental stressor, specifically in Canada, but potentially for any temperate industrialized country with active mining operations.

We thank the reviewer for the positive review of our work!

I only had two substantial comments, neither of which negate the quality of the manuscript (though #2 may), and addressing each I think would improve an already strong submission.

First, little attempt is made to extrapolate and infer whether the improvements to deposition (i.e. climatic adjustment for Ndep and Sdep and emissions adjustments for BCdep), which appear very important for Alberta and Saskatchewan, may or may not be advised in other industrialized parts of the world. My suspicion is that in vast areas of the US, Europe, and China, similar adjustments may be warranted.

The key issue here is that air-quality model estimates of N_{dep}, S_{dep} and BC_{dep} are subject to a host of possible errors, ranging from errors in the emissions inputs to the level of the model's ability to accurately simulate the chemical and physical processes leading to deposition. In that respect, correcting the model output using comparisons to the measurements in some fashion is something we can definitely recommend. However, these corrections must be done on a case-by-case basis. For example, while we show that our model estimates for the component of S_{dep} in precipitation are highly correlated with observations, they were almost a factor of 2 too high relative to observations. In a different jurisdiction, with different emissions (and emissions accuracy, and/or a different air-quality model), a completely different bias might result. So yes, we would advise that some form of model-measurement fusion, whether as simple as what we have carried out here, or using a more complex methodology as pioneered by one of us (Robichaud), should be carried out for future critical load exceedance estimates using air-quality models, in order to improve on their accuracy. We have added a sentence to that effect at the end of the last paragraph in the revised Abstract, viz, "We strongly recommend the use of observation-based correction of model-simulated deposition in estimating critical load exceedances, in future work," and have also added a fifth point to our Summary and

Conclusions section: "(5) We have found that corrections of model estimates of S_{dep}, N_{dep} and BC_{dep} using observations, and using direct observation-based emissions data for base cations, have a significant impact on model estimates of critical load exceedances. Here, relatively simple corrections using model-observation relationships were employed. We note that other means of model-measurement fusion for acidifying pollutants are under investigation, and show great promise for creating observation-corrected air-quality model deposition fields (e.g. Robichaud et al., 2018)."

Second, the use of the 5th percentile for lakes (or the minimum) may be flawed. This is elaborated more below in the specific comments, but the accuracy of the 5th percentile as truly representing the 5th depends on the underlying sample. If there are many lakes in the grid cell (e.g. >20), it will be accurate, if there are not, (e.g. <10), it will not. This is exacerbated when the authors decided to select the minimum when the sample is very small. In these cases, the minimum of the small sample is unlikely to be anywhere near the true minimum, and is probably closer to the mean. Some discussion of this is needed or edits to the methods for the aquatic. This is the same problem that Clark et al. (2018) fell into, and needs to be mentioned (https://doi.org/10.1002/eap.1703).

The original lines of text were poorly worded, and this has been corrected first of all to clarify the procedure used in the Jeffries et al (2010) work to collect the CL data mentioned, and an additional several lines of discussion has been added. We note in the latter that the Jeffries et al (2010) data is an historical dataset included here due to its availability and to allow us to compare to more recent data and methodology, described in section 2.1.4: "The SSWC critical load values for each surveyed lake contained within each AURAMS grid-cell were compared – when data from multiple lakes within the same grid cell were available, the fifth percentile of the resulting critical load values was assigned to that grid cell (for grid cells containing less than 20 lakes, the critical load for the most sensitive lake was used). The lake critical load data thus represent the most sensitive lake ecosystems within the given grid cell based on the available data. We note, however, that this procedure used in the creation of this dataset (Jeffries et al., 2010) becomes less accurate as the number of lakes per grid cell becomes small, with either over- or under-estimates of local ecosystem sensitivity. This was one of the factors leading to more recent updates in aquatic critical load maps for Canada, discussed in more detail in section 2.1.4."

These two issues raised are important, but neither is a "deal breaker" in terms of acceptance for publication, as there are many important strengths and insights in the manuscript. Other, specific comments below.

Specific Comments:

Abstract:

"Aircraft-observation-based estimates of fugitive dust" is awkward, how about "Aircraft-based estimates of fugitive dust" or "Aircraft observations of fugitive dust"

Changed to "aircraft-based".

"Aircraft-observation-based estimates of fugitive dust emissions, shown to be a factor of ten higher than reported values". Clarify "reported", is this from ground observations, reported in some governmental permit, modeled?
Changed to "higher than reported to national emissions inventories".

Introduction:

Pg 4 lines 13-17: Hard to follow multiple embedded proportions, just proportionalize everything to Canada.
Done.

Pg 4 line 17-18: If NOx and NHx emissions from the oil sands are only 3.8 and 1%, respectively, of the total emissions of NOx and NHx in Alberta, how are they the main anthropogenic sources? Everything else is natural?
The first two sentences of this paragraph have been changed to "The provinces of Alberta and Saskatchewan are home to the majority of Canada's petrochemical extraction and refining infrastructure, in addition to other industries such as coal-fired power generation, and account for a substantial fraction of the Canadian anthropogenic emissions of sulphur dioxide (34%), nitrogen oxides (43%), and ammonia (50 %), see Zhang et al., 2018). Emissions originating within the Athabasca oil sands region account for approximately 6.5, 1.3, and 0.3% of the Canadian anthropogenic emissions of these three chemicals, based on inventories used in Zhang et al. (2018). ". The original sentence referred to the total Alberta anthropogenic emissions, and implies that the sum of other sources in Alberta contribute to the Alberta totals to a greater degree than the Athabasca oil sands.

Methods:
18 pages of methods is ridiculous, but if this is ok with the journal, it's ok with me. I'd prefer to see this in an Appendix and have a brief methods section in the main text.

We have moved the sections dealing with the snowpack observation protocol to the Supplemental Information to reduce the Menthods section; the SI also includes a detailed description of the gas-phase deposition, and is now 14 pages long. We are reluctant to move more of the methods to the SI for two reasons. First, this is the first time that the deposition algorithms used in GEM-MACH have appeared in the literature, and the details of algorithms (and inputs) selected for deposition calculations can have a substantial impact on a model's estimates of deposition. That is, they form a substantial portion of the "novel" part of the work, being unreported in the past, and have a significant impact on the overall results, as we demonstrate in later figures. Second, the critical load estimates, while largely a review of past work, are often difficult to find in the peer-reviewed literature, and yet are also critical to the results of the paper. For example, some of the gridded Canadian estimates we include for historical comparison purposes (section 2.3.2) only appear in the "grey" internal government literature, and a description of how these are ultimately derived from the same source of information as the more recent CLRTAP protocols is also difficult for researchers to access. The descriptions of the CL data employed thus shows the

historical record of CL development in Canada, and present information on their construction which up until now have not been easily available to the general scientific public. To clarify our intent for the latter section, we have changed the title of the CL section to "Estimates of Critical Loads of Acidic Deposition in Canada– A Review of Recent Work", and added the text, "In this section, we review recent work on the estimation of critical loads in Canada, starting from the UNECE definitions, in order to provide a complete description of the critical load datasets used in our subsequent estimates of exceedances.".

Pg 9 line 19-23: The subsampling is likely flawed. Using the 5th percentile is only appropriate if there are many lakes in a grid cell (i.e. > 20). If there are very few lakes in a grid cell, assuming a normal distribution, the lakes will more approximate the mean than anything else. Thus, selecting the "minimum" when there are only a few lakes is the minimum in name only, as these lakes more likely represent the mean. We ran into the same problem in Clark et al. (2018) Ecological Applications and discussed its implications (https://doi.org/10.1002/eap.1703). Please consider revising the methodology (i.e. only use grid cells with > 20 lakes) or discuss this issue in the paper.

The Jeffries et al (2010) dataset was only available to us in its final form (which is why the resolution is much lower than our 2.5km resolution); the section describes how that data was constructed in the original reference. We agree that this is an issue, however, and have modified the text accordingly: "The SSWC critical load values for each surveyed lake contained within each AURAMS grid-cell were compared – when data from multiple lakes within the same grid cell were available, the fifth percentile of the resulting critical load values was assigned to that grid cell (for grid cells containing less than 20 lakes, the critical load for the most sensitive lake was used). The lake critical load data thus represent the most sensitive lake ecosystems within the given grid cell based on the available data. We note, however, that this procedure used in the creation of this dataset (Jeffries et al., 2010) becomes less accurate as the number of lakes per grid cell becomes small, with either over- or under-estimates of local ecosystem sensitivity. This was one of the factors leading to more recent updates in aquatic critical load maps for Canada, discussed in more detail in section 2.1.4."

Parse out in the figures and captions of Figs 2-4 the "No Data" category. There are many possible reasons for no data, and knowing and communicating that is helpful. What that "No Data" because it was not the right land cover type (e.g. non-forested) or because there was no estimate of data (e.g. BC dep), or some other reason. These are very different. Please separate the reason for no data into at least two categories (i.e. "No appropriate cover" and "No data").

This has been indicated in the revised figure captions, with the addition of the following sentences to the captions:
Figure 2: No Data: (a) No lake observations were available in the given 45 x 45 km grid cell; (b) No forest data were available and/or the "No Data" regions were not forested".
Figure 3: No Data: data was only collected within the province of Alberta (outside of Alberta, no data reflects the limitation of data collection); within Alberta, data was only collected for natural terrestrial ecosystems (no data within Alberta thus refers to landscapes modified by human activities such as agriculture).

Figure 4: No Data: data were not collected for the largest lakes and river systems within the coloured region; the boundaries of the coloured region represent the limit of the catchment basins for which data were collected.

Results:

Figure 5: Interesting that most of the N dep is from NH4+ wet, which did not seem to be mentioned much in the introduction. Maybe introduce this a bit more so it's not a surprise.

Given the material discussed, we assume that the reviewer is referring to Figure 6 (total and percent components of N_{dep}); Figure 5 is the corresponding S_{dep} figure. We note that "most of" is in the sense of a relative local contribution. One has to be a bit careful here in that the relative contributions in Figures 5 and 6 are percent contributions at each location, not total masses. That is, NH_4^+ is the dominating relative contribution to total N production for downwind regions far from major anthropogenic emissions sources. The absolute values of N deposition (and hence NH_4^+ in those regions (such as northern Saskatchewan and Manitoba)) are low. The manuscript has been modified to mention this, within the discussion of Figure 6: "The bulk of the relative fraction of total S_{dep} close to the sources of emissions is due to dry deposition of $SO_2(g)$ and wet deposition of HSO_3^-, while the wet deposition of $SO_4^{(2-)}$ dominates in downwind regions. The relative fraction of N_{dep} near the sources is dominated by dry deposition of $NO_2(g)$ and $NH_3(g)$ near sources and dry deposition of $HNO_3(g)$ and $NH_4^{(+)}$ further downwind. Figure 5 (b-e) and Figure 6 (b-i) show that for sites downwind of the source regions (hot-spots in panel (a) of these figures), wet deposition dominates. We note that the mass of S_{dep} and N_{dep} deposited decreases with distance from the sources; for example, $NH_4^{(+)}$ dominates the relative fraction of N_{dep} in locations more distant from the sources, where total N_{dep} is relatively low. ".

Pg. 24-25: Please add a bit more discussion on the sources of error that could be attributable to the model and could be attributable to the observed estimates. Both are potential sources of error and I found this a bit too brief.

We have modified and added to the last few sentences of the last paragraph of page 24 to read, "Air-quality models such as GEM-MACH are quite complex, with many possible sources of model error; some possibilities include but are not limited to errors in the input emissions data (as we examine below for base cation emissions and deposition), errors in the plume rise algorithms leading to potential errors in the relative distribution of deposition near versus far from the sources (Gordon et al., 2018, Akingunola et al., 2018), potential errors in the magnitude of N_{dep} associated with the absence of bi-directional fluxes of NH_3 (Whaley et al., 2018) in the simulations carried out here, and biases within the meteorological forecast components of the model. As we discuss below, the model predictions nevertheless correlate well with wet deposition observations at precipitation-monitoring stations located downwind of

emissions sources, and these relationships allow for an approximate correction of model S_{dep} and N_{dep} estimates using observations. This allows us to reduce the potential impact of sources of model error on estimates of critical load exceedances.".

Pg. 25: Very nice that you used uncorrected and corrected deposition estimates in calculations of exceedance.

Thank you. As noted above, we have stressed the importance of these corrections and have recommended in the revised manuscript that some form of model-measurement fusion be employed wherever possible for estimation of total deposition, to reduce model errors.

As mentioned earlier "Aircraft-observation-based" is a mouthful and not necessary. Use "aircraft-based." It would be silly to take a computer up in the aircraft to make this an "aircraft-simulation-based" estimate.

Done.

Pg 27, line 12-13. I don't follow the logic of why this following from the preceding sentences: "This in turn suggests that the primary particles may rapidly deposit with increasing distance from the emissions sources." If the emission inventories are too low, why does that mean they deposit faster? Couldn't this explain the bias in the BCdep (i.e. that the actual emissions are higher, and thus the model estimates BCdep as too low)?

Larger particles have higher deposition velocities, hence the finding that much of the particle mass containing base cations resides in the coarse mode implies that those particles should not travel far from the sources. The process is well-known from laboratory studies of particle deposition, but implies that the particles containing base cations, which originate in fugitive dust emissions and are largely in the coarse mode, will deposit faster than smaller particles. With increasing distance from fugitive dust sources, then, the neutralization effect associated with base cations contained within those particles would be expected to decrease. This has been clarified in the revised manuscript with the following sentences: "Larger particles have higher deposition velocities compared to particles with diameters of 1□m (c.f. Zhang et al., 2001), and hence these larger, "coarse mode" primary particles would be expected to rapidly deposit with increasing distance from the emissions sources. This in turn implies a reduction in BC_{dep} with increasing distance from the sources, associated with this differential deposition of the larger fugitive dust particles earlier in the transportation process. "

Pg 27 line 18-19. It shouldn't be "aircraft emissions estimates" (i.e. the emissions of the aircraft) it should be "aircraft-based emissions estimates"
Done.

Pg. 27-28. Would be nice to have a "take home message" in terms of how far from a large point source do you need to be before one needs to worry. Seems like from Figure 8 you need to be >100 km, which would be a useful rule of thumb to include. Are these underestimates for Canada

likely occurring elsewhere in the world as well?...Later I see that the 142 km threshold (pg. 33) is presented, which is slightly different but related and useful.

It's problematic to conclusively state that the 142km distance we see here will hold in other parts of the world, in that the drop-off with distance from the (area, not point) sources of fugitive dust will depend on the size distribution of the emitted particles. In that sense, to the extent that the fugitive dust size distribution of the region studied is "typical", then yes, we would expect a similar drop-off with distance from the sources of fugitive dust. To our fourth point in the Discussion section, we have added the following: "We also note that the 142 km drop-off distance associated with BC_{dep} shown here is a function of the size distribution of the emitted fugitive dust particles – while our expectation is that the bulk of fugitive dust emissions are likely to be in the coarse mode (sizes greater than 2.5 μm diameter) as they are here, differences in the initial size distribution may lead to different decrease functions with distance from fugitive dust sources. However, a general result from our findings is that fugitive dust base cation neutralization will be limited in spatial scope, due to the effect of particle deposition increasing with increasing size in the coarse mode.".

Pg 29 line 1-2. Unclear why the improvement in the BC emissions using the aircraft observations also improves the Sdep and Ndep, please clarify.
Whoops – that should have read "the use of this correction and other observation-based corrections on the original model estimates"; this has been corrected in the revised manuscript.

Section 3.4. It's not really clear to me what value the comparison with snowpack adds except to say that the snowpack isn't a very useful comparison. If that is the case, I'd move all this to the supplement, and just have a short statement to that effect. This would shorten an already very long paper.
The main addition (and one as a result of which we think this section is worth retaining in the revised manuscript) is one of measurement methodology, and how the measurements can/should be compared to model values. We have identified the "open" versus "throughfall" deposition estimates as a potential confounding factor, of which modellers of atmospheric deposition may be unaware. We have added the following sentence to our fifth discussion point: "Snowpack deposition observations should attempt to measure both "throughfall" and "open" deposition, in order to more accurately estimate total deposition to snow-covered vegetation. ".

Figure 12 a, what is the red hotspot to the NE of the Athabasca oil sands where BC_{dep} again dominates? Is that another source or evidence of long range transport?
No – rather, it suggests potential regions of base cation accumulation in surface waters. The given panel shows the ratio two different base cation fluxes, the first an estimate of BCdep to the region from sparse observations gathered to the south, and the second an estimate of the amount of base cations leaving the region via export in catchment waters, as was described in the text referencing this figure. Areas where the ratio is greater than unity thus represent places where accumulation of base cations might be expected to occur, and hence where, over time, BC_{dep} might be expected to have a greater role in the neutralization of S_{dep} and N_{dep}, at 2013 emissions levels.

Figure 14 b-c: Unclear whether the S and N dep are precipitation adjusted, which I think they should be in one of either b or c? The description in Figure 13 is more clear and complete (i.e. "GEM-MACH S+N deposition scaled according to precipitation observations, base cations scaled using precipitation and aircraft data".
This has been corrected in the revised caption for Figure 14.

Not really clear what Figures 15 and 19 on the Regions adds, please clarify.

An additional paragraph has been added to describe what these figures show (they are very policy-relevant, in that they show how exceedances could be reduced in different areas), referencing the regions of Figure 1:
Figure 15 added text: "Figure 15 presents possible avenues to reduce the impacts of deposition. Areas within Regions 1,2, and 3 with respect to Figure 1 may be brought below exceedance levels through a combination of reductions in S_{dep} and N_{dep}, the relative magnitude of each depending on the location of the current N_{dep},S_{dep} on Figure 1, with more than one reduction strategy often possible. However, areas within region 4 may only be brought below exceedance by reductions in S_{dep}. Figure 15 thus may be of use to policy-makers in determining strategies to reduce deposition to levels below critical load exceedance."
Figure 19 added text: "Figure 19 shows that most of the exceedances for aquatic ecosystems reside within Regions 1 or 2 with respect to the regions shown in Figure 1, and thus may be brought to below exceedance conditions by different combinations of reductions in S_{dep} and N_{dep}, depending on the location of the current N_{dep},S_{dep} on Figure 1."

Discussion:

This is fantastic work for Canada, but some discussion of whether the results and lessons would hold for other parts of the world would be nice if briefly discussed (e.g. Europe and the US?).

Pg 46 line 29-30: In addition to exceedances not helping with the timeline or recovery, they also don't really comment on the magnitude of effect, also an important note.
The line has been modified to read, "As noted earlier, exceedances to critical loads indicate the potential for ecosystem damage, but not the timeline over which damage may be expected to occur or has occurred, the time to ecosystem recovery (if acidifying deposition is reduced), or the magnitude of the ecosystem impacts of exceedance".

Pg 47 and Figure 20: This is a really nice addition, but it seems to me that comparing exceedances with actual impact is a much bigger effort than this would suggest. If it's just included as a preview, it's fine, otherwise, maybe caveat that much more comparison with observed effects is needed (e.g. forest tree growth??).

It has been included to indicate that some observation data suggests that there is some observational evidence that the effects of exceedances are starting to appear in lakes closest to the emissions region – but also that more direct observations and monitoring over time is needed. In that respect, the Figure is intended to show the importance of maintaining aquatic ecosystem observations in the region at risk. We have added "Our calculations of aquatic critical

load exceedances imply that acidification will eventually occur; Figure 20 highlights the need for ongoing monitoring of aquatic ecosystems in this region."

Please add a non-spatial plot to simplify the information in Figure 20. The take home point appears to be that exceedance does not translate to effect.

See the above response – we have added text to indicate the intent and implications of Figure 20.

Pg 49 line 15: I would not characterize a radius of 142 km as "rapid". I'd say 10 km would be rapid, but that circle in the figures is pretty large!

That part of the sentence has been changed to "rapidly with distance in comparison to the size of the predicted areas of aquatic critical load exceedance"

Reviewer # 2:

General remarks:

This rather extensive paper reports on detailed deposition calculations for the two Canadian provinces as well as their use in exceedance calculations for different sets of critical loads (CLs) for terrestrial and aquatic ecosystems. As the larger part – and more of the novel material – is concerns atmospheric depositions, I suggest to change the title to "Estimates of Acidifying Deposition and Critical Load Exceedances in Alberta and Saskatchewan" (or similar), and also to restructure the paper accordingly, i.e. first depositions, then CLs and their exceedances.

With respect to depositions I suggest to move some of the material to the 'Supporting Information', since its mostly material taken from existing literature.

We have reorganized the paper's methodology to follow the section order as described by the reviewer. We have also moved the details of the snowpack methods section to the SI, as later recommended by the reviewer, to reduce the length of the methods section. While we agree with the reviewer that the estimates of deposition are novel (as are our corrections of those estimates using observations), we feel that the use of those deposition estimates to predict exceedances of the critical loads is also novel (and the main point of the paper). The original title was not "Estimates of Critical Loads for Acidifying Deposition and their Exceedances in Alberta and Saskatchewan", which would imply we are presenting the CL values for the first time, but "Estimates of Exceedances of Critical Loads for Acidifying Deposition in Alberta and Saskatchewan", which makes the point that the estimates of exceedances are the main point of the paper, and does not imply that the critical loads themselves are a result of our work. Hence we have left the title unchanged.

With regards to moving the deposition description to the SI, the reviewer may have missed the existing SI and the line in the original manuscript "A detailed description of the gas-phase dry deposition module of GEM-MACH (with an emphasis on the chemical species which contribute to S_{dep} and N_{dep}) appears in the Supplementary Information; here we provide an overview" (a later comment by the reviewer regarding references appearing in the reference list but not in the paper would seem to confirm this; most of those 'superfluous' references are quoted in the SI). In the 12 page SI for the original manuscript, the gas-phase deposition algorithm of GEM-MACH is described in much more detail, including tables for all of its input parameters. That is, what appears in the main body of the manuscript is already the "condensed" version.

With regards to the reviewer's suggestion that the deposition material is taken from the existing literature: a sometimes overlooked aspect of the use of air-quality models such as GEM-MACH for deposition calculations is that there are a large number of different parameterizations present in the literature for deposition, a large number of choices for input variables for those parameterizations, and the choice of parameterization and input variables can have a substantial impact on the model results. Yes, all of the components of the GEM-MACH deposition algorithms appear (separately) in the literature, but the specific combination used in GEM-MACH has not appeared in the literature. That combination is critical to the model results, and as noted in the manuscript and SI, some of the choices are known to result in a factor of two variation in gas-phase deposition levels. Given that the crux of our work is dependent on the GEM-MACH deposition estimates (albeit corrected by observations), we thought it best to include the full description of the GEM-MACH deposition algorithms, particularly since that combination had yet to be presented in the literature. Most of the detailed information has already been moved to the SI, in that respect. We do, however agree with the reviewer's later suggestion that the details of the snowpack observation methodology need not appear in the main body of the manuscript, and have moved this to the SI.

The paper (and the reviewer) would have benefitted if the authors had carefully read the paper before submission: there are close to 30 references that are there and not cited or cited and not in the reference list (see below); also the equation number is quite faulty in some parts.

These errors have been corrected. Note that most of the "there and not cited" papers appeared in the supplemental information description of GEM-MACH's gas-phase dry deposition module.

Furthermore, the definition of critical load exceedances (in case of non-exceedance) requires some attention (see below).

We have modified the manuscript descriptions following the reviewer's comments, see details below.

Apart from this, I consider the material of paper suitable for publication, after the authors have also taken into consideration the (often minor) remarks/corrections listed below.

Thank you – we are very grateful for your careful look through the manuscript; with the large number of co-authors and the multiple sources of information, it was very helpful to have someone with a detailed knowledge of CL calculations and procedures examine the manuscript.

Detailed remarks:

Note: 'X →Y' means: replace 'X; by 'Y' (in the text).

Title:

See 'General remarks' above.

Abstract:

P[age]1,L[ine] 33: Suggest to change 'protocols' to 'methods' (throughout the paper!), as 'protocol' has its own meaning in the context of CLRTAP!]

Done.

P1, L34: Delete 'forest and': forests are terrestrial ecosystems!

Fair enough – the idea here was to differentiate the earlier and later data for these ecosystems using "forest ecosystem" for one and "terrestrial ecosystem" for the other, but we can see how that causes confusion in the abstract.

P2, L2: Delete 'emissions and'.

The emissions levels used as inputs to the model are the key values, here. The sentence start has been changed to "Potential ecosystem damage using 2011/13 emissions data was predicted for regions"

P2, L7: 'was shown to have' → 'has' (otherwise it sounds the authors have shown that in this paper).

This has been made more specific: "Base cation deposition was shown to be sufficiently high in the region to have a neutralizing effect on acidifying deposition", which we have shown in this paper.

P2, L11: 'primary particle dust particles' → 'primary dust particles'

Deleted.

Introduction:

P2, L17: Delete 'regional and'.

Deleted.

P2, L18: The reference to the CLRTAP Manual sh/could be simplified (throughout the whole paper!) as it's always the same source. Just call it CLRTAP (2017) – with the text in the References as is now under 'CLRTAP, 2004' – since 2017 is the (last) time you accessed it.

Done.

P3, L16: 'Estimates of critical loads' → 'Critical loads'

Done.

P4, L1-2: No! If BCdep is greater than Sdep + Ndep, a large part of that BCdep could be taken up by forests and harvested (i.e. taken away) and thus not be available for neutralizing the S and N deposition; and a case could be made for the converse – If the statement were true, then the CL would be equal to BCdep!

Very true. The sentence has been changed to: "Both terrestrial and aquatic critical loads are based on the concept of ion charge balance (cations – anions), as well as terms describing the perturbation of the charge balance through, for example, removal of specific ions or groups of ions through , leaching, harvesting of biomass, etc.".

P4, L5: 'emissions levels' → 'emission levels'.

Done.

P4, L7: What is 'alkylization'? (I guess the authors mean 'alkalinisation'?)

Should have been 'alkalinization'; fixed this.

P4, L24: 'aquatic and terrestrials' → 'aquatic and terrestrial ecosystems'.

Done.

P4, L25: Insert 'deposition' after 'surface'.

Done.

Methodology:

P5, L15: 'sum of in equivalents of' → 'sum of'; the criteria is generally reported as 'molar Bc:Al (or Al:Bc) ratio! That's the way the factor of 3/2 appears in eq 4 to convert it to equilvalents!

The sentence has been changed to: "The most widely used soil chemical criterion is based on the molar ratio of base cations to aluminum (Bc:Al where Bc is the molar sum of calcium (Ca^{2+}), magnesium

(Mg^{2+}) and potassium (K^{+})) in soil solution (the factor of 3/2 in equation (4) converts this term to equivalents)."

P5, L19: There is no 'level of protection' defined for CLs.

The sentence has been changed to "The critical level of the leaching of acid neutralizing capacity for the ecosystem ($ANC_{le,crit}$) is defined via equation 4.".

P5, L19-20: It's the chemical criterion (here Bc:Al ratio) that *defines* the critical ANC leaching – the user does not specify the critical ANC leaching (in the case described here), he just computes it!

We've changed the word "specified" to "defined".

P5, eq.2: 'CLmax(S)/(1-fde))' → CLmax(S)/(1-fde): i.e. drop the superfluous parentheses.

We've rearranged eq 2 to have the fraction as in eq. 4, ie. $\frac{CL_{max}(S)}{1-f_{de}}$

P5, eq. 4: Delete the superfluous parentheses (twice); only the square brackets are needed.

A minor point, but we disagree – the additional brackets prevent any possible confusion if someone was to re-write the formula (e.g. mistakenly including the 3 into the numerator, the 2 into the denominator of the start of the next function).

P5, L30: Bc is already explained above (line 15).

Removed this repeat definition.

P5, L31: Insert 'annual' after 'long-term'.

Done.

P6, L1: 'due to other forms of removal (e.g. harvesting)' → 'due to, e.g., harvesting'. … and all other variables in the text should be in ***italics*** if they are so in the equations (also further below)!

Changed as suggested and variables have been written in italics throughout the text.

P6, L8: 'Q' is already defined on line 1.

Change to "Q as defined above" here.

P6, eq6 : Y does not stand for Ca+Mg+K+Na-Cl, but Sy stands for the sum of base cations minus chloride (Ca+Mg+K+Na-Cl).

The equation has been replaced by:

$$S_{runoff} + N_{runoff} = Ca_{runoff} + Mg_{runoff} + K_{runoff} + Na_{runoff} - Cl_{runoff} - ANC_{limit}$$

P6, L28: '(i)' → '(subscript i)', etc.

Corrected. We also noticed in this sentence that the subscript "u" definition had been repeated twice; the second definition was removed.

P7, L4: What is the 'charge x mole equivalent'? moles? moles of charge? …

We were trying for a definition of the "eq" unit here. We have converted the text to "converted to units of molar equivalent (eq) deposition of SO_4^{2-} (number of moles of the ion times number of charges associated with the ion).

P7, L22: There is a change in font size from that line onwards – Any reason?

Probably multiple versions and we missed it (a one point difference in font size in that paragraph). We've made it uniform in the revised version.

P8, L1: 'In some instances, S deposition (or N) must be reduced to achieve non-exceedance' What do the authors want to say? As it stands it's trivial/obvious.

Yes – we've removed the sentence.

P8, Figure 1: (a) Why is the slope of the Critical Load Function (CLF) shown as 45^o? This is a special case only for f_{de}=0 (see eq.2): (b) the point (N_0,S_0), computed in eqs. 12, 13 should be shown on the Figure; (c) It should be indicated in the Figure how the quantity E0 is derived, i.e. where N_A and S_A are located on the CLF.

(a) *It's a sketch – it was not intended to represent any particular case. Presumably the sensitivity here relates to the earlier CLRTAP protocols referencing constant values of denitrification (which result in the 45^o slope) versus later revisions to the protocols which result in shallower slopes from the horizontal for non-constant denitrification. We've modified the diagram slightly so that it depicts the more general case.*

(b) *Done.*

(c) *Given the reviewer's later comment, below, SA and NA themselves are superfluous, but we've added an arrow indicating the value of E_0 for the point N_{dep1},S_{dep1}.*

P8, L5: 'denotes ecosystem': No, it does not denote ecosystems, it denotes 'the case for which'.

Changed to "denotes cases for which S_{dep} and N_{dep} to an ecosystem".

P8, L15: E_0, as a negative quantity, cannot be a distance, only a positive quantity can; e.g. $|E_0|$ = - E0 (thus it would be better to define E0 as a positive quantity and make it $-E_0$ in eq. 11)!

See response to P8,L15 comment, below.

P8, L15: There are no 'exceedance lines' – what you mean is the critical load function.

"The sentence has been changed to "We define here E_0, a negative quantity defining the smallest decrease in deposition from the critical load function (i.e. the boundary between the exceedance and non-exceedance regions of Figure 1) to reach the N_{dep}, S_{dep} point on Figure 1."

P8, eq.15: In fact, NA is the Ndep-value on the CLF for a given Sdep, and the SA the Sdep-value on the CLF for a given Ndep. It can be easily shown that Sdep-SA is always greater than (or equal to) Ndep-NA, or, to express it in positive terms (i.e. distances): SA-Sdep ≤ NA-Ndep. Thus eq.15 simplifies to:

$$(15)\ E_0 = \begin{cases} S_{dep} - CL_{max}(S) & for\ N_{dep} \le CL_{min}(N) \\ m(N_{dep} - CL_{max}(N) & for\ CL_{min}(N) < N_{dep} < CL_{max}(N) \end{cases}$$

… and eq. 16 becomes superfluous

Almost. We think the reviewer may have made a typo on the second line of the revised (15), above; it should be:

$$(15)\ E_0 = \begin{cases} S_{dep} - CL_{max}(S) & for\ N_{dep} \le CL_{min}(N) \\ S_{dep} - m(N_{dep} - CL_{max}(N) & for\ CL_{min}(N) < N_{dep} < CL_{max}(N) \end{cases}$$

The reviewer is quite right – we had solved for the more general case, where the slope of the line joining ($CL_{min}(N)$,$CL_{max}(S)$) and ($CL_{max}(N)$,0) could have a steeper slope than 45 degrees. However, the reviewer has a good point in that equation (2) guarantees that the value of $CL_{max}(N)$-$CL_{min}(N)$ will always be greater than or equal to $CL_{max}(S)$, and hence the minimum value of the slope is 45 degrees. Consequently, the maximum of S_{dep}-SA,N_{dep}-NA becomes unnecessary, since the fastest approach to exceedance will always be via the S path. Thanks for pointing this out! We've dropped equation (16) and related text, and have simplified the equation (15) as per the second version above.

P9, L5: insert 'critical loads' after 'estimated'.

Done. Thanks for catching this!

Note: for computing E_0 is a different distance measure is used than for computing positive exceedances. This is not really faulty, but peculiar, and should at least be mentioned (and maybe 'justified'). More generally, the authors should give reasons why they map negative exceedances, as policy makers might not be so much interested in them; generally, they are 'happy' when there is non-exceedance (however small)… But it makes 'nice' maps; and maybe there is another reason as well…

This is not just a case of making nice maps, as the reviewer is suggesting. Our own experience with policy makers (and the reason why we included the additional E0 term) is that they are also interested in areas which, if emissions are likely to increase in the future, are likely to be in exceedance. The issue here is that the air-quality models such as GEM-MACH provide deposition estimates which are relative to a particular meteorological year but more importantly for a specific emissions inventory year. The emissions inventories used in the models are updated as new emissions data becomes available, usually on a two to three year basis by the relevant agencies (US EPA, ECCC and Mexican government, in the case of the outer domain used for our simulations in this case. Emissions activities and the amount of emissions may change from year to year – and hence the relative sensitivity of regions which are not currently in exceedance, but could be, were emissions to increase, is valuable information for policymakers. To address this point more clearly, following equation (15), the following paragraph has been added:

"For deposition levels below exceedance, i.e. within the grey region of Figure 1, the value of E_0 describes the proximity to exceedance; the fastest path by which exceedance could occur, relative to current deposition levels. Given that equation (2) guarantees that the slope of the line joining $(CL_{min}(N),CL_{max}(S))$ and $(CL_{max}(N),0)$ will always have an inclination of less than 45^o, the shortest path to exceedance will always be via the S_{dep} path. E_0 is of potential interest to policymakers, in that this term describes the proximity of regions which are not yet in exceedance of critical loads to exceedance. Small magnitude values of E_0 thus describe ecosystems for which small increases in S_{dep} or N_{dep} may result in exceedances of critical loads."

P9, L11: '… in order to obtain data for critical load estimates': Only for that purpose?

That was indeed the main purposes of the work in Jeffries et al 2010 – the work was carried out specifically to obtain data to carry out the first estimates of acidification sensitivity of lakes in northern Manitoba and Saskatchewan; these data were used in that paper to calculate critical loads of acidity using the SSWC model.

P9, L15/16: '…and other related information': What else c/would that be?
Sentence has been changed to end at "biological surveys".

P9, L16,17: 'estimates … were conducted': Do you really conduct estimates?
Changed "conducted" to "created".

P9, L20: Delete 'lowest'.
Done.

P9, L21: 'for grid cells containing smaller number of lakes, the… most sensitive lake was used': Smaller than what? (20? …). And, by the way, percentiles can be compared for any number…

This was poorly worded on our part. The idea in the original sentence describing the Jeffries et al (2010) reference was that (1) percentiles were calculated for the lakes critical loads within each grid cell and the 5th percentile was used but (2) for lakes less than 20, the idea of a lowest 5th percentile becomes more of an approximation, so in the latter case the CL for the most sensitive lake within the grid cell was used. The sentence has been changed to "…when data from multiple lakes within the same grid cell were available, the fifth percentile of the resulting critical load values was assigned to that grid cell (for grid cells containing less than 20 lakes, the critical load for the most sensitive lake was used).

P9, L22/23: 45 km2 grid cell – What's that? If it's a 45 km x 45 km grid cell its size is 2025 km2, if it's area is 45 km2, what are the lengths of the sides? - It's no problem to call it a 45 km grid cell in the former case…

The sentence has been changed to "…within the given grid cell." The dimensions were specified in a sentence just above the one mentioned, so it's unnecessary here.

P10, L5: Only BC deposition is needed for CL alculations.

Disagree – the context here is the entire suite of variables (aka "inputs") required to create a critical load, which includes the $BC_w(T)$ and $Bc_w(T)$ terms, for example. In case the reviewer is disagreeing with the use of the generic word "inputs", which may be misinterpreted, we have replaced this with "; the key spatial data-sets (or base maps) or formulae required for calculating critical loads"

P10, L6: Critical alkalinity leaching is not an input, but calculated from, e.g., a critical Bc:Al ratio.

The sentence fragment has been modified to read, "…and a critical base cation to aluminum ratio (used to calculate critical alkalinity leaching)".

P10, L14: '(a) a critical Bc:Al ratio of 10 and a Kgibb of 3000.0 were used': This is not a simplifying assumption! Furthermore, provide units for this numbers!

The sentence has been modified to "…several simplifying assumptions and/or specified functions and values were applied to terms in equations (1) through (4)..." As the reviewer has noted in an earlier comment, Bc:Al is defined as a molar ratio (we've also added text elsewhere, see responses to comments below, which make this more clear, as well as use "molar ratio" rather than "ratio" in the given sentence. The units of Kgibb have been stated as $m^6\ mol_{charge}^{-2}$.

P10, L16: Replace 'invariant' by 'spatially uniform'.

Done.

P10, L16/17: 'the equivalent of the (CLmax(S)/1-fde)) term…': Although I can infer what you want to say, it's confusing for the non-expert. What you are doing is modelling denitrification as

a constant flux Nde, (i.e. CLmin(N) = Ni + Nu + Nde) and not with the fraction fde, as in eq.2 – but this has to be explained (better)!

We've used the reviewer's wording in the revised sentence, which reads "…both N_i and the $\left(CL_{max}(S)/(1-f_{de})\right)$ term of equation (2) were set to 35.7 eq ha^{-1} yr^{-1}, the latter modelling denitrification as a constant flux)."

P10,L17: Why the somewhat 'awkward' number 35.7? Why not a 36, or 40? Tell the reader that it comes from a nice round number in a different unit and an assumed soil depth of 0.5 m (this is a simplifying assumption that should be mentioned!)

The original text, "(c) denitrification and net N immobilization was assumed to occur, but at a spatially uniform low level appropriate for well-drained upland forest ecosystems (both N_i and the $\left(CL_{max}(S)/(1-f_{de})\right)$ term of equation (2) were set to 35.7 eq ha^{-1} yr^{-1}, the latter modelling denitrification as a constant flux), (d) ", has been modified to read: "(c) as in section 2.3.3, net N immobilization (N_i) was based on a 50 cm depth rooting and assumed to be equivalent to 0.5 kg N ha^{-1} yr^{-1} (35.7 eq ha^{-1} yr^{-1}) (CLRTAP, 2018) , (d) denitrification (N_{de}) was also set to 0.5 kg N ha^{-1} yr^{-1} (35.7 eq ha^{-1} yr^{-1}) following recommendations in CLRTAP (2018) as an upper limit for well-drained soils, (e)"

P10, L18: 'weathering … was assumed to be dependent on temperature': This is not really a simplifying assumption to me.

The sentence has been modified from using "…several simplifying assumptions and/or specified functions and values were applied to terms in equations (1) through (4)..."

P10,eq.17: (a) the minus side should be a plus sign! (b) Why do you insert the numbers (2 times 35.7) for Ni and Nde, but not for (Bc:Al)crit and Kgibb? (c) Some reason should be given why this is now called CL(S+N) and not CLmax(N) as in eq.2.

(a) *Yes, we caught that typo when going through the paper post-submission as well – thanks for catching it, nevertheless. (b) All specified constant values have replaced the original variable names in the revised formula (c) See the detailed response to the comment about equation (19), below.*

P10, eq.18: The square brackets are superfluous.

Perhaps, but they are more precise. The problem: to our experience, sometimes readers will misinterpret an exponential such as this to only apply to the numerical constant, and not to the whole temperature function, mistakenly multiplying by the latter instead of including it in the exponential. Keeping the square brackets for the entire expression for the exponential is therefore safer; less likely to be misinterpreted.

P10, L23: '$Bc_{we} = 0.75\ BC_{we}$': this is another simplifying assumption, that should be mentioned above.

The assignment has been removed from that line in favour of an addition to the earlier list, viz. "and (f) Bc_w was assumed to be equal to 0.75 BC_w".

P10, L27: (a) I guess it's 2.5km x 2.5km (or 2.5km for short) grid cells. (b) Delete 'lowest'.

Changed to "2.5km x 2.5km ", and "lowest" were deleted.

P10, L31: Parentheses around $S_{dep} + N_{dep}$ superfluous.

We've changed the line to "simplified for deposition of sulphur and nitrogen", and modified the deposition calculation itself (see following comment and response).

P11, eq 19: This is a 'dangerous' equation! What if $N_{dep} < N_i + N_{de}$? The remaining N-sink can not compensate any S deposition! Maybe it does never happen in AL and SK(?), but it has to be said that the (potentially) remaining N sink is not used to compensate S_{dep}, as the equation does as it stands!

We agree with the reviewer on this. This is one of the drawbacks of the NEG-ECP protocol, and we should have made that clear in the original document. We've included the ECCC Forest ecosystem dataset, constructed for that methodology, since the methodology appears in the literature (Ouiment 2005). The NEG-ECP methodology itself is based on an earlier approach appearing as equation V.19 in the CLRTAP manual; the separation of the CL into separate terms for S_{dep} and N_{dep} via equations (1) through (4) resulted from recognition in the community of the potential drawbacks, such as the one pointed out by the review, of that earlier approach. To address this issue in the revised manuscript, while still attempting to make use of the historical data constructed for this earlier approach, we've done the following:

In the sentence following equation (18), we've added the following caveat, "We note that equation (18), which follows the NEG-ECP methodology (Ouiment, 2005) may lead to potential errors at very low values of N_{dep}, in that the nitrogen sinks could potentially compensate sulphur deposition. To avoid that possibility, we have added the caveat to equation (16) that the rightmost term is replaced by the minimum of 71.4 eq ha^{-1} yr^{-1} and N_{dep} (that is, the calculated nitrogen sink will not be used to compensate S_{dep}, in the event that N_{dep} is below the sum of nitrogen immobilization and denitrification (71.4 eq ha^{-1} yr^{-1})). "

When we re-examined the code for Figure 17, we realized that we had inadvertently used 37.5 eq ha^{-1} yr^{-1} for the two constants, rather than 35.7 eq ha^{-1} yr^{-1}. When this was corrected, a small increase in the exceedance area for each of the panels of Figure 17 resulted (2^{nd} decimal place for the total area exceeded in each case). We have corrected this error in the revised figure (the conclusions with regards to this figure are unchanged).

Having applied that correction for (min(71.4, Ndep) in equation (16), we have seen a minimal impact on the predicted CL exceedances. The actual area in exceedance with and without the correction is the same to three figures, and the differences are very hard to spot on the resulting revised Figure 13, though we have incorporated the revised values into that Figure in the paper. For the reviewer's benefit we also add an expanded version of Figure 13 here, below, which compares the original figure panels (first column of panels) with those using the value of 71.4 for the final term of equation (16) (second column of panels), versus using min(71.4,N_{dep}) (3rd column of panels, as well as, in the 4th column, the differences in calculated exceedances for each of the panels (with correction –without correction). The main effect of the min(71.4,N_{dep}) correction is to make some of the regions which

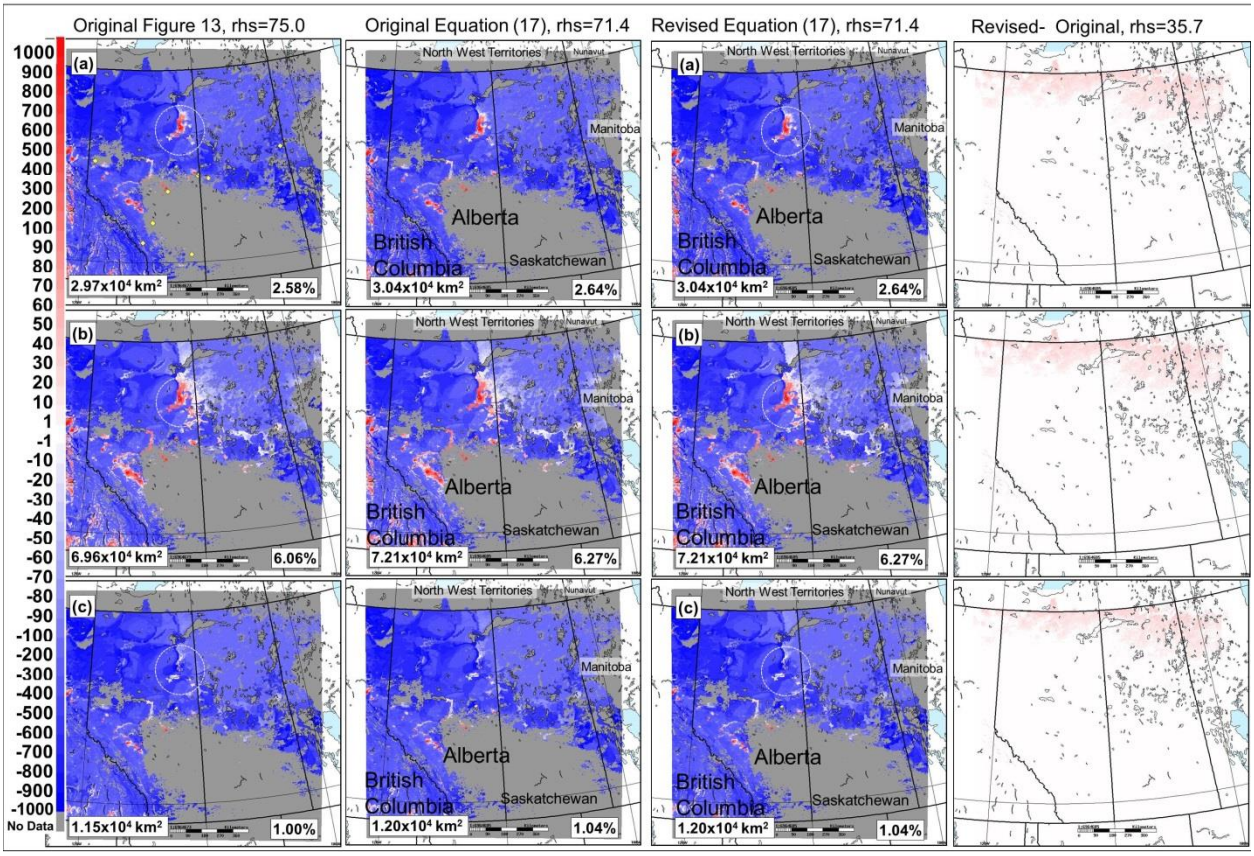

below the exceedance threshold slightly closer to exceedance. However, the total area in exceedance was unchanged, to 3 significant figures. Given that the impact of the correction is minimal, to the above text we have added the sentence, "In our application of this methodology (see section 3.6.1), this additional correction was found to bring areas which were already below exceedance slightly closer to exceedance, but had no impact on the estimate of the size of areas over exceedance, to three significant figures."

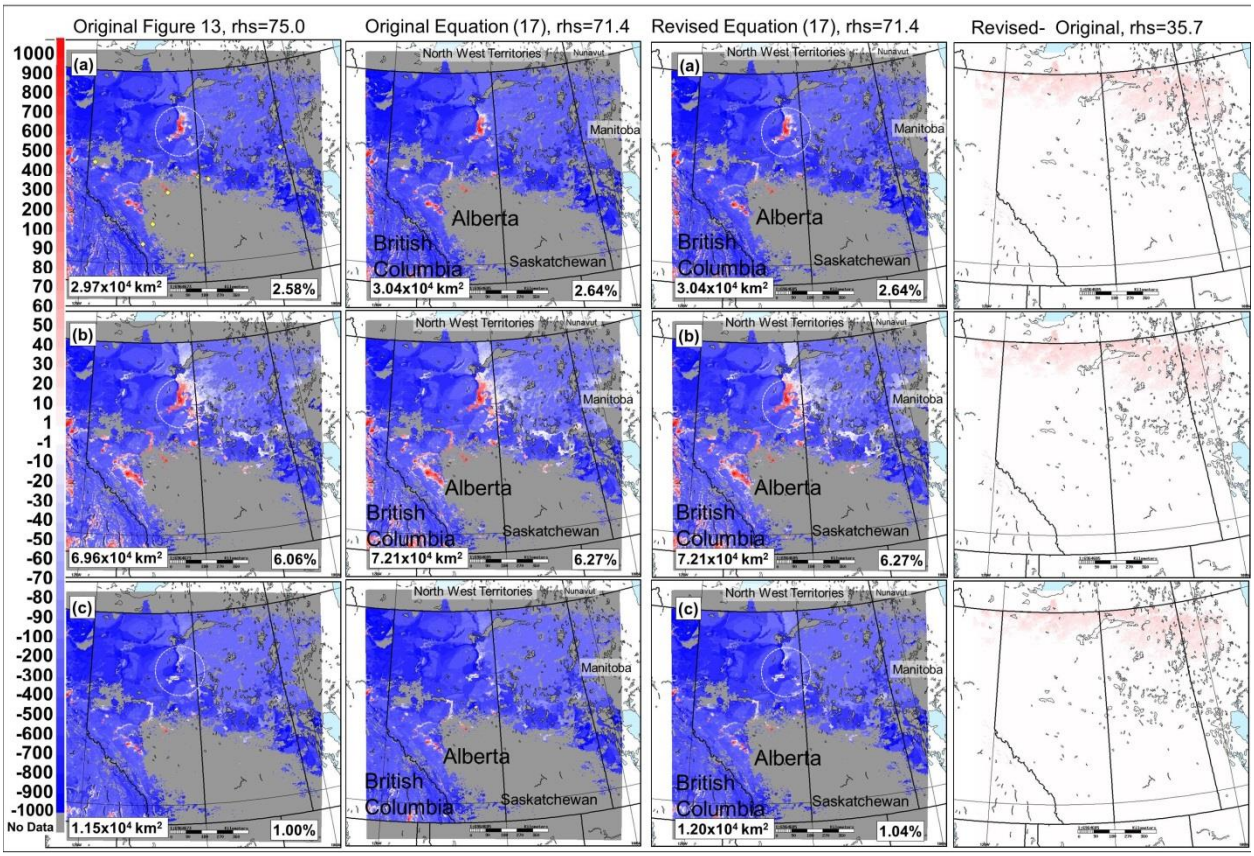

Figure R1. Left column of panels: As in Figure 13, Makar et al, 2018. Middle column: using "min(71.4,N_{dep})" instead of "71.4" as the last term in equation (16). Right column: impact on calculated exceedances as a result of modifying the last term of equation (16) (revised methodology exceedances) subtracted by (original NEG-ECP methodology exceedances). While the proximity to exceedance (E0 region) is reduced in the northern part of the domain, the given increases are insufficient to bring these areas into exceedance (the total area in exceedance does not change to 3 significant figures).

P12, L1: 'permutations' seems a strange expression in this context!

Changed to "permutations on" to "different estimates of".

P12, L11: 'Soils' → 'Soil'.

Done.

P12, L20: How deep was the rooting zone?

This was mentioned earlier in the same paragraph – 50 cm. We've added it again here for clarity.

P12, L27: Comparing $CL_{max}(S)$ with CL(S+N) does not make much sense, as the latter includes N-terms; thus CL(S+N) could be compared to $CL_{max}(N)$.

Good point. The sentence has been changed to read, "$CL_{max}(S)$ and $CL_{max}(N)$" values. The point we were trying to make here is that the forest critical loads for (S+N) calculated through the ECP-NEG protocol imply slightly less sensitive ecosystems than via the more detailed

CLRTAP protocol. This being a little difficult, given that the calculation methodology has changed as well.

P14, L4: '(equations 1 through 16)': This is misleading; e.g. eqs. 1-4 describe the CLs for terrestrial ecosystems. Improve the citation of equation numbers in the whole paragraph! By the way: the exceedance calculations given in eqs. 11-16 are not fully correct for FAB CL functions, as also the first segment of the CLF is tilted.

Quite right – that should have been '1 through 14, with the addition of our equation 15', and the last equation references should have been 1-10, 11-15, respectively. Corrected in the text. We've added the following sentence to the description of Figure 1: "We also note that equations 11-14 themselves are a slight simplification for the FAB model, which allows for a slight inclination of the CLF for $N_{dep} < CL_{min}(N)$*.*

P14,L6: 'predictive maps': wouldn't 'interpolated maps' be more appropriate?

This has been changed to "maps", the word "predictive" has been removed.

P14,L6/7: 'four target variables': In the next 2 lines only 3 variables are mentioned (BC, DOC, $SO4^{2-}$); what's the 4^{th} one?

The "four" has been changed to "three".

P19, L1: 'Yao' → 'Yau'

Corrected.

P21, L20 – P22, L4: This paragraph goes into very much detail… Maybe to Supp Info?

Yes, we agree with the reviewer – the sections dealing with the details of the snowpack sampling protocol have been moved to the SI.

P22, L7: Isn't sulphate an anion?

Yes, that should be removed. Apologies; should have caught that.

P22, L12: 'Manzaono' → 'Manzano'

Corrected.

P22, L13 and eqs: The equation numbers are wrong: On page 11 yu had already eq.19!!

Sorry! This was a case of 'version control'; different versions of the paper having different equation numbers, and the ordering of the sections moving around between different versions of the paper prior to submission. These last three equation numbers have been corrected.

P22, L14: 'used in equation (18)': Which eq. 18?

See above.

P22, L24: Delete 'in 2014'(?)

The date is relevant here in that other criteria were used for site selection in other years, so we have retained the date as in the original submission.

P25, L1: Insert 'in' after 'result'.

Done. Thanks for catching this.

P25, L3: 'input emissions' → 'emissions inputs'

Done.

P26, L4: Sub-header: 'oil sands' →'Oil Sands region'(?)

Changed to 'Athabasca oil sands'. There are several oil sands regions in that part of Canada (in addition to Athabasca, where the study data was collected, there are also oil sands in the Peace River area, and the Cold Lake area.

P27,L28: 'simulation, of' → 'simulations by'

Done (was on line 28).

P31,L30/31: merge lines.

Done.

P33,L13: Delete parentheses around 'BCdep-Sdep-Ndep'

Sorry – we think the parenthesis around the term is justified in this case; the bracket is intended to denote the explicit definition being added as a sideline to the main conversation; we've added an "i.e." within the brackets to make that more clear.

P34,L16: 'sampling for' →'sampling to monitor'

Done.

P35,L9: 'critical load exceedances' → 'critical loads and their exceedances'

Done.

P35,L13: Sub-header: 'Exceedances with respect to' → 'Exceedances of'

Done.

P36,L18: 'Columbia': NO! Columbia is 100 times larger (about 1.14×10^6 km^2)!

Thanks for catching this; there was a transcription error in reading from a list of country sizes. The country name in that line has been changed to Qatar ($1.15x10^4$ km^2).

P38, L3: 'have increased in size relative to' → 'are larger than'

Done.

P40, L1: Sub-header: 'Exceedances with respect to' → 'Exceedances of"

Done.

P40, L6: 'equation (7)': No, it's equ.(5), I presume.

Correct – thanks for catching this; corrected.

P40, L11: 'superimposed in' → 'superimposed om'

*Changed to 'superimposed o**n**'.*

P40, L20: 'to be in exceedance' → 'to be exceeded'

Changed to "in exceedance of critical loads".

Discussion:

P46,L12: 'improve the bias and correlation' → 'reduce the bias and improve the correlation'.

Changed as suggested.

P46,L30: 'expected to occur' → 'expected to occur or has occurred'.

Good point; we've added that correction.

P47,L4: 'of Figure 17(b)': Or 18(b)? As said in the caption of Fig. 20

The text was correct; the caption to Figure 20 was corrected (should have been 17b, there).

Author Contribution:

P51,L7: 'Lakes and Forest' → 'lakes and forest'

Done.

References:

The following references are **cited** in the text, but **missing** here:

- NPRI, 2013

  We've changed this one to Zhang et al., 2018, which describes both the emissions inventory used as well as the sources of information which were included in that inventory.
- Aherne, 2013

We've replaced this one with Aherne and Posch, 2013 (that being a more publicly accessible reference which includes the same material; other was an internal report).
- Aklilu, 201x

Updated to Aklilu et al, 2018
- ECCC, 2014

We couldn't find this one in the text of the article and are assuming that the reviewer mistook an "ECCC (2017)" for "ECCC (2014)".
- Nasr et al., 2010

  Added.
- Whitfield et al, 2010

Added.
- Pregitzer et al, 1990

  Added.
- Stockwell et al, 1989

Changed to Stockwell and Lurmann (1989) and Lurmann et al., 1986, and both were added to the reference list.
- Gong et al, 2003a

Added.
- Gong et al, 2003b

Added.
- Makar et al, 2017

  Added.
- Wesely et al, 1989 [or is this the same as Wesely, 1989?]

  The former – corrected.
- Slinn, 1982

Added.
- Jacobson, 2003 [or should it be Jacobson, 1999, which is given, but not cited?]

Should have been the 1999 reference – fixed this.
- Watmough et al., 2015 [or should it be 2014?]

Should have been 2014 – corrected this.
- Whaley et al., 2017

Updated to Whaley et al, 2018 (was in Discussion phase in 2017, full acceptance in 2018, and we did miss it in the reference list!

The following **references** are **superfluous**, as they are not cited in the text:

Actually, for most of these (exceptions Henriksen, 1984, and Sverdrup and DeVries, 1994) the references were cited – in the SI on the gas dry deposition module of GEM-MACH (maybe the reviewer missed the SI).

- Brook et al, 1999

In the SI.

- Dasch and Cadle, 1986

In the SI.

- Ellsworth and Reich, 1993

In the SI.

- Environment and Climate Change Canada, 2017 [I guess that's ECCC, 2017, cited in the text!?]

It's cited in the text as ECCC 2017 and appears as such in the references, too.

- Henriksen, 1984

This one was removed.

- Hicks et al, 1987

In the SI.

- Hosker and Lindberg, 1982

In the SI.

- Jacobson, 1999 [maybe 2003? – see above]

Should have been 1999 in the text; corrected.

- Meyers et al., 1998

In the SI

- Sverdrup and De Vries, 1994

Reference added to the text.

- Voldner et al., 1986

In the SI.

- Wesely and Hicks, 2000

In the SI.

Figures:

Figure 1: Improve as suggested above

Done.

Figure 2: Caption: 'Lake (S_{dep})' is a somewhat starnge notation. Why not give the equation number used to calculate the CL. Same for 'Forest ($S_{dep}+N_{dep}$)'.
Changed to "(a) Critical load for acidity (eq. 5) and (b) Forest ecosystems (eq. 18) (eq ha^{-1} yr^{-1}).".

Figure 4: Caption: Replace '$S_{dep}+N_{dep}$' by 'S_{dep} and N_{dep}' [and add (FAB model)' after it].
Done.

Figure 5: Caption: 'Sulphur' → 'sulphur' or 'S'.
Done.

Figure 6: Caption: 'Nitrogen' → 'nitrogen' or 'N'.
Done.

- Plate (i): Isn't it the **sum of** particulate nitrate (dry), gaseous organic nitrate (dry), etc.? And not **each of**?

No it's "each of"; the point being that each of these species contributes less than the lowest colour interval of the chosen scale; i.e. less than 10%, as stated in the original figure caption.

Figure 13: Caption: Add that Alberta and Saskatchewan are shown in the maps (?) [also in other Figures!]
Labelling of provinces has been added to all Figures which did not already include that labelling.
Figure 14: Caption: Add that Alberta is shown in the maps (?) [also in other Figures!]
Labelling of provinces has been added to all Figures which did not already include that labelling.

- Year after Wang *et al*. is missing.
- *Year has been added back in.*

Figure 15: Caption: Add '(see Figure 1)' to explain the regions 1,2,3,4! The term 'region' in this context is a bit confusing – e.g. 'cases' would be clearer, to distinguish from geographical regions.

The caption has been changed to "Predicted sub-types of terrestrial ecosystem critical load exceedance (see Figure 1), with panels arranged as in Figure 14. Inset information shows the area within S + N exceedance sub-types 1, 2, 3, and 4 (km^2) and the corresponding percentage of the total area of exceedance. Circled region: 140 km radius diameter circle around the Athabasca oil sands."

Figure 19: Caption: Add '(see Figure 1)' to explain regions 1,2,3,4!

This portion of the caption has been modified to read, "Predicted sub-types of aquatic ecosystem critical load exceedance (see Figure 1), with respect to deposition of sulphur and nitrogen deposition.. Boxed numbers give the area in exceedance within each of exceedance sub-types 1, 2, 3 and 4 (km^2) and the corresponding percentage of the total area in exceedance."

Figure 20: Caption incomplete!

Last sentence of the caption has been modified to "Note that the colour of the symbols, which are for illustration purposes only, does not correspond to numerical exceedance values on the colour scale.".

Estimates of Exceedances of Critical Loads for Acidifying Deposition in Alberta and Saskatchewan

Paul A. Makar[1], Ayodeji Akingunola[1], Julian Aherne[2], Amanda S. Cole[1], Yayne-abeba Aklilu[3], Junhua Zhang[1], Isaac Wong[4], Katherine Hayden[1], Shao-Meng Li[1], Jane Kirk[5], Ken Scott[6], Michael D. Moran[1], Alain Robichaud[1], Hazel Cathcart[2], Pegah Baratzedah[1], Balbir Pabla[1], Philip Cheung[1], Qiong Zheng[1], Dean S. Jeffries[7]

[1]Air Quality Research Division, Environment and Climate Change Canada
[2]Environmental and Resource Studies, Trent University
[3]Environmental Monitoring and Science Division, Alberta Environment and Parks
[4]Watershed Hydrology and Ecology Research Division, Canada Centre for Inland Waters, Environment and Climate Change Canada
[5]Aquatic Contaminants Research Division, Environment and Climate Change Canada
[6]Technical Resources Branch, Environment Protection Division, Saskatchewan Ministry of the Environment
[7]Canada Centre for Inland Waters, Environment and Climate Change Canada

For submission to Atmospheric Chemistry and Physics, Oil Sands Special Issue

Correspondence to: Paul A. Makar (paul.makar@canada.ca)

Abstract. Estimates of potential harmful effects to ecosystems in the Canadian provinces of Alberta and Saskatchewan due to acidifying deposition were calculated, using a one year simulation of a high resolution implementation of the Global Environmental Multiscale – Modelling Air-quality and Chemistry (GEM-MACH) model, and estimates of aquatic and terrestrial ecosystem critical loads. The model simulation was evaluated against two different sources of deposition data; total deposition in precipitation and total deposition to snowpack in the vicinity of the Athabasca oil sands. The model captured much of the variability of observed ions in wet deposition in precipitation (observed versus model sulphur, nitrogen and base cation R^2 values of 0.90, 0.76 and 0.72, respectively), while being biased high for sulphur deposition, and low for nitrogen and base cations (slopes 2.2, 0.89 and 0.40, respectively). Aircraft ~~observation~~-based estimates of fugitive dust emissions, shown to be a factor of ten higher than reported ~~values~~to national emissions inventories (Zhang *et al.*., 2017), were used to estimate the impact of increased levels of fugitive dust on model results. Model comparisons to open snowpack observations were shown to be biased high, but in reasonable agreement for sulphur deposition when observations were corrected to account for throughfall in needleleaf forests. The model-observation relationships for precipitation deposition data, along with the expected effects of increased (unreported) base cation emissions, were used to provide a simple observation-based correction to model deposition fields. Base cation deposition was estimated using published observations of base cation fractions in surface collected particles (Wang *et al.*., 2015).

Both original and observation-corrected model estimates of sulphur, nitrogen and base cation deposition were used in conjunction with critical load data created using the NEG-ECP (2001) and CLRTAP (~~2004, 2016,~~ 2017) ~~protocols~~methods for calculating critical loads, using variations on the Simple Mass Balance model for ~~forest and~~ terrestrial ecosystems, and

the Steady State Water Chemistry and the First-order Acidity Balance models for aquatic ecosystems. Potential ecosystem damage ~~at 2013/14~~using 2011//13 emissions ~~and deposition levels~~data was predicted for regions within each of the ecosystem critical load datasets examined here. The spatial extent of the regions in exceedance of critical loads varied between $1x10^4$ and $3.3x10^5$ km^2, for the more conservative observation-corrected estimates of deposition, with the variation dependant on the ecosystem and critical load ~~protocol.~~calculation methodology. The larger estimates (for aquatic ecosystems) represent a substantial fraction of the area of the provinces examined.

Base cation deposition was shown to be sufficiently high in the region to have a neutralizing effect on acidifying deposition, and the use of the aircraft and precipitation observation-based corrections to base cation deposition resulted in reasonable agreement with snowpack data collected in the oil sands area. However, critical load exceedances calculated using both observations and observation-corrected deposition suggest that the neutralization effect is limited in spatial extent, decreasing rapidly with distance from emissions sources, due to the rapid deposition of emitted primary ~~particles~~ dust particles as a function of their size. We strongly recommend the use of observation-based correction of model-simulated deposition in estimating critical load exceedances, in future work.

1 Introduction

Acidifying deposition was one of the first transboundary air pollution issues recognized as having ecological and economic consequences. In the late 1970's the UN Economic Commission for Europe (UNECE) developed a framework to assess the impacts of acidifying deposition, via the Convention on Long-Range Transboundary Air Pollution (LRTAP, or CLRTAP). The Convention described the scientific basis for the assessment of acidifying precipitation, and provided an internationally binding legal framework for mitigation and control of this and associated issues relating to ~~regional and~~ transboundary air pollution, and entered into force in 1983 (CLRTAP, ~~2016~~ 2017). This and similar legislation elsewhere resulted in a requirement to be able to link sources of acidifying pollutants with downwind ecosystem impacts. While measurement networks were constructed to estimate acidifying deposition in sensitive ecosystems (and continue to be used for this purpose today, see Vet *et al.* (2014) for a review of current global acidifying precipitation networks and their status), the measurement sites are sparse due to their expense and the availability of the infrastructure to make observations in remote sensitive ecosystems. A further requirement thus arose: to provide estimates of acidifying pollution to sensitive ecosystems to complement the available observations.

This requirement drove the development of the first generation of chemical transport models (CTM's), which made use of inventories of the emissions of different pollutants, detailed descriptions of gas, aqueous-phase and particle chemistry, speciated gas and particle and meteorological forecast model information, to describe the downwind transformation and deposition of acidifying pollutants (cf. Eliassen *et al.*, 1982; Calvert and Stockwell, 1983; Venkatram and Karamchandani, 1988; Chang *et al.*, 1987). The models increased in sophistication over the years to include more detailed descriptions of gas and aqueous chemistry, particle chemistry and particle microphysics (cf. Binkowski and Shankar, 1995; Binkowski and

Roselle, 2003; Gong *et al.*, 2006). The next generation of models was extended to merge previously separate chemistry and meteorological forecasting models into unified frameworks (Grell *et al.*, 2005; Vogel *et al.*, 2009; Moran *et al.*, 2010, Baklanov *et al.*, 2014). The most recent versions of these models included incorporation of the impacts of model-generated aerosols into radiative transfer, and hence estimation of the impacts of feedbacks between atmospheric pollution and weather forecasting (ensemble comparisons of these fully coupled models with observations may be found in Makar *et al.*, 2015(a,b) and Im *et al.*, 2015 (a,b)).

Concurrent to the ongoing CTM development, methodologies were extended to improve the estimation of the effects of acidifying emissions on sensitive ecosystems. A key tool for this work are spatial maps of ecosystem "critical loads", where a critical load is defined (Nilsson and Grennfelt, 1988) as "A quantitative estimate of an exposure to one or more pollutants below which significant harmful effects on specified sensitive elements of the environment do not occur according to present knowledge". In the context of acidifying deposition, the critical load is the upper limit to the deposition flux of acidifying pollutants, below which ecosystem damage due to that deposition will not occur. A critical load *exceedance* is thus defined as the *excess* deposition of acidifying pollutants *above* the critical load. Guidelines for the determination of UNECE CLRTAP critical load data were first published in 1996, with subsequent updates (CLRTAP, ~~2004, 2016,~~ 2017). In North America, modified ~~protocols~~critical load calculation methodologies were initially adopted, to provide upper limit estimates of critical loads, for cases in which more detailed data were unavailable, via an agreement between the eastern US States and eastern Canadian provinces (New England Governors – Eastern Canadian Premiers; NEG-ECP, 2001).

~~Estimates of critical~~Critical loads for acidifying deposition for different ecosystems are calculated using different models, but all are predicated on the concept of charge balance at steady-state; the critical load models determine the excess flux of cations available in the natural ecosystem, which could potentially balance the anions added due to acidifying deposition. The critical load calculations may thus depend on estimates of the deposition flux of both anions and cations. The anions of interest are the total (wet plus dry) atmospheric deposited sulphur, S_{dep}, and total atmospheric deposited nitrogen, N_{dep}, where the sulphur deposition is assumed to have two negative charges (all forms of S_{dep} are assumed to eventually be transformed to, and contribute to deposition as, SO_4^{2-}), and nitrogen is assumed to have one negative charge (all forms of N_{dep} are assumed to eventually be transformed to, and contribute to deposition as, NO_3^-). Cations of interest include Mg^{2+}, Ca^{2+}, K^+, and Na^+, collectively referred to as base cations, and their net deposition from the atmosphere when converted to molar charge equivalents, is referred to as BC_{dep}. For terrestrial ecosystems BC_{dep} must be estimated from observations or CTM predictions, while for aquatic ecosystems, the total base cation concentrations within water due to atmospheric deposition and other sources are derived from direct sampling and laboratory analysis of ecosystem surface water.

We note that while an exceedance of critical loads identifies the *potential* for ecosystem damage to occur, critical loads are based on the concept of a chemical steady-state, and depending on the buffering mechanisms available in an ecosystem, the steady-state defined by an exceedance of critical loads may not take place until some point in the future. Once exceedances

of critical loads have been identified, dynamic models may be used to assess the time delay until damage occurs and/or the time required for recovery of the ecosystem subsequent to that damage (CLRTAP, ~~2015~~2017).

Atmospheric deposition of S_{dep}, N_{dep} and BC_{dep} may thus influence the estimation of critical load exceedances. ~~For terrestrial ecosystems, if the value of BC_{dep} – S_{dep} – N_{dep} is positive, then critical loads will not be exceeded.~~Both terrestrial and aquatic critical loads are based on the concept of ion charge balance (cations – anions), as well as terms describing the perturbation of the charge balance through, for example, removal of specific ions or groups of ions through , leaching, harvesting of biomass, etc. For aquatic ecosystems, if the value of the total charge balance of the critical load (which includes all forms of input of base cations to the system including BC_{dep}) is greater than the added anions, critical loads will not be exceeded. Emissions sources of base cations may thus act to counteract the emissions sources of S_{dep} and N_{dep}, depending on the relative ~~emissions~~emission levels, the locations of the sources, etc. For example, some observations in the immediate environs (within 135 km) of emission sources located within the Athabasca oil sands region of Canada have shown that BC_{dep} exceeds S_{dep} and N_{dep}, implying that ~~alkylization~~alkalinization (rather than acidification) may be happening in this region (Watmough *et al.*, 2014). While the disturbance to the ecosystems due to the increase in pH associated with the excess base cations may cause other ecosystem effects, this finding has been used to imply that acidifying deposition, and the consequent potential ecosystem damage due to emissions from these facilities is unlikely. This implication has been re-evaluated on a larger scale in the present work.

The provinces of Alberta and Saskatchewan are home to the majority of Canada's petrochemical extraction and refining infrastructure, in addition to other industries such as coal-fired power generation, and account for a substantial fraction of the Canadian anthropogenic emissions of sulphur dioxide~~,~~ (34%), nitrogen oxides~~,~~ (43%), and ammonia (~~34, 43, and~~ 50 ~~%, respectively, NPRI, 2013). Within the province of Alberta , emissions~~%), see Zhang *et al.*, 2018). Emissions originating ~~in~~within the Athabasca oil sands region account for approximately ~~38.4, 3.8, and~~6.5, 1.3, and 0.3% of the ~~Alberta total~~Canadian anthropogenic emissions of these three chemicals~~.~~, based on inventories used in Zhang *et al.* (2018). These three pollutants, and their gas, particulate and aqueous-phase reaction products, are the main anthropogenic sources of S_{dep} and N_{dep} within this region. As we will show below, the provinces are also home to terrestrial and aquatic ecosystems which are sensitive to acidifying deposition (i.e. have relatively low critical loads for acidifying deposition). Calculations of exceedances of critical loads within this region are therefore of interest, to assess the potential for ecosystem damage associated with these emissions, and are the focus of our work.

We use a combination of a fourth-generation CTM (the Global Environmental Multiscale – Modelling Air-quality and CHemistry; GEM-MACH), critical load estimates for aquatic and ~~terrestrials~~terrestrial ecosystems determined using different ~~protocols~~methodologies, and two different surface deposition observation datasets, to predict the extent to which critical loads are being exceeded, over large portions of the Canadian provinces of Alberta and Saskatchewan.

We begin with a description of the critical load data used in our evaluation, follow with a description of GEM-MACH (with a focus on its components which pertain to S_{dep} and N_{dep}), an evaluation of the model performance, corrections to the model predictions based on observations, and end with estimates of exceedances for terrestrial and aquatic ecosystems and our conclusions.

2 Methodology

2.1 Global Environmental Multiscale – Modelling Air-quality and CHemistry (GEM-MACH), Version 2

2.1.1 GEM-MACH v2 Overview

GEM-MACH is Environment and Climate Change Canada's comprehensive chemical reaction transport model. The model follows the on-line paradigm (in that atmospheric chemistry modules have been incorporated directly into a weather forecast model (GEM) (Moran *et al.*, 2010; Makar *et al.*, 2015 (a,b)). The parameterizations include gas-phase chemistry (42 species, ADOM-II mechanism, Stockwell and Lurmann, 1989), aerosol microphysics (Gong *et al.*, 2003(a,b)) and cloud processing of gases and aerosols including uptake and wet deposition (Gong *et al.*, 2006; Gong *et al.*, 2015). The model's aerosol size distribution makes use of the sectional (bin) approach, with two possible configurations: (1) a processing-time efficient two-bin configuration used for operational forecasting and longer scenario simulations (fine and coarse particle sizes are subdivided within certain aerosol microphysics processes in order to preserve solution accuracy while minimizing advective transport time) and (2) a more detailed 12 bin size distribution used to more accurately simulate aerosol microphysics and the size spectrum of particles. The aerosols in GEM-MACH are also speciated chemically into particle sulphate, nitrate, ammonium, primary organic aerosol, secondary organic aerosol, elemental (aka "black") carbon, sea-salt and crustal material, within each size bin. The crustal material component includes all particulate matter not speciated under the other components, and hence includes base cations as a fraction of its total mass. As will be discussed below, the observations of Wang *et al.* (2015) were used to approximate the base cation fraction of GEM-MACH's crustal material, and hence estimate the mass of base cation deposition predicted by the model.

A comparison of GEM-MACH version 1.5.1 against other peer on-line models appears elsewhere (Makar *et al.*, 2015(a,b)), as does a description of the main updates associated with version 2 of the model (Makar *et al.*, 2017). Comparisons of the operational 2-bin version of the model against observations have also appeared in the literature (Pavlovic *et al.*, 2016; Munoz-Alpizar *et al.*, 2017). Our description below will focus on the model's modules for gas-phase dry deposition, particle phase dry deposition, cloud processing and aqueous phase chemistry (wet deposition).

2.1.2 Gas-phase dry deposition in GEM-MACH

A detailed description of the gas-phase dry deposition module of GEM-MACH (with an emphasis on the chemical species which contribute to S_{dep} and N_{dep}) appears in the Supplementary Information; here we provide an overview. Gas-phase deposition is handled using the commonly used "resistance" approach, where the deposition velocity is the inverse of the sum of aerodynamic, quasi-laminar sublayer and net surface resistances. The aerodynamic resistance is the same for all gases, the quasi-laminar sublayer resistance depends on gas diffusivity, but these terms are relatively minor compared to the net surface resistance, which tends to control the deposition velocity for many of the gases (notable exceptions being HNO_3 and NH_3 which have a relatively low surface resistance and hence the overall resistance is strongly dominated by meteorological factors). The net surface resistance follows the approach of Wesely (1989) with a parameterization following Jarvis (1976) for the stomatal resistance. For plants, the overall resistance has terms for the contributions associated with the stomata, mesophyll, and cuticles, the resistance of gases to buoyant convection, the resistance associated with leaves, twigs, bark and other exposed surfaces in the vegetated canopy, the resistance associated with the height and density of the vegetated canopy (referred to here as canopy resistance), and the resistance associated with soil, leaf litter, etc., at the surface. The net surface resistance includes a term to account for the impact of precipitation and high humidity on stomatal and mesophyll resistances, and a temperature-dependent correction term for snow-covered surfaces.

Soil resistances are calculated following Wesely (1989) with a parameterization based on the values for SO_2 and O_3, with a seasonal dependence (Midsummer, Autumn, Late Autumn, Winter and Transitional spring). Canopy resistances are based on Zhang *et al.* (2003), with the same seasonality as above. The resistance for the lower canopy follows Wesely (1989) using a function of the effective Henry's law constant and terms for SO_2 and O_3 resistances. The mesophyll and cuticle resistances follow Wesely (1989), with seasonal variations as above and vegetation-dependent leaf area index values. The resistance of gases to buoyant convection follows Wesely (1989), and is a function of the visible solar radiation. The stomatal resistance follows a similar approach to Jarvis (1976), Zhang *et al.* (2002, 2003), Baldocchi *et al.* (1987), and ValMartin *et al.* (2014), and results from several terms describing its dependence on light ($k_s(Q_p)$), water vapour pressure deficit ($k_s(\delta e)$), temperature (k_{st}), CO_2 concentration (k_{sca}), the leaf area index (LAI), and the ratio of the molecular diffusivities of water to the gas being deposited ($\frac{D_{H2O}}{D_{gas}}$). The approach taken for the dependence on light provides stomatal resistance values similar to those of Baldocchi *et al.* (1987), but are lower than those of Zhang *et al.* (2002) for the same vegetation types, decreasing stomatal resistances and thus increasing the stomatal resistance contribution to deposition velocities, relative to Zhang *et al.* (2002). The other terms in the stomatal resistance employed curve fitting where possible across different sources of deposition data, due to the wide variation noted in the underlying measurement literature.

Deposition velocities are calculated for the S_{dep} and N_{dep} contributing gases SO_2, H_2SO_4, NO, NO_2, HNO_3, PAN, HONO, NH_3, organic nitrates, as well as several other transported gases of the ADOM-II gas phase mechanism. We note that the rapid conversion of gaseous sulphuric acid (H_2SO_4) to particulate sulphate due to its low vapour pressure ensures that the

Formatted: Font: Italic

Formatted: Font: Italic

direct contribution of H_2SO_4 deposition to S_{dep} is relatively minor. Further details on the deposition velocity formulation, and tabulated coefficients for the species contributing to S_{dep} and N_{dep}, appear in the Supplementary Information.

Gas-phase dry deposition velocities are incorporated as a flux lower boundary condition in the solution of the vertical diffusion equation within GEM-MACH.

2.1.3 Particle phase dry deposition in GEM-MACH

Particle dry deposition in GEM-MACH makes use of the size-segregated formulation of Zhang *et al.* (2001), which in turn follows Slinn (1982). The gravitational settling velocity (a function of the particle density, wet diameter, air viscosity, and the temperature and air pressure) is calculated for each particle size at each model level. At the lowest level, the settling velocity is added to the inverse of the sum of the aerodynamic resistance above the canopy and the surface resistance. The aerodynamic resistance is a function of atmospheric stability, surface roughness, and the friction velocity, while the surface resistance is the inverse of the sum of collection efficiencies for Brownian diffusion, impaction and interception, multiplied by correction factors to account for the fraction of particles which stick to the surface. The Brownian diffusion is a function of the Schmidt number of the particle (ratio of the kinematic viscosity of the air to the particle's Brownian diffusivity). The impaction term is dependent on the Stokes number (itself a function of the gravitational settling velocity) and the land-use type, and the interception term is taken to be a simple function of the particle diameter and a land-use and seasonal dependent characteristic radius.

The resulting deposition velocities have the characteristic strong dependence on particle size noted in observations, with minimum deposition values occurring at particle diameters of about 1 μm, with an increase in deposition velocities of up to two orders of magnitude with decreasing or increasing particle size. As will be discussed later in this work, one of the consequences of the size-dependence of particle deposition velocity is that particles which are larger (or smaller) than 1 μm diameter settle more rapidly than the latter particles, and hence have shorter transport distances than 1 μm diameter particles. This phenomena is responsible for the rapid decrease in surface deposition with increasing distance from sources of base cations.

Particle gravitational settling and deposition velocities are handled in this version of GEM-MACH using a semi-Lagrangian advection approach in the vertical for each column; vertical backtrajectories are calculated from the settling and deposition velocities, and mass-conservative interpolation is used to determine the new concentration profile and the flux to the surface. The particle deposition component of S_{dep} and N_{dep} (via the deposition of particle sulphate, particle nitrate, and particle ammonium) is typically very small compared to the gaseous dry deposition of primary emitted gases (SO_2, NO_2, NH_3), secondary gases (HNO_3), and wet deposition of ions (HSO_3^-, SO_4^{2-}, NO_3^-, NH_4^+).

2.1.4 Cloud processing of gases and aerosols, and inorganic particle chemistry in GEM-MACH

The cloud chemistry and aqueous processing of gases and aerosols in GEM-MACH makes use of the methodologies used in GEM-MACH's precursor model, A Unified Regional Air-quality Modelling System (AURAMS), and are described in detail in Gong *et al.* (2006). Aqueous chemistry includes the transfer of gaseous SO_2, O_3, H_2O_2, ROOH, HNO_3, NH_3 and CO_2 to cloud droplets, along with the oxidation of S(IV) to S(VI) within the cloud droplets by several pathways. The stiff system of equations described by the aqueous chemistry is solved using a bulk approach and a computationally efficient predictor-corrector algorithm. Aerosol sulphate, nitrate and ammonium may be taken up into cloud droplets following activation, and may be returned to the aerosol phase following aqueous chemistry via particle evaporation. Rebinning of mass transferred back to the particle phase is accomplished through a mass-conservative rebinning algorithm similar to that described in Jacobson (1999).

Wet deposition processes (tracer transfer from cloud droplets to raindrops, scavenging of aerosols and soluble gases by falling hydrometers, downward transport by precipitation, and evaporation of raindrops and potential loss of mass prior to deposition) are explicitly included in GEM-MACH. Cloud droplet to raindrop tracer transfer is handled using a bulk autoconversion rate obtained from the meteorological model. Impact scavenging of size-resolved aerosols is parameterized using a scavenging rate based on the precipitation rate and the mean collision efficiency. Irreversible scavenging of soluble gases makes use of the Sherwood number and diffusivity of the gas, the precipitation rate, the Reynolds and Schmidt numbers, and the raindrop diameter, while reversible scavenging makes use of equilibrium partitioning.

The cloud fields provided to the aqueous phase chemistry module depend on the model resolution – for the high resolution simulations carried out here, the hydrometeors are explicitly simulated and transported using the 2-moment scheme of Milbrandt and Yau (2005 (a,b)). A full description of the cloud processing model and the formulation of its components appears in Gong *et al.* (2006).

Inorganic particle chemistry makes use of the HETV system of equations for sulphate, nitrate and ammonium described in detail in Makar *et al.* (2003), based on the ISORROPIA algorithms of Nenes *et al.* (1999). The concentrations of particle sulphate, nitrate, ammonium, and gaseous NH_3 and HNO_3 are solved in bulk for non-ideal high concentration solutions via first determining the chemical subspace in which the total nitrate, sulphate, ammonium and relative humidity resides (breaking the problem into twelve subspaces for the different combinations of gases, salts, and aqueous ions which may exist under those conditions), then solving a double iteration including the full system of equations incorporating activity coefficient calculations and vectorization across the subspaces for computational efficiency. Following the bulk calculations, the resulting aerosol mass of sulphate, nitrate and ammonium are rebinned using an approach similar to that of Gong *et al.* (2006).

2.1.5 Emissions and Simulation Setup

The emissions used in the simulations carried out here are described in detail in Zhang *et al.* (2017, this special issue).

All simulations used a nested model setup, feeding into the meteorological and chemical boundary conditions for a 2.5km resolution Alberta and Saskatchewan simulation. The latter domain is depicted in Figures 2 and 3 (the 2.5km resolution domain is the entire coloured and grey shaded region). Archived GEM 10km forecast simulations were driven by data assimilation analysis fields, and were used to in turn drive successive overlapping 30 hour forecasts of both a Canadian domain 2.5km resolution meteorological forecast, and a 10km GEM-MACH forecast. The final 24 hours of these simulations provided the meteorological and chemical boundary conditions respectively for a series of 24-hour simulations of GEM-MACH on the domain shown in Figures 2 and 3. This nesting approach was selected to provide the best possible meteorological and chemical inputs for the 2.5km high resolution domain. The output from the 24-hour simulations were then brought together to create the continuous time record of concentrations and deposition on the high resolution model grid Three simulations were carried out with this setup. The first of these is made use of the two aerosol bin configuration of GEM-MACH, for an entire year of simulated chemistry and meteorology (August 1, 2013 to July 31, 2014), in order to obtain a year of model output, required for critical load calculations. The outer 10km North American domain of the simulation made use of the operational GEM-MACH forecast emissions inventories for the years 2010 (Canada), 2011 (USA) and 1999 (Mexico), while the inner nest made use of 2013 (Canada) and 2011 (USA) inventories (see Zhang *et al.*, 2017). The predicted deposition thus represents the model predictions using emissions reported under current Canadian regulatory requirements. Two additional simulations were then carried out, for the period August 13th to September 10th, making use of the 12-bin version of the model: a base case and a primary particulate scenario. The primary particulate scenario made use of aircraft-based estimates of primary particulate emissions from six oil sands facilities, and both making use of continuous emissions monitoring data for Alberta for SO_2 and NO_x emissions from large stack sources (see Zhang *et al.*, 2017, this issue, for the full description of these emissions). This second pair of simulations was carried out to investigate the potential impact of possible under-reporting of primary particulate emissions on model critical load exceedance predictions. About 96% of these primary particulate emissions by mass are associated with fugitive dust emissions sources, and over 68% of this mass is in the coarse mode (diameters greater than 2.5 μm) (Zhang *et al.*, 2017). The potential impact of these sources of base cations on acidifying deposition will be discussed in Sections 3.3, 3.5 and 3.6.

2.2 Deposition Observations

2.2.1 Deposition of ions in precipitation

Wet-only precipitation measurements were collected at six sites in Alberta (AB) by Alberta Environment and Parks and two sites in Saskatchewan (SK) by the Canadian Air and Precipitation Monitoring Network (CAPMoN) (Figure 2(b)). In wet-only samples, a heated precipitation sensor opens the collector lid when precipitation is detected, and closes the lid when precipitation ends. For the SK samples, the collector bucket was lined with a polyethylene bag which was removed, weighed, sealed, refrigerated, and shipped to the laboratory for major ion analysis. For the AB samples, the samples were transferred from the clean collection bucket to a smaller sample bottle, capped, refrigerated if stored on site, and shipped to the

laboratory for analysis. Collection occurred approximately daily at the SK sites and approximately weekly at the AB sites. Quality control was performed by the collecting networks.

Annual precipitation-weighted mean concentrations of SO_4^{2-}, NO_3^- and NH_4^+ were calculated from the daily or weekly samples using recommended methods and completeness criteria (WMO/GAW, 2004, 2015) and the resulting deposition fluxes were compared with model values. Where there were measurement gaps of > 3 weeks (two sites), or where there was only partial coverage of the 12 months (one site), fluxes were compared over shorter measurement periods. The collector buckets described above tend to underestimate the total precipitation, so the flux of ions derived from their records must be corrected using independent observations of total precipitation. At the SK sites, separate on-site rain and snow gauges were used to manually record the daily precipitation amount. At the AB sites, precipitation gauges for independent quantification of total precipitation were not available, hence weekly deposition fluxes were calculated using daily precipitation depth data from the nearest meteorological station, or combination of meteorological stations, with the most complete coverage (ECCC, 2017, AAF, 2017).

Total precipitation depth collected in the AB wet deposition collectors, summed over all collection periods at the sites, was 51-96% of the estimated precipitation depth at meteorological stations. Our deposition flux calculations implicitly assume that the ion concentrations measured in the sample are representative of all the precipitation during the period. However, the mechanism of precipitation loss (undercatch due to wind, evaporative loss, delay in lid opening) may lead to unrepresentative concentration values. Additional uncertainty is introduced by the use of precipitation depth from collectors that are not co-located, particularly at Kananaskis. Therefore, wet deposition fluxes from the AB sites have higher uncertainty than the fluxes at the two SK sites, where 105% and 78% of the standard gauge precipitation was captured by the collector.

2.2.2 Deposition of S and N compounds to snowpack

Observations of total deposition of sulphur, nitrogen, and base cations to snow-covered open surfaces were collected in two separate studies. Samples were collected in the immediate vicinity of the oil sands by Environment and Climate Change Canada, and snowpack samples in northern Saskatchewan were collected by Saskatchewan Environment (snowpack station locations are discussed in Section 3.4). Both sets of data were collected in open clearings and thus deposition is to snow-covered *open* surfaces. They thus provide *minimum* estimates of deposition, particularly for gases. One method of accounting for deposition to forests and related vegetation is via collection of precipitation samples below foliage, which assumes that deposited materials leaves the vegetation via precipitation and/or melting of snow, to reach the collector ("throughfall"). Watmough *et al.* (2014) compared winter throughfall versus open deposition in the oil sands region, and showed maximum throughfall values to be about 1.9 times their open deposition counterparts. However, throughfall observations do not account for the portion of the deposited material which remains on or within the vegetated surfaces, and hence must also be considered a conservative estimate of total deposition. Using the algorithms of GEM-MACH's gas-phase deposition module, typical ratios of dry deposition velocity between a needle leaf forest and an open snow covered

surface for SO_2 and NH_3 respectively are 2.63 and 1.97 (temperature -5C, u*= 0.1 m s^{-1}, solar radiation = 100 W m^{-2}, z_0 = 0.1m, Monin-Obukhov length = 50). However, the ratios for dry deposition of particles with diameters of 2.5 and 10 μm are 0.76 and 0.82, respectively (Zhang *et al.*, 2001), indicating that the open snowpack observations may slightly overestimate BC_{dep} and Bc_{dep} (in contrast to the Watmough *et al.* (2014) observations), but significantly underestimate S_{dep} and N_{dep}.

Further details on the methodology used for snowpack analysis may be found in the Supplemental Information for this paper.

2.3 Estimates of Critical Loads of Acidic Deposition in Canada– A Review of Recent Work

In this section, we review recent work on the estimation of critical loads in Canada, starting from the UNECE definitions, in order to provide a complete description of the critical load datasets used in our subsequent estimates of exceedances.

2.~~1~~3.1 Critical Loads and Critical Load Exceedances – Definitions

Critical loads were estimated following methodologies set out under the UNECE Convention on Long-range Transboundary Air Pollution (CLRTAP, ~~2016,~~ 2017; de Vries, *et al.*, 2015). We define first the equations used for determining critical loads, and follow with the description of the data used to estimate critical loads of acidifying sulphur (S) and nitrogen (N) for terrestrial and aquatic ecosystems in Alberta and Saskatchewan, based on a Canada-wide implementation (Carou *et al.*., 2008), and two more recent studies focused on terrestrial ecosystems in the province of Alberta, and aquatic ecosystems in northern Alberta and Saskatchewan (Cathcart *et al*., 2016).

For terrestrial ecosystems, critical loads of acidity were estimated using the steady-state (or simple) mass balance (SSMB) model~~,~~ which links deposition to a chemical variable (the 'chemical criterion') in the soil, or soil solution, associated with ecosystem effects~~.~~ (Sverdrup and DeVries, 1994). The violation of a specific value (the 'critical limit') for the chemical criterion is associated with potential ecosystem damage. The most widely used soil chemical criterion is based on the molar ratio of base cations to aluminum (*Bc:Al* where *Bc* is the molar sum of ~~in equivalents of~~ calcium (Ca^{2+}), magnesium (Mg^{2+}) and potassium (K^+)) in soil solution~~.~~ (the factor of 3/2 in equation (4) below converts this term to equivalents). The acidifying impact of S and N define a critical load function (CLF) incorporating the most important biogeochemical processes that affect long-term soil acidification (CLRTAP, ~~2004~~2017). The function is defined by three quantities (see ~~Equations~~equations 1 to ~~3~~4): the maximum critical load of S ($CL_{max}(S)$); minimum critical load of N ($CL_{min}(N)$); and the maximum critical load of N ($CL_{max}(N)$). The critical level of ~~protection for~~ the ~~chosen receptor ecosystem (e.g., forests) is specified via the receptor ecosystem's critical~~ leaching of acid neutralizing capacity for ~~leaching~~the ecosystem ($ANC_{le,crit}$~~,~~ ~~Equation~~) is defined via equation (4). Critical loads of acidity for terrestrial ecosystems are defined in units of "equivalents" (ionic charge × moles).

$$CL_{max}(S) = BC_{dep} + BC_w - Cl_{dep} - Bc_u - ANC_{le,crit} \quad (1)$$

Formatted: Superscript
Formatted: Subscript
Formatted: English (U.K.)
Formatted: English (U.K.)
Formatted: Font: Italic, English (U.K.)
Formatted: English (U.K.)
Formatted: Font: Italic, English (U.K.)
Formatted: English (U.K.)
Formatted: English (U.K.)
Formatted: English (U.K.)
Formatted: Font: Not Italic
Formatted: Font: Not Italic

$$CL_{max}(N) = CL_{min}(N) + \frac{CL_{max}(S)}{1-f_{de}} \quad (2)$$

$$CL_{min}(N) = N_i + N_u \quad (3)$$

$$ANC_{le,crit} = -Q^{\frac{2}{3}}\left[\frac{3}{2}\left(\frac{Bc_w+Bc_{dep}-Bc_u}{(Bc:Al)_{crit}K_{gibb}}\right)\right]^{\frac{1}{3}} - \frac{3}{2}\left(\frac{Bc_w+Bc_{dep}-Bc_u}{(Bc:Al)_{crit}}\right) \quad (4)$$

The remaining terms in these equations include: BC_{dep}, the non-marine annual base cation deposition, BC_w, is the release of soil base cations owing to physical and chemical breakdown (weathering) of rock and soil minerals, Cl_{dep} the non-marine chloride deposition, Bc_u, the average base cation removal due to the harvesting of base-cation-containing biomass from the ecosystem, f_{de}, the denitrification fraction (loss of nitrogen to N_2), N_i, the long-term annual net immobilization of nitrogen in the rooting zone, and N_u, the average removal of nitrogen from an ecosystem due to, e.g., harvesting), Q is defined above, $(Bc:Al)_{crit}$, is the critical value of the non-sodium base cation to aluminum ion ratio described above, and K_{gibb} is the Gibbsite equilibrium constant.

For aquatic ecosystems, two steady-state models have been widely used for calculating critical loads (Henriksen and Posch, 2001; CLRTAP, 2017; de Vries *et al.*, 2015): the Steady-State Water Chemistry (SSWC) model and the First-order Acidity Balance (FAB) model.

The SSWC model requires volume-weighted mean annual water chemistry and runoff volume (Q) to calculate critical loads of S acidity.

$$CL(A) = Q([BC]_0^* - ANC_{limit}) \quad (5)$$

where $[BC]_0^*$ is the sea salt corrected pre-acidification concentration of base cations in the surface water, and ANC_{limit} is the ANC (concentration) limit above which no damage to the specified biological indicator (e.g., fish) occurs. The sea salt correction, denoted by a superscript asterisk, assumes all chloride originates from sea salt; the current concentrations of base cations, SO_4^{2-}(aq) and NO_3^-(aq) in water along with empirical functions (see below) are used to estimate $[BC]_0^*$, following CLRTA methodologies (CLRTAP protocols (CLRTAP, 2016, 2017); further details regarding the sensitivity of the critical load estimates to these functions are described in Cathcart *et al.* (2016).

The FAB model (Posch *et al.*, 2012) allows the simultaneous calculation of critical loads of acidifying S and N deposition similar to the SSMB model widely used for forest soil critical loads. In addition to processes in the terrestrial catchment soils, such as uptake, immobilization and denitrification, the FAB model includes in-lake retention of N and S. The derivation of the FAB model starts from the charge balance at the outlet of a lake:

Formatted: Font: Italic

Formatted: Font: Italic

Formatted: Font: Italic

~~$$Y = \frac{S_{runoff} + N_{runoff} - \sum_X Y_{runoff} - ANC_{limit}}{Ca + Mg + K + Na - Cl} \quad (6)$$~~

$$S_{runoff} + N_{runoff} = Ca_{runoff} + Mg_{runoff} + K_{runoff} + Na_{runoff} - Cl_{runoff} - ANC_{limit} \quad (6)$$

Steady-state mass balance equations for the runoff terms for each ion (X) are then derived as a function of the total amount of ions entering the lake (X_{in}) and dimensionless retention factors ~~(ρ_X)~~:(ρ_X):

$$X_{runoff} = (1 - \rho_X) X_{in} \quad (7)$$

The formulae for X_{in} depends on the specific ion; S_{in} depends on deposition alone, N_{in} includes terms for net immobilization (subscript *i*), growth uptake (subscript *u*), and denitrification (f_{de}), and base cations includes terms for deposition (subscript dep), weathering (subscript *w*) ~~and uptake (u).~~ An equation of the following form results (the summation is over the different components within the catchment, usually simplified to be "lake" and "non-lake" (i.e. m=1 in the equation which follows), and A_j/A is the relative area of the components (A_j) to the total catchment area (A):

$$\begin{aligned}(1-\rho_S)\sum_{j=0}^{m}\frac{A_j}{A}S_{dep,j} + \sum_{j=0}^{m}\frac{A_j}{A}\left(1-f_{de,j}\right)\left(N_{dep,j}\left(1-f_{u,j}\right) - N_{i,j} - N_{u,o,j}\right)_+ = \\ \sum_Y\left[(1-\rho_Y)\sum_{j=0}^{m}\frac{A_j}{A}\left(Y_{dep,j} - Y_{w,j} - Y_{u,j}\right)_+\right] - Q\cdot ANC_{limit}\end{aligned} \quad (8)$$

where the "+" subscript refers to the maximum value of the term within the brackets across the catchment components j (lake and non-lake). S_{dep} includes all forms of sulphur deposition (gaseous SO_2 dry deposition, particulate dry deposition, and wet deposition of bisulphate and sulphate ions), converted to charge x mole equivalent deposition of SO_4^{2-}. N_{dep} includes all forms of nitrogen deposition (gas phase dry deposition of NO, NO_2, NH_3, HONO, HNO_3, peroxyacetylnitrate, organic nitrates, dry deposition of particulate nitrate and ammonium, and wet deposition of ammonium and nitrate ions), converted to the charge x mole equivalent deposition of NO_3^-. Setting N_{dep} = 0 in (8) results in a formula for $CL_{max}(S)$, and setting S_{dep} = 0 results in a formula for $CL_{max}(N)$. The denitrification fraction was estimated as f_{de} = 0.1 + 0.7 ·f_{peat}, where f_{peat} is the fraction of wetlands in the terrestrial catchment, and $CL_{min}(N)$ was taken to be N_i+N_u (N_i was set to the regional default value of 35.7 eq ha^{-1}), and N_u was based on estimates of forest biomass (Canadian Forestry Service National Forest Inventory) and literature data for the concentration of N in biomass). The net uptake of N on land was assumed to be constant ($f_{u,I}$=0), and the flux of base cations (right-hand-side of (8)) is determined using the SSWC model via equation (5). In both the SSWC and FAB models, the value of $[BC]_0^*$ is derived using an "F-factor" equation describing the change in charge balance over time from pre-industrial (time 0) to current (time t) conditions:

$$[BC]_0^* = [BC]_t^* - F\cdot\left([SO_4]_t^* + [NO_3]_t - [SO_4]_0 - [NO_3]_0\right) \quad (9)$$

The F-factor in (9) depends on the pre-industrial base cation concentration and (~~9~~12) is solved iteratively. The in-lake retention coefficients for S and N (ρ_S and ρ_N, respectively) are modelled by a kinetic equation (Kelly *et al.*, 1987) making them a function of runoff, the lake:catchment ratio and net mass transfer coefficients for S and N. It is assumed that the lakes and their catchments are small enough to be properly characterised by average soil and lake-water properties; furthermore, all of the lakes examined here are treated as headwater lakes, and larger lakes are excluded from the analysis.

Formatted: Font: Italic
Formatted: Font: Italic
Formatted: Font: Italic
Formatted: Font: Italic
Formatted: Font: Italic
Formatted: Font: Italic
Formatted: Font: Italic
Formatted: Font: 10 pt

The risk of negative impacts owing to acidifying S and N deposition, i.e. deposition in excess of the critical load,- is based on the magnitude and areal extent of exceedance. Exceedance of the critical load of S acidity for aquatic ecosystems under the SSWC model is defined as

$$Ex(S_{dep}) = S_{dep} - CL(A) \quad (10)$$

Where S_{dep} is the sum of deposition of all forms of S, where each mole of S is treated as SO_4^{2-} (i.e. two equivalents per mole of S deposited). Exceedances of acidity are defined as instances where the addition of acidity in the form of S exceeds the net buffering capacity. In contrast, under the SSMB and FAB models there is no unique amount of S and N to be reduced to reach non-exceedance; Exceedance for a given S and N deposition pair is the sum of the S and N deposition reductions required to reach the critical load function (CLF) by the 'shortest' path (Figure 1). The computation of the exceedance function followed the methodology described in CLRTAP (~~2004, 2016, 2017). In some instances, S deposition (or N) must be reduced to achieve non-exceedance.~~2017).

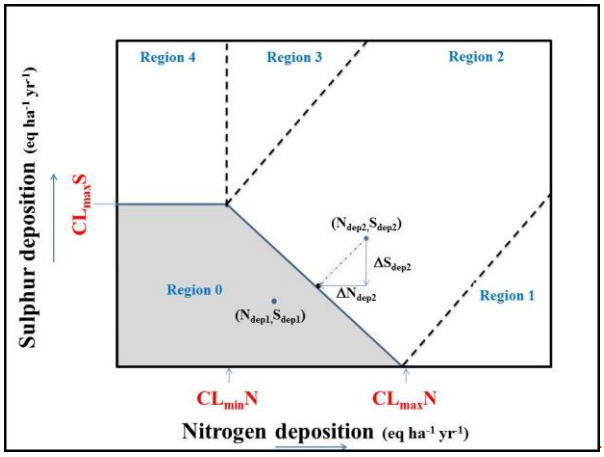

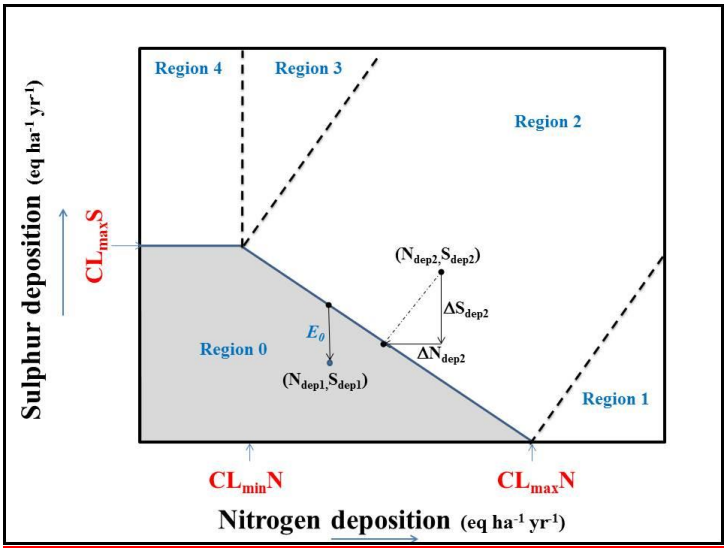

Figure 1. Critical Load Function, showing exceedance Regions 1 through 4 and the "below exceedance" region 0.

Region 0 in Figure 1 denotes ~~ecosystems~~cases for which S_{dep} and N_{dep} to an ecosystem are *below* exceedance levels (i.e. deposition does not exceed critical load). For this region, we introduce a term E_0, a negative number indicating the proximity of deposition in region 0 to the nearest bordering exceedance region. Exceedances are calculated as follows:

$$Ex(N_{dep}, S_{dep}) = \begin{cases} E_0 & (S_{dep}, N_{dep}) \in Region\ 0 \\ N_{dep} - CL_{max}(N) + S_{dep} & (S_{dep}, N_{dep}) \in Region\ 1 \\ N_{dep} - N_0 + S_{dep} - S_0 & (S_{dep}, N_{dep}) \in Region\ 2 \\ N_{dep} - CL_{\min}(N) + S_{dep} - CL_{max}(S) & (S_{dep}, N_{dep}) \in Region\ 3 \\ S_{dep} - CL_{max}(S) & (S_{dep}, N_{dep}) \in Region 4 \end{cases} \quad (11)$$

For Region 2, the exceedance is defined with respect to the closest point between the diagonal line joining the points ($CL_{min}(N)$,$CL_{max}(S)$) and ($CL_{max}(N)$,0)), defined via:

$$N_0 = \frac{N_{dep} + mS_{dep} + m^2 CL_{max}(N)}{1+m^2} \quad (12)$$

$$S_0 = m(N_0 - CL_{max}(N)) \quad (13)$$

where

$$m = \frac{CL_{max}(S)}{CL_{min}(N) - CL_{max}(N)} \quad (14)$$

We define here E_0, a negative quantity defining the ~~minimum distance below~~smallest decrease in deposition from the critical load function (i.e. the boundary between the exceedance ~~lines from the~~ and non-exceedance regions of Figure 1) to reach the N_{dep}, S_{dep} point on Figure 1~~:~~.

~~$E_0 = \max[(S_{dep} - S_A), (N_{dep} - N_A)]$~~ ~~(15)~~

~~where~~

~~$S_A = \begin{cases} CL_{max}(S) & N_{dep} < CL_{min}(N) \\ m(N_{dep} - CL_{max}(N)) & CL_{min}(N) \le N_{dep} < CL_{max}(N) \end{cases}$~~ ~~(16)~~

~~$N_A = \frac{S_{dep}}{m} + CL_{max}(N)$~~

$$E_0 = \begin{cases} S_{dep} - CL_{max}(S) & for\ N_{dep} \le CL_{min}(N) \\ S_{dep} - m(N_{dep} - CL_{max}(N) & for\ CL_{min}(N) < N_{dep} < CL_{max}(N) \end{cases} \quad (15)$$

For deposition levels *below* exceedance, i.e. within the grey region of Figure 1, the value of E_0 describes the proximity to exceedance; the fastest path by which exceedance could occur, relative to current deposition levels. Given that equation (2) guarantees that the slope of the line joining ($CL_{min}(N)$,$CL_{max}(S)$) and ($CL_{max}(N)$,0) will always have an inclination of less than 45°, the shortest path to exceedance will always be via the S_{dep} path. E_0 is of potential interest to policymakers, in that this term describes the proximity of regions which are not yet in exceedance of critical loads to exceedance. Small magnitude values of E_0 thus describe ecosystems for which small increases in S_{dep} or N_{dep} may result in exceedances of critical loads. We also note that equations 11-14 themselves are a slight simplification for the FAB model, which allows for a slight inclination of the CLF for $N_{dep} < CL_{min}(N)$.

Three different sources of critical load data were used in this work. We begin with Canada-wide critical loads of acidity, which employ modifications to the above UNECE methodology (CLRTAP, ~~2004~~2017), used in eastern North America (NEG-ECP, 2001, Ouimet, 2005), and then expanded across Canada (Carou *et al.*, 2008; Jeffries *et al.*, 2010; Aherne and Posch, 2013). We follow with more recent estimated critical loads determined using the UNECE ~~protocols~~methodologies, for terrestrial ecosystems for the province of Alberta (Aklilu~~, 201x~~ *et al.*, 2018), and aquatic ecosystems in northern Alberta and Saskatchewan (Cathcart *et al.*, 2016).

2.~~1~~3.2 Canada-wide Critical Loads of Acidity: Lakes and Forest Soils

The earliest critical load data used in the current work are for forest and lake ecosystems, and resulted from updates to Environment and Climate Change Canada databases, subsequent to the publication of the Canadian Acid Deposition Science Assessment (ECCC, 2004; Jeffries and Ouimet, 2005).

Lake chemistry surveys were conducted in Canada in order to obtain data for critical load estimates (Jeffries *et al.*, 2010). Critical loads of acidity for each sampled lake were estimated using the SSWC model (Henriksen and Posch, 2001). In addition to the lake survey data, other inputs to the SSWC include ecosystem-specific characteristics that were estimated using a mixture of methods, including broad mineralogical, geological, hydrological and biological surveys~~, and other related information.~~ At the time these aquatic critical load data were collected, acidic deposition estimates at ECCC were

~~conducted~~created using A Unified Regional Air-quality Modelling System (AURAMS; Gong *et al.*, 2006). The critical load values for lakes were therefore gridded to the map of Canada used by the AURAMS model, with a grid-cell resolution of 45 km × 45 km. The SSWC critical load values for each surveyed lake contained within each AURAMS grid-cell were compared – when data from multiple lakes within the same grid cell were available, the ~~lowest~~ fifth percentile of the resulting critical load values was assigned to that grid cell (for grid cells containing ~~smaller numbers of~~less than 20 lakes, the critical load for the most sensitive lake was used~~).~~.). The lake critical load data thus represent the most sensitive lake ecosystems within the given ~~45 km~~^{2} ~~g~~grid cell~~.~~ based on the available data. We note, however, that this procedure used in the creation of this dataset (Jeffries *et al.*, 2010) becomes less accurate as the number of lakes per grid cell becomes small, with either over- or under-estimates of local ecosystem sensitivity. This was one of the factors leading to more recent updates in aquatic critical load maps for Canada, discussed in more detail in section 2.3.4. The ~~data~~resulting 45 km resolution resulting CL maps were subsequently re-mapped to the higher resolution GEM-MACH grid used here; the centroids of those 2.5 km GEM MACH grid-cells falling within the AURAMS lake critical load polygons were assigned the corresponding AURAMS grid critical load values. The resulting critical loads are shown in Figure 2 (a), with red values indicating the most sensitive ecosystems and blue values indicating the least sensitive ecosystems. AURAMS cells for which no lake information was available were assigned "null" values (shown in grey). These critical load data identified lake ecosystems in north-eastern Alberta, northern Saskatchewan, and north-western Manitoba as particularly sensitive to acidifying precipitation.

The forest ecosystem critical loads used here began with provincial and regional surveys that were combined to form a unified Canada-wide critical load dataset (Carou *et al.*, 2008). Critical load and exceedance of S and N were estimated for forest soils following the methodology and guidelines established by the NEG-ECP (NEG-ECP 2001, Ouimet 2005), which largely follow the UNECE methodology (CLRTAP, ~~2004, 2016,~~ 2017). The long-term critical load was estimated using SSMB model; the key spatial data-sets (or base maps) or formulae required ~~as inputs~~for calculating critical loads are atmospheric deposition, base cation weathering rate and a critical base cation to aluminum ratio (used to calculate critical alkalinity leaching~~.~~). Average annual total (wet plus dry) atmospheric base cation deposition data during the period 1994–1998 was estimated using observed wet deposition, observed air concentrations, and modelled meteorological data along with land-use specific dry deposition velocities, and mapped on the Global Environmental Multiscale (GEM) grid at a resolution of 35 km × 35 km (see Section 2.~~2~~1 for details on GEM and its companion on-line chemistry module, GEM-MACH). Under the NEG-ECP ~~protocol~~methodology, weathering rates were estimated using a soil type–texture approximation method (Ouimet, 2005). The approach estimates weathering rate from texture (clay content) and parent material class. This method was used in conjunction with the Soil Landscapes of Canada (SLC, version 2.1) to estimate base cation weathering rates across western Canada. Under the NEG-ECP (2001) ~~protocol~~methodology, several simplifying assumptions and/or specified functions and values were applied to terms in equations (1) through (4): (a) a critical $Bc{:}Al$ molar ratio of 10, and a K_{gibb} of 3000.0 $m^6\ mol_{charge}^{-2}$ were used, (b) harvesting removals were not considered; therefore, long-term net uptake N_u and Bc_u were set to zero, (c) ~~denitrification and~~ as in section 2.3.3, net N immobilization (N_i) was

Formatted: English (U.K.)

Formatted: Font: Italic

Formatted: Font: Italic

Formatted: Font: Italic

Formatted: Font: Italic

Formatted: English (U.K.)

Formatted: English (U.K.)

Formatted: English (U.K.)

~~assumed to occur, but at an invariant low level appropriate for well-drained upland forest ecosystems (both N, and the~~ based on a 50 cm depth rooting and assumed to be equivalent ~~of the $(CL_{max}(S)/(1-f_{de}))$ term of equation (2) were set to~~ to 0.5 kg N ha^{-1} yr^{-1} (35.7 eq ha^{-1} yr^{-1}~~),~~) (CLRTAP, 2017) , (d) ~~the~~ denitrification (N_{de}) was also set to 0.5 kg N ha^{-1} yr^{-1} (35.7 eq ha^{-1} yr^{-1}) following recommendations in CLRTAP (2017) and Aherne and Posch (2013) as an upper limit for well-drained soils, (e) the deposition of Cl ions was assumed to be zero, ~~and (e~~(f) the weathering release of soil base cations (BC_w) was assumed to be dependent on temperature, (g) Bc_w was assumed to be equal to 0.75 BC_w, and (h) Bc_{dep} was assumed to be equal to 0.75 BC_{dep}. The net critical load functions for the forest ecosystems with these simplifications becomes:

$$CL(S+N) = BC_{dep} + BC_w(T) + Q^{\frac{2}{3}}\left[\frac{3}{2}\left(\frac{Bc_w(T)+Bc_{dep}}{(Bc:Al)_{crit}K_{gibb}}\right)\right]^{\frac{1}{3}} - \frac{3}{2}\left(\frac{Bc_w(T)+Bc_{dep}}{(Bc:Al)_{crit}}\right) + 2\,(35.7)$$

~~(17~~$\left[\frac{3}{2}\left(\frac{0.75(BC_w(T)+BC_{dep})}{3x10^4}\right)\right]^{\frac{1}{3}} + \frac{3}{2}\left(\frac{0.75(BC_w(T)+BC_{dep})}{10}\right) + 71.4$ (16)

With

$$BC_w(T) = BC_w e^{\left[3600\left(\frac{1}{281}-\frac{1}{274+T}\right)\right]} e^{\left[3600\left(\frac{1}{281}-\frac{1}{274+T}\right)\right]}$$ (~~18~~17)

Where T is the temperature in degrees C~~, and $Bc_w = 0.75\ BC_w$~~. (NEG-ECP, 2001, Nasr *et al.*, 2010, Whitfield *et al.*, 2010, Aherne, 2011).

The resulting critical load values were referenced to the corresponding GIS polygons under the SLC containing that soil type, resulting in a Canada-wide map of forest soil critical loads for acidity. These polygons were superimposed on the map of GEM-MACH 2.5 ~~km~~^{2}km x 2.5 km resolution grid cells. Similar to the approach for lake critical loads described above, the ~~lowest~~ 5th percentile value from the forest critical load polygons existing within each GEM-MACH grid cell was assigned to that grid cell. The forest soil critical load values on the resulting GEM-MACH grid cell thus represent the most sensitive forest ecosystems within that grid cell. Polygons for which forest soils were not present were assigned "null" values. Under the NEG-ECP ~~protocol~~methodology (NEG-ECP, 2001) critical loads were simplified ~~for acidic~~ deposition ~~(S_{dep} + N_{dep}),~~of sulphur and nitrogen, as such exceedance was defined for combined deposition:

$$Ex(N_{dep}, S_{dep}) = S_{dep} + N_{dep} - CL(S+N)$$ (~~19~~18)

We note that equation (18), which follows the NEG-ECP methodology (Ouiment, 2005) may lead to potential errors at very low values of N_{dep}, in that the nitrogen sinks could potentially compensate sulphur deposition. To avoid that possibility, we have added the caveat to equation (16) that the rightmost term is replaced by the minimum of 71.4 eq ha^{-1} yr^{-1} and N_{dep} (that is, the calculated nitrogen sink will not be used to compensate S_{dep}, in the event that N_{dep} is below the sum of nitrogen immobilization and denitrification (71.4 eq ha^{-1} yr^{-1})). In our application of this methodology (see section 3.6.1), this additional correction was found to bring areas which were already below exceedance further below exceedance, but had no impact on the estimate of the size areas over exceedance, to three significant figures.

Formatted: English (U.K.)

Formatted: English (U.K.)

Formatted: Font: Italic

The resulting critical load map for forest soils for the first of these approaches is shown in Figure 2(b), with the same colour scale as Figure 2(a). The lake ecosystems can be seen to be more sensitive to acidic deposition compared to forest soil ecosystems (lower critical load values, red shades in Figure 2).

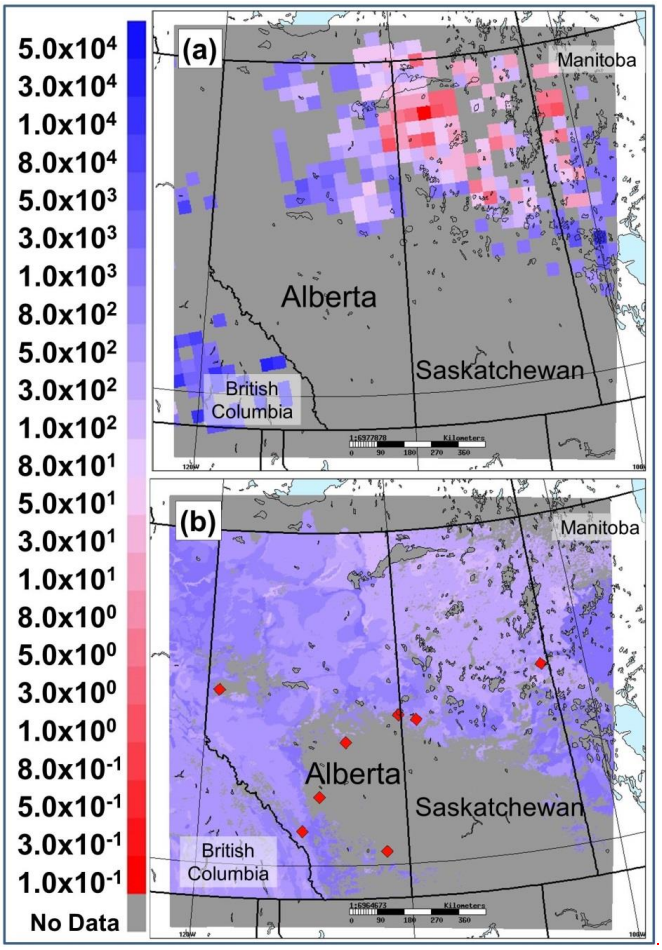

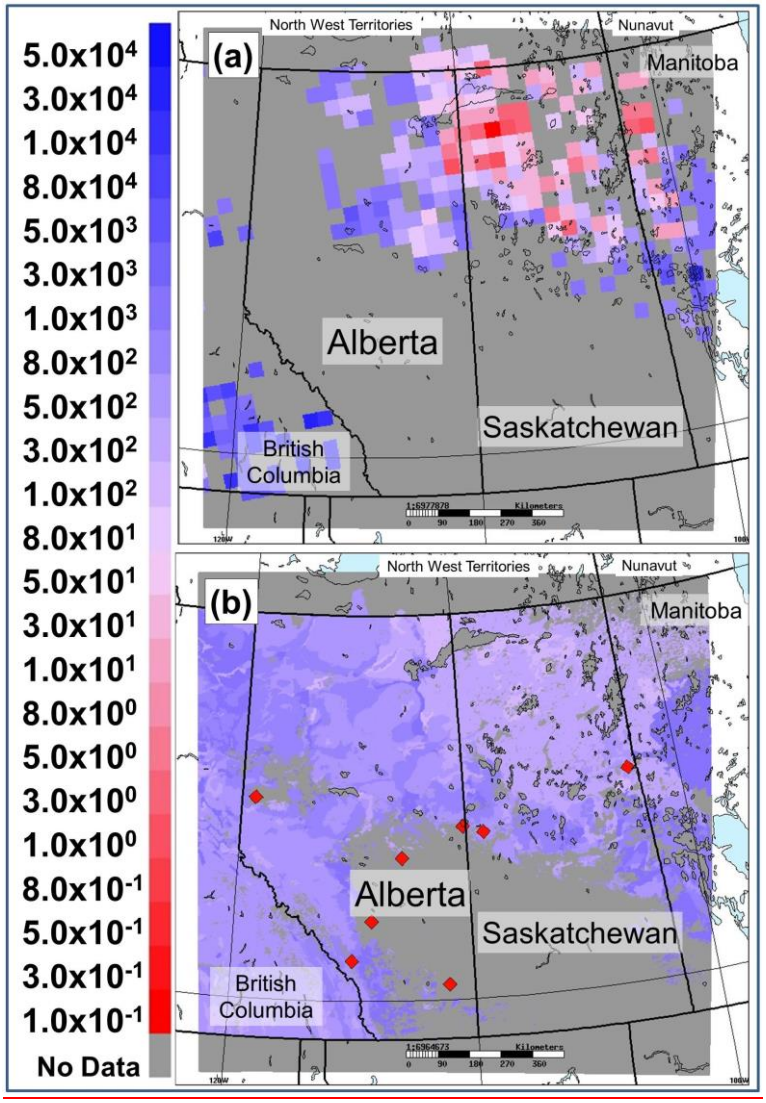

Figure 2. Critical loads of acidity on the 2.5km GEM-MACH domain, based on a Canada-wide implementation: (a) ~~Lake~~ (~~S_{dep}~~Critical load for acidity (eq. 5) and (b) Forest (~~S_{dep} + N_{dep}~~) ecosystems (eq. 18) (eq ha^{-1} yr^{-1}). Forest values were calculated using 1994-1998 interpolated/extrapolated BC_{dep} observations (diamonds show the location of those Canada-wide stations used to estimate BC_{dep}, which reside within the 2.5km resolution model domain). Red regions (low numbers) on the scale have the lowest critical loads, hence are the most sensitive to deposition. No Data: (a) No lake observations were available in the given 45 x 45 km grid cell; (b) No forest data were available and/or the "No Data" regions were not forested".

Later in this work, we discuss the effect of ~~permutations on~~different estimates of the assumed level of atmospheric base cation deposition in the above calculations towards the resulting estimates of critical load and critical load exceedances.

2.~~1~~3.3 Province of Alberta: Critical Loads of Acidity for Terrestrial Ecosystems

The SSMB model was used to estimate $CL_{max}(S)$, $CL_{max}(N)$, and $CL_{min}(N)$, for terrestrial ecosystems in the province of Alberta following methods recommended under the Convention on Long-Range Transboundary Air Pollution (CLRTAP, ~~2016,~~ 2017). Critical loads were not derived for areas comprising cultivated or agricultural land, rock, and exposed or developed soil. Our initial estimate of non-marine annual base cation deposition (BC_{dep}) was the interpolated/extrapolated 1994-1998 base cation database described above. The release of base cations as a result of chemical dissolution from the soil mineral matrix (BC_w) followed the soil texture approximation method (equation ~~18~~17), with soil information vertically weighted to a rooting depth of 50 cm to create a homogeneous soil layer for calculations. Soil information for this calculation was obtained from the Soils Landscape Canada version 3.2 database (AAFC, 2010). The average base cation removal in harvested biomass (Bc_u) was calculated using the Alberta Vegetation Index dominant forest cover database to determine type and distribution of forests (ABMI, 2010), harvest information (AAF, 2015), and information on nutrient uptake by forest type (Paré *et al.*., 2012). For unmanaged ecosystems (i.e. not harvested) Bc_u was set to zero, and the removal of biomass due to grazing in grasslands was set to 8 eq ha^{-1} yr^{-1}. The acid neutralization capacity leaching ($ANC_{le,crit}$) was determined using critical Bc:Al ratios applied by vegetation type (a $(BC:Al)_{crit}$ ratio of 6 was used for Mixed Forest, Shrubland and Broadleaf Forest, while Coniferous Forest and Grassland made use of ratios of 2 and 40, respectively). The denitrification fraction (f_{de}) was assigned using a seven level scale (AAFC, 2010; CLRTAP, ~~2016,~~ 2017). f_{de} values for "very rapid", "well", "moderately well", "imperfectly", "poorly", and "very poorly" drained ~~soils~~soil were respectively 0.0, 0.1, 0.2, 0.4, 0.7, and 0.8. The long-term net immobilization of N in the 50 cm depth rooting zone was assumed to be 0.5 kg N ha^{-1} yr^{-1} (35.7 eq ha^{-1} yr^{-1}) (CLRTAP, ~~2016,~~ 2017). The average removal of N from an ecosystem (N_u) followed Pregitzer *et al.* (1990), using Alberta Vegetation Index dominant forest cover data to identify the type and distribution of forests (Alberta, 2016), and nutrient information from the Canadian Tree Nutrient Database (Paré *et al*., 2012). For grasslands the value of N_u was set to 43 eq ha^{-1} yr^{-1} to account for nitrogen removal due to grazing.

The resulting maps for $CL_{max}(S)$, $CL_{max}(N)$, and $CL_{min}(N)$ for Alberta Terrestrial Ecosystems are shown in Figure 3 (using the same colour scale as Figure 2). $CL_{max}(S)$ and $CL_{max}(N)$ values (Figure 3(a)) are lower than the forest critical load values created under the NEG-ECP (2001) ~~protocol~~methodology (Figure 2(b)), reflecting the more detailed treatment of the acid neutralizing capacity term, and the impacts of harvesting on estimated critical loads. NEG-ECP (2001) ~~protocol~~methodology critical load estimates were intended as "upper limits", that is, they were expected to underestimate ecosystem sensitivity, relative to the more detailed calculation used in the creation of Figure 3.

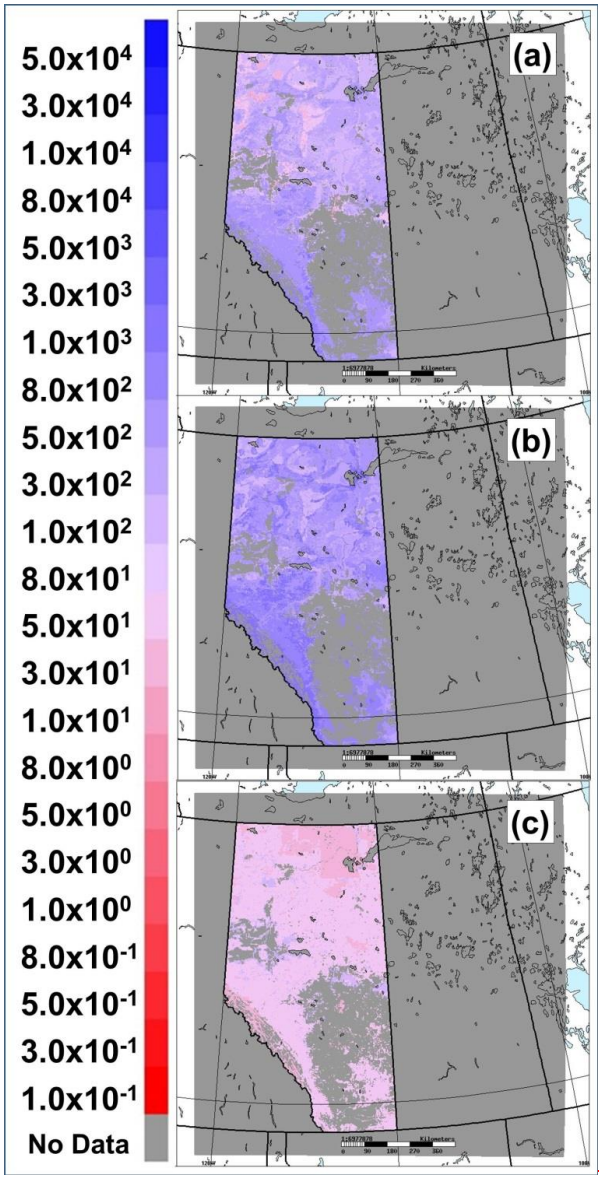
5.0x10^4
3.0x10^4
1.0x10^4
8.0x10^4
5.0x10^3
3.0x10^3
1.0x10^3
8.0x10^2
5.0x10^2
3.0x10^2
1.0x10^2
8.0x10^1
5.0x10^1
3.0x10^1
1.0x10^1
8.0x10^0
5.0x10^0
3.0x10^0
1.0x10^0
8.0x10^-1
5.0x10^-1
3.0x10^-1
1.0x10^-1
No Data
(a)
(b)
(c)

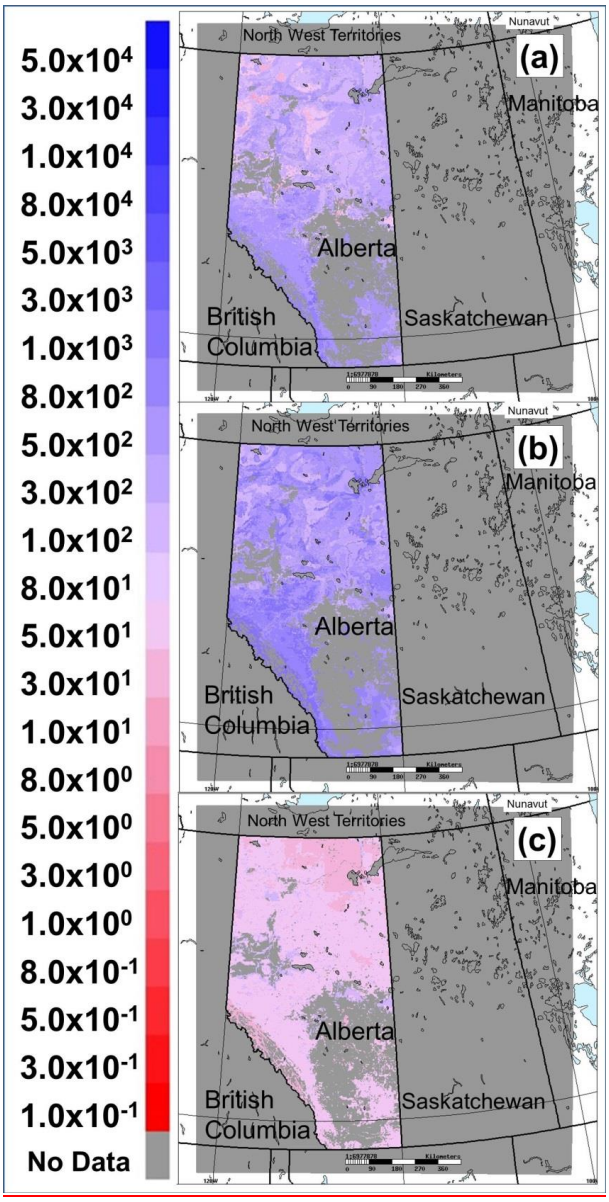

Figure 3. Critical loads of acidity with respect to sulphur and nitrogen for terrestrial ecosystems, Province of Alberta implementation (eq ha^{-1} yr^{-1}), using BC_{dep} from interpolated/extrapolated 1994-1998 observations. (a) Maximum critical load for

sulphur. (b) Maximum critical load for nitrogen. (c) Minimum critical load for nitrogen. No Data: data was only collected within the province of Alberta (outside of Alberta, no data reflects the limitation of data collection); within Alberta, data was only collected for natural terrestrial ecosystems (no data within Alberta thus refers to landscapes modified by human activities such as agriculture).

2.~~1~~3.4 Northern Alberta and Saskatchewan: Critical Loads of Acidity for Aquatic Ecosystems

The critical load data for lake ecosystems described in Section 2.~~1~~3.2 were updated for aquatic ecosystems in northern Alberta and Saskatchewan,as part of an ongoing project to update previous Canada-wide critical load data, following the full UNECE ~~protocols~~methodologies (equations 1 through ~~16~~14, with the addition of our equation 15), resulting in new spatially georeferenced critical load maps for acidity with respect to S_{dep} and $S_{dep} + N_{dep}$ (equations (1-~~9,17,18~~10,11-15) respectively).

Formatted: Font: Italic

Formatted: Font: Italic

Water chemistry from 2409 observations of 1344 lakes were used to produce ~~predictive~~ maps of lake concentrations for ~~four~~three target variables across northern Alberta and Saskatchewan for the determination of critical loads: base cations (BC), dissolved organic carbon (DOC) and sulphate (SO_4^{2-}). A regression kriging approach was used to generate (predict) water chemistry for 137,587 lake catchments following Cathcart *et al*. (2016). Regression kriging is a spatial interpolation method wherein a regression of the target variable on covariate variables (e.g., landscape characteristics such as soil, climates, vegetation; a total of 185 covariates were included) is combined with kriging on the regression residuals (Hengl *et al*., 2007; Hengl, 2009). The water chemistry (target variable) data were obtained from Environment and Climate Change Canada's Level 1 and 2 monitoring networks in Saskatchewan, Alberta and the Northwest Territories (Jeffries *et al*., 2010), lake surveys undertaken by the Government of Saskatchewan (Scott *et al*., 2010), the RAMP monitoring network in Alberta (RAMP, 2016), and from the Alberta Environment and Parks surface water quality data portal (Alberta Environment and Parks, 2016). Critical loads of acidity for lakes were calculated from the predictive maps of lake concentration using the SSWC and the FAB models. As previously noted, the FAB model extends the SSWC model to consider terrestrial and aquatic sources and sinks of S and N, similar to the SSMB (Henriksen and Posch, 2001; Posch *et al*., 2012). A variable ANC_{limit} was used, adjusted for the strong acid anion contribution from organic acids (DOC) after Lydersen *et al*. (2004). Long-term normals for catchment runoff (Q) were estimated from meteorological data and soil properties using a model similar to MetHyd (a meteo-hydrological model; Slootweg *et al*.,2010). Long-term (1961–90) average monthly temperature, precipitation and cloudiness were derived from a 0.5° × 0.5° global database (Mitchell *et al*., 2004). Default net mass transfer coefficients for N (6.5 m a^{-1}) and S (0.5 m a^{-1}) were applied to all lakes (Kaste and Dillon, 2003; Baker and Brezonik, 1988). Nitrogen immobilization in catchment soils was set at 0.5 kg N ha^{-1} yr^{-1} (35.7 eq ha^{-1} yr^{-1}) following the Mapping Manual (CLRTAP ~~2004~~2017). The denitrification fraction in the catchment soils was estimated as $f_{de} = 0.1 + 0.7 \cdot f_{peat}$, where f_{peat} is the fraction of wetlands in the terrestrial catchment; landcover fractions of peat were obtained from the 2010 USGS North American Landcover database (USGS, 2013). Nitrogen removal in harvested biomass was estimated using biomass and species composition obtained from the National Forest Inventory (Beaudoin *et al*., 2014) in combination with nutrient concentrations from the Canadian Tree Nutrient Database (Paré *et al*., 2012) and the Tree Chemistry Database (Pardo *et al*., 2005).

The resulting *CL(A), $CL_{max}(S)$,$CL_{max}(N)$ and $CL_{min}(N)$* maps created using the above data (Figure 4) cover much of the same region as depicted in Figure 2(a). Figures 2, 3 and 4 have matching colour scales, showing the relative sensitivity of the different ecosystems estimated using the critical load calculation ~~protocols~~methodologies employed in each data set. The lakes and aquatic ecosystem data, shown in Figure 2(a) and Figure 4, are in general more sensitive to acidifying deposition than the forest (Figure 2(b)) and terrestrial ecosystem data (Figure 3), a theme which recurs in our subsequent calculation of critical load exceedances (Section 3.6).

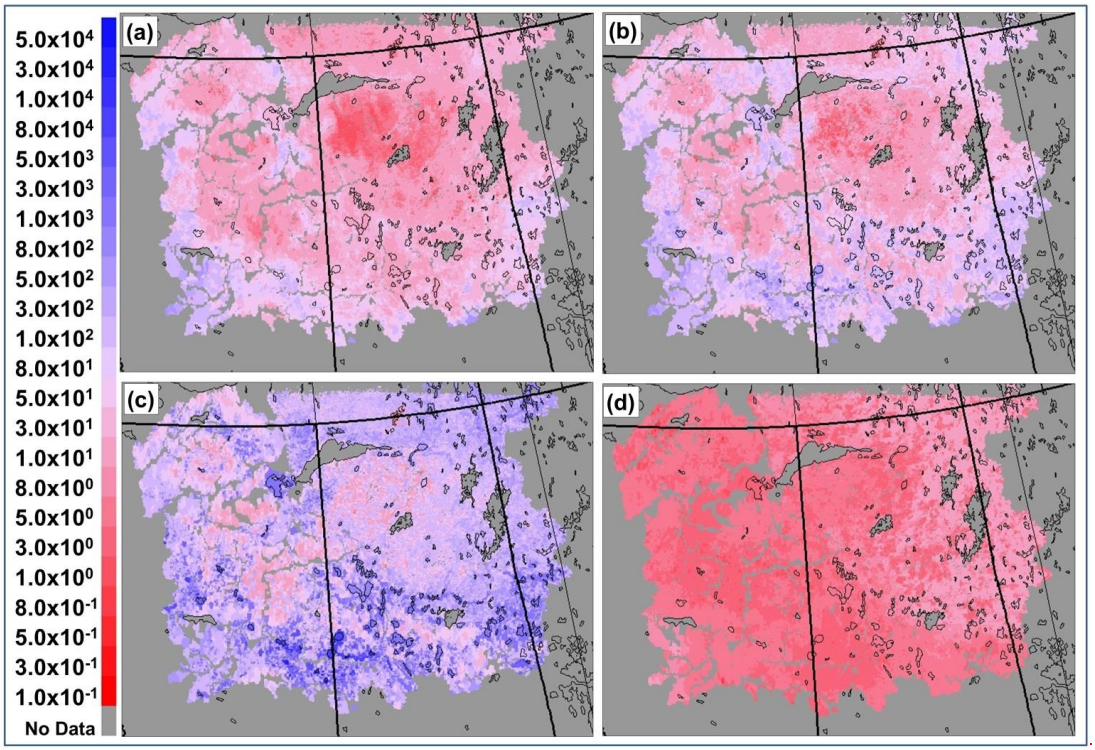
5.0x10^4
3.0x10^4
1.0x10^4
8.0x10^4
5.0x10^3
3.0x10^3
1.0x10^3
8.0x10^2
5.0x10^2
3.0x10^2
1.0x10^2
8.0x10^1
5.0x10^1
3.0x10^1
1.0x10^1
8.0x10^0
5.0x10^0
3.0x10^0
1.0x10^0
8.0x10^-1
5.0x10^-1
3.0x10^-1
1.0x10^-1
No Data
(a)
(b)
(c)
(d)

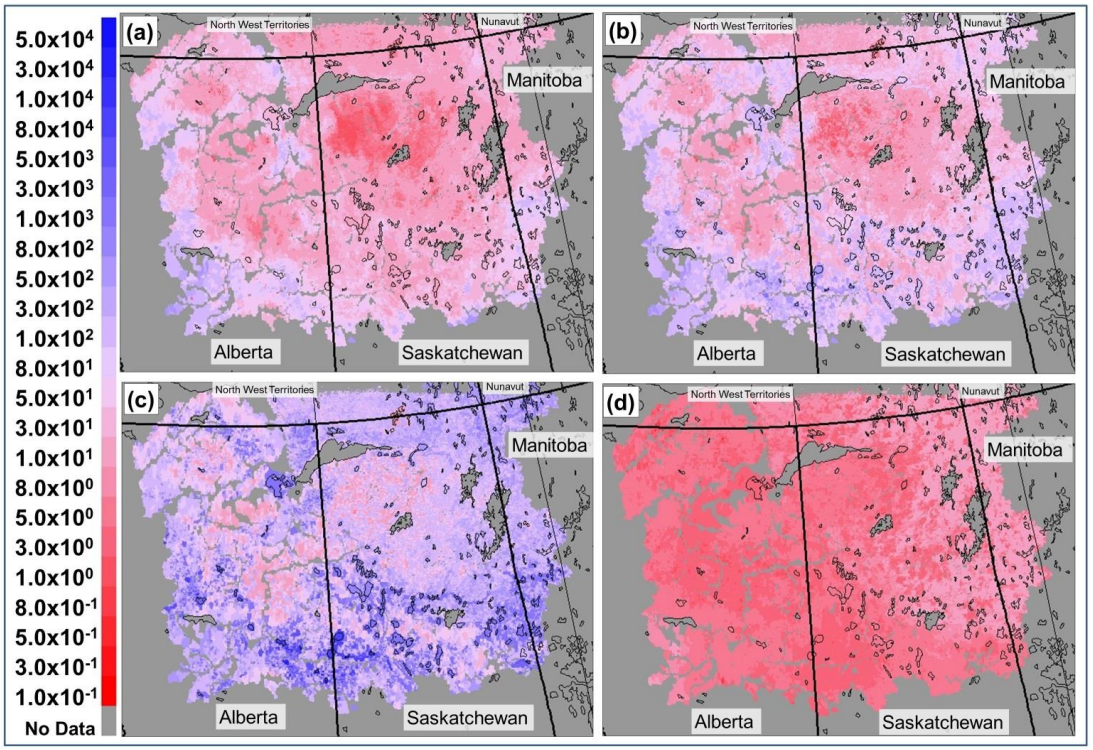

Figure 4. Critical loads of acidity with respect to S_{dep} ($CL(A)$), and S_{dep} ~~+~~ *and* N_{dep}; (FAB model) for aquatic ecosystems (eq ha^{-1} yr^{-1}). (a) $CL(A)$ (b) $CL_{max}(S)$. (c) $CL_{max}(N)$. (d) $CL_{min}(N)$.

~~2.2 Global Environmental Multiscale – Modelling Air-quality and CHemistry (GEM-MACH) , Version 2~~

~~2.2.1 GEM-MACH v2 Overview~~

~~GEM-MACH is Environment and Climate Change Canada's comprehensive chemical reaction transport model. The model follows the on-line paradigm (in that atmospheric chemistry modules have been incorporated directly into a weather forecast model (GEM) (Moran *et al.*, 2010; Makar *et al.*, 2015 (a,b)). The parameterizations include gas phase chemistry (42 species, ADOM-II mechanism, Stockwell *et al.*, 1989), aerosol microphysics (Gong *et al.*, 2003(a,b)) and cloud processing of gases and aerosols including uptake and wet deposition (Gong *et al.*, 2006; Gong *et al.*, 2015). The model's aerosol size distribution makes use of the sectional (bin) approach, with two possible configurations: (1) a processing-time efficient two-bin configuration used for operational forecasting and longer scenario simulations (fine and coarse particle sizes are subdivided within certain aerosol microphysics processes in order to preserve solution accuracy while minimizing advective~~

transport time) and (2) a more detailed 12-bin size distribution used to more accurately simulate aerosol microphysics and the size spectrum of particles. The aerosols in GEM-MACH are also speciated chemically into particle sulphate, nitrate, ammonium, primary organic aerosol, secondary organic aerosol, elemental (aka "black") carbon, sea salt and crustal material, within each size bin. The crustal material component includes all particulate matter not speciated under the other components, and hence includes base cations as a fraction of its total mass. As will be discussed below, the observations of Wang *et al.* (2015) were used to approximate the base cation fraction of GEM-MACH's crustal material, and hence estimate the mass of base cation deposition predicted by the model.

A comparison of GEM-MACH version 1.5.1 against other peer-on-line models appears elsewhere (Makar *et al.*, 2015(a,b)), as does a description of the main updates associated with version 2 of the model (Makar *et al.*, 2017). Comparisons of the operational 2-bin version of the model against observations have also appeared in the literature (Pavlovic *et al.*, 2016; Munoz-Alpizar *et al.*, 2017). Our description below will focus on the model's modules for gas-phase dry deposition, particle phase dry deposition, cloud processing and aqueous phase chemistry (wet deposition)..

2.2.2 Gas-phase dry deposition in GEM-MACH

A detailed description of the gas phase dry deposition module of GEM-MACH (with an emphasis on the chemical species which contribute to S_{dep} and N_{dep}) appears in the Supplementary Information; here we provide an overview. Gas-phase deposition is handled using the commonly used "resistance" approach, where the deposition velocity is the inverse of the sum of aerodynamic, quasi-laminar sublayer and net canopy resistances. The aerodynamic resistance is the same for all gases, the quasi-laminar sublayer resistance depends on gas diffusivity, but these terms are relatively minor compared to the net canopy resistance, which tends to control the deposition velocity for many of the gases (notable exceptions being HNO_3 and NH_3 which have a relatively low canopy resistance). The net canopy resistance follows the approach of Wesely (1989) and Jarvis (1976), with terms for the resistance contributions associated with deposition to plant stomata, mesophyll, and cuticles, the resistance of gases to buoyant convection, the resistance associated with leaves, twigs, bark and other exposed surfaces in the vegetated canopy, the resistance associated with the height and density of the vegetated canopy, and the resistance associated with soil, leaf litter, etc., at the surface. The net canopy resistance includes a term to account for the impact of precipitation and high humidity on stomatal and mesophyll resistances, and a temperature dependent correction term for snow-covered surfaces.

Soil resistances are calculated following Wesely (1989) with a parameterization based on the values for SO_2 and O_3, with a seasonal dependence (Midsummer, Autumn, Late Autumn, Winter and Transitional spring). Canopy resistances are based on Zhang *et al.* (2003), with the same seasonality as above. The resistance for the lower canopy follows Wesely (1989) using a function of the effective Henry's law constant and terms for SO_2 and O_3 resistances. The mesophyll and cuticle resistances follow Wesely *et al.* (1989), with seasonal variations as above and vegetation dependent leaf area index values. The resistance of gases to buoyant convection follows Wesely *et al.* (1989), and is a function of the visible solar radiation. The stomatal resistance follows a similar approach to Jarvis (1976), Zhang *et al.* (2002, 2003), Baldocchi *et al.* (1987), and

Formatted: Font: Italic

Formatted: Font: Italic

ValMartin *et al.* (2014), and results from several terms describing its dependence on light ($k_s(Q_p)$), water vapour pressure deficit ($k_s(\delta e)$), temperature (k_{st}), CO_2 concentration (k_{sca}), the leaf area index (LAI) , and the ratio of the molecular diffusivities of water to the gas being deposited ($\frac{D_{H2O}}{D_{gas}}$). The approach taken for the dependence on light provides stomatal resistance values similar to those of Baldocchi *et al.* (1987), but are lower than those of Zhang *et al.* (2002) for the same vegetation types, decreasing stomatal resistances and thus increasing the stomatal resistance contribution to deposition velocities, relative to Zhang *et al.* (2002). The other terms in the stomatal resistance employed curve fitting where possible across different sources of deposition data, due to the wide variation noted in the underlying measurement literature.

Deposition velocities are calculated for the S_{dep} and N_{dep} contributing gases SO_2, H_2SO_4, NO, NO_2, HNO_3, PAN, HONO, NH_3, organic nitrates, as well as several other transported gases of the ADOM-II gas phase mechanism. We note that the rapid conversion of gaseous sulphuric acid (H_2SO_4) to particulate sulphate due to its low vapour pressure ensures that the direct contribution of H_2SO_4 deposition to S_{dep} is relatively minor. Further details on the deposition velocity formulation, and tabulated coefficients for the species contributing to S_{dep} and N_{dep}, appear in the Supplementary Information..

Gas phase dry deposition velocities are incorporated as a flux lower boundary condition in the solution of the vertical diffusion equation within GEM-MACH.

2.2.3 Particle phase dry deposition in GEM-MACH

Particle dry deposition in GEM-MACH makes use of the size-segregated formulation of Zhang *et al.* (2001), which in turn follows Slinn (1982). The gravitational settling velocity (a function of the particle density, wet diameter, air viscosity, and the temperature and air pressure) is calculated for each particle size at each model level. At the lowest level, the settling velocity is added to the inverse of the sum of the aerodynamic resistance above the canopy and the surface resistance. The aerodynamic resistance is a function of atmospheric stability, surface roughness, and the friction velocity, while the surface resistance is the inverse of the sum of collection efficiencies for Brownian diffusion, impaction and interception, multiplied by correction factors to account for the fraction of particles which stick to the surface. The Brownian diffusion is a function of the Schmidt number of the particle (ratio of the kinematic viscosity of the air to the particle's Brownian diffusivity). The impaction term is dependent on the Stokes number (itself a function of the gravitational settling velocity) and the land use type, and the interception term is taken to be a simple function of the particle diameter and a land use and seasonal dependent characteristic radius.

The resulting deposition velocities have the characteristic strong dependence on particle size noted in observations, with minimum deposition values occurring at particle diameters of about 1 μm, with an increase in deposition velocities of up to two orders of magnitude with decreasing or increasing particle size. As will be discussed later in this work, one of the consequences of the size dependence of particle deposition velocity is that particles which are larger (or smaller) than 1 μm diameter settle more rapidly than the latter particles, and hence have shorter transport distances than 1 μm diameter particles.

This phenomena is responsible for the rapid decrease in surface deposition with increasing distance from sources of base cations.

Particle gravitational settling and deposition velocities are handled in this version of GEM-MACH using a semi-Lagrangian advection approach in the vertical for each column; vertical backtrajectories are calculated from the settling and deposition velocities, and mass-conservative interpolation is used to determine the new concentration profile and the flux to the surface. The particle deposition component of S_{dep} and N_{dep} (via the deposition of particle sulphate, particle nitrate, and particle ammonium) is typically very small compared to the gaseous dry deposition of primary emitted gases (SO_2, NO_2, NH_3), secondary gases (HNO_3), and wet deposition of ions (HSO_3^-, SO_4^{2-}, NO_3^-, NH_4^+).

2.2.4 Cloud processing of gases and aerosols, and inorganic particle chemistry in GEM-MACH

The cloud chemistry and aqueous processing of gases and aerosols in GEM-MACH makes use of the methodologies used in GEM-MACH's precursor model, A Unified Regional Air-quality Modelling System (AURAMS), and are described in detail in Gong *et al.* (2006). Aqueous chemistry includes the transfer of gaseous SO_2, O_3, H_2O_2, ROOH, HNO_3, NH_3 and CO_2 to cloud droplets, along with the oxidation of S(IV) to S(VI) within the cloud droplets by several pathways. The stiff system of equations described by the aqueous chemistry is solved using a bulk approach and a computationally efficient predictor-corrector algorithm. Aerosol sulphate, nitrate and ammonium may be taken up into cloud droplets following activation, and may be returned to the aerosol phase following aqueous chemistry via particle evaporation. Rebinning of mass transferred back to the particle phase is accomplished through a mass-conservative rebinning algorithm similar to that described in Jacobson (2003).

Wet deposition processes (tracer transfer from cloud droplets to raindrops, scavenging of aerosols and soluble gases by falling hydrometers, downward transport by precipitation, and evaporation of raindrops and potential loss of mass prior to deposition) are explicitly included in GEM-MACH. Cloud droplet to raindrop tracer transfer is handled using a bulk autoconversion rate obtained from the meteorological model. Impact scavenging of size-resolved aerosols is parameterized using a scavenging rate based on the precipitation rate and the mean collision efficiency. Irreversible cavenging of soluble gases makes use of the Sherwood number and diffusivity of the gas, the precipitation rate, the Reynolds and Schmidt numbers, and the raindrop diameter, while reversible scavenging makes use of equilibrium partitioning.

The cloud fields provided to the aqueous phase chemistry module depend on the model resolution – for the high resolution simulations carried out here, the hydrometeors are explicitly simulated and transported using the 2-moment scheme of Milbrandt and Yao (2005 (a,b)). A full description of the cloud processing model and the formulation of its components appears in Gong *et al.* (2006).

Inorganic particle chemistry makes use of the HETV system of equations for sulphate, nitrate and ammonium described in detail in Makar *et al.* (2003), based on the ISORROPIA algorithms of Nenes *et al.* (1999). The concentrations of particle sulphate, nitrate, ammonium, and gaseous NH_3 and HNO_3 are solved in bulk for non-ideal high concentration solutions via

first determining the chemical subspace in which the total nitrate, sulphate, ammonium and relative humidity resides (breaking the problem into twelve subspaces for the different combinations of gases, salts, and aqueous ions which may exist under those conditions), then solving a double iteration including the full system of equations incorporating activity coefficient calculations and vectorization across the subspaces for computational efficiency. Following the bulk calculations, the resulting aerosol mass of sulphate, nitrate and ammonium are rebinned using an approach similar to that of Gong *et al.* (2006).

2.2.5 Emissions and Simulation Setup

The emissions used in the simulations carried out here are described in detail in Zhang *et al.* (2017, this special issue).

All simulations used a nested model setup, feeding into the meteorological and chemical boundary conditions for a 2.5km resolution Alberta and Saskatchewan simulation. The latter domain is depicted in Figures 2 and 3 (the 2.5km resolution domain is the entire coloured and grey shaded region). Archived GEM 10km forecast simulations were driven by data assimilation analysis fields, and were used to in turn drive successive overlapping 30 hour forecasts of both a Canadian domain 2.5km resolution meteorological forecast, and a 10km GEM-MACH forecast. The final 24 hours of these simulations provided the meteorological and chemical boundary conditions respectively for a series of 24 hour simulations of GEM-MACH on the domain shown in Figures 2 and 3. This nesting approach was selected to provide the best possible meteorological and chemical inputs for the 2.5km high resolution domain. The output from the 24 hour simulations were then brought together to create the continuous time record of concentrations and deposition on the high resolution model grid. Three simulations were carried out with this setup. The first of these is made use of the two aerosol bin configuration of GEM-MACH, for an entire year of simulated chemistry and meteorology (August 1, 2013 to July 31, 2014), in order to obtain a year of model output, required for critical load calculations. The outer 10km North American domain of the simulation made use of the operational GEM-MACH forecast emissions inventories for the years 2010 (Canada), 2011 (USA) and 1999 (Mexico), while the inner nest made use of 2013 (Canada) and 2011 (USA) inventories (see Zhang *et al.*, 2017). The predicted deposition thus represents the model predictions using emissions reported under current Canadian regulatory requirements. Two additional simulations were then carried out, for the period August 13th to September 10th, making use of the 12 bin version of the model: a base case and a primary particulate scenario. The primary particulate scenario made use of aircraft observation based estimates of primary particulate emissions from six oil sands facilities, and both making use of continuous emissions monitoring data for Alberta for SO_2 and NO_x emissions from large stack sources (see Zhang *et al.*, 2017, this issue, for the full description of these emissions). This second pair of simulations was carried out to investigate the potential impact of possible under reporting of primary particulate emissions on model critical load exceedance predictions. About 96% of these primary particulate emissions by mass are associated with fugitive dust emissions sources, and over 68% of this mass is in the coarse mode (diameters greater than 2.5 μm) (Zhang *et al.*, 2017). The potential impact of these sources of base cations on acidifying deposition will be discussed in Sections 3.3, 3.5 and 3.6.

2.3 Deposition Observations

2.3.1 Deposition of ions in precipitation

Wet-only precipitation measurements were collected at six sites in Alberta (AB) by Alberta Environment and Parks and two sites in Saskatchewan (SK) by the Canadian Air and Precipitation Monitoring Network (CAPMoN) (Figure 2(b)). In wet-only samples, a heated precipitation sensor opens the collector lid when precipitation is detected, and closes the lid when precipitation ends. For the SK samples, the collector bucket was lined with a polyethylene bag which was removed, weighed, sealed, refrigerated, and shipped to the laboratory for major-ion analysis. For the AB samples, the samples were transferred from the clean collection bucket to a smaller sample bottle, capped, refrigerated if stored on site, and shipped to the laboratory for analysis. Collection occurred approximately daily at the SK sites and approximately weekly at the AB sites. Quality control was performed by the collecting networks.

Annual precipitation-weighted mean concentrations of SO_4^{2-}, NO_3^- and NH_4^+ were calculated from the daily or weekly samples using recommended methods and completeness criteria (WMO/GAW, 2004, 2015) and the resulting deposition fluxes were compared with model values. Where there were measurement gaps of > 3 weeks (two sites), or where there was only partial coverage of the 12 months (one site), fluxes were compared over shorter measurement periods. The collector buckets described above tend to underestimate the total precipitation, so the flux of ions derived from their records must be corrected using independent observations of total precipitation. At the SK sites, separate on-site rain and snow gauges were used to manually record the daily precipitation amount. At the AB sites, precipitation gauges for independent quantification of total precipitation were not available, hence weekly deposition fluxes were calculated using daily precipitation depth data from the nearest meteorological station, or combination of meteorological stations, with the most complete coverage (ECCC, 2017; AAF, 2017).

Total precipitation depth collected in the AB wet deposition collectors, summed over all collection periods at the sites, was 51-96% of the estimated precipitation depth at meteorological stations. Our deposition flux calculations implicitly assume that the ion concentrations measured in the sample are representative of all the precipitation during the period. However, the mechanism of precipitation loss (undercatch due to wind, evaporative loss, delay in lid opening) may lead to unrepresentative concentration values. Additional uncertainty is introduced by the use of precipitation depth from collectors that are not co-located, particularly at Kananaskis. Therefore, wet deposition fluxes from the AB sites have higher uncertainty than the fluxes at the two SK sites, where 105% and 78% of the standard gauge precipitation was captured by the collector.

2.3.2 Deposition of S and N compounds to snowpack

Observations of total deposition of sulphur, nitrogen, and base cations to snow-covered open surfaces were collected in two separate studies. Samples were collected in the immediate vicinity of the oil sands by Environment and Climate Change Canada, and snowpack samples in northern Saskatchewan were collected by Saskatchewan Environment (snowpack station

locations are discussed in Section 3.4). Both sets of data were collected in open clearings and thus deposition is to snow-covered open surfaces. They thus provide *minimum* estimates of deposition, particularly for gases. One method of accounting for deposition to forests and related vegetation is via collection of precipitation samples below foliage, which assumes that deposited materials leaves the vegetation via precipitation and/or melting of snow, to reach the collector ("throughfall"). Watmough *et al.* (2014) compared winter throughfall versus open deposition in the oil sands region, and showed maximum throughfall values to be about 1.9 times their open deposition counterparts. However, throughfall observations do not account for the portion of the deposited material which remains on or within the vegetated surfaces, and hence must also be considered a conservative estimate of total deposition. Using the algorithms of GEM-MACH's gas-phase deposition module, typical ratios of dry deposition velocity between a needle leaf forest and an open snow covered surface for SO_2 and NH_3 respectively are 2.63 and 1.97 (temperature -5C, u*= 0.1 m s^{-1}, solar radiation = 100 W m^{-2}, z_0 = 0.1m, Monin-Obukhov length = 50). However, the ratios for dry deposition of particles with diameters of 2.5 and 10 μm are 0.76 and 0.82, respectively (Zhang *et al.*, 2001), indicating that the open snowpack observations may slightly overestimate BC_{dep} and Be_{dep} (in contrast to the Watmough *et al.* 2015 observations), but significantly underestimate S_{dep} and N_{dep}.

2.3.2.1 Environment and Climate Change Canada oil sands snowpack sampling

Snowpack sampling: To assess winter-time atmospheric deposition of acidifying emissions to the oil sands region, snowpack samples were collected at varying distances from the major oil sands development area in early spring 2014 (n=130), as well as at 9-12 sites in the Peace-Athabasca River Delta (PAD) located ~200 km north of the major oil sands developments (See Figure 9(a)). Based on historical snow accumulation data for the Fort McMurray region (Environment Canada. National Climate **No Data** and Information Archive), the onset of permanent freezing began on November 6th of 2013, and all samples were collected within an 8-day period ending March 6th, to ensure maximum snowpack depth and minimize snowpack alterations over the course of sampling. Sampling sites were accessed by helicopter, and snow samples were collected at 50-100 m upwind of landing sites, to reduce potential contamination by helicopter exhaust. Stainless steel tools used snow collection were acid washed prior to use in the field and a standard two-person protocol was used to minimize potential contamination. Snow pits were dug to the bottom of the snowpack using a stainless steel shovel and 10 cm diameter custom-made stainless steel corers and stainless steel spatulas were used for snow collection, which ensured an even sampling of the complete snowpack profile. Snow sampling equipment was cleaned with snow at each site prior to collection. Snow for water chemistry and multi-element analyses was collected into 13 L pre-cleaned high density polypropylene pails. The weight and depth of ~10 cores was recorded at each site for further determination of snow water equivalence (SWE). After collection, snow was kept frozen until processing at the Canada Centre for Inland Waters (CCIW), in Burlington, Ontario, Canada.

As part of QA/QC protocol, field blanks and duplicate (5% of sites) and triplicate samples (1% sites) were also collected at random sites.

Formatted: Superscript

Formatted: Subscript

Formatted: Font: 9 pt, Bold, English (U.S.)

~~*Water Chemistry analysis*: Snow was analyzed for water chemistry parameters, including pH, major cations, anions, and sulphate, and 45 elements including crustal elements, following standard procedures at the National Laboratory for Environmental Testing (NLET) in Burlington, Ontario, Canada. NLET is a certified member of the Canadian Association for Environmental Analytical Laboratories (CAEAL) and undergoes regular external reviews to maintain this accreditation.~~

~~*Snow Water Equivalent and Loadings*: Average SWE were determined at each site and used to calculate loadings as described previously (Kelly *et al.* (2009), Kelly *et al.* (2010), Kirk *et al.* (2014), Manzaono *et al.* (2016)). Briefly, equations [16], [17] and [18] were used to calculate SWE and Aerial Water Volume (AWV), which was used to obtain sulphate, nitrate, ammonium and base cations loadings, depending on the parameter used in equation (18):~~

$$SWE\left(\frac{kg}{m^2}\right) = \frac{snowpack\ weight\ (kg)}{\pi[corer\ radius\ (m)]^2} \quad (16)$$

$$AWV\left(\frac{L}{m^2}\right) = \frac{SWE\left(\frac{kg}{m^2}\right)}{\rho_{water}\left(\frac{kg}{m^3}\right) \times \frac{1}{10^3}\left(\frac{m^3}{L}\right)} \quad (17)$$

$$\sum Ion\ loading\left(\frac{\mu g}{m^2}\right) = AWV\left(\frac{L}{m^2}\right) \times \sum Ion\ concentration\left(\frac{\mu g}{L}\right) \quad (18)$$

~~**2.3.2.2 Saskatchewan Environment Snow Sampling**~~

~~*Sampling Design:* Snowpack surveys were conducted by Saskatchewan Ministry of Environment at 18 sites during Feb 16th – 22nd (n=13) and Apr 1st – 2nd (n=5), of 2014. Snow cores were collected at the centre of frozen~~**: data were not collected for the largest, lakes** ~~to minimize the influence of trees and topography on deposition and chemistry. Distances from the approximate centre of emissions in the Athabasca Oil Sands operations ranged from 106-291 km. Site selection in 2014 was based on criteria used to select lakes for a sediment coring study, described by Laird *et al.*, (2017).~~**and river systems within the coloured region; the boundaries of the coloured region represent the limit of the catchment basins for which data were collected.**

~~*Sample collection*~~

~~Sampling equipment was cleaned with snow at each site prior to collection. Multiples (10-20) of intact snow cores were collected using an acrylic 7.62 cm diameter tube and a stainless steel spatula and composited into Teflon™ bags. Snow water equivalents (SWE) and snowpack loadings were determined as described for the ECCC snowpack samples, above. Samples were delivered frozen to the Biogeochemistry Analytical Laboratory at the University of Alberta, Edmonton.~~

~~*Water Chemistry analysis:* Samples were melted in a temperature controlled clean room and stirred prior to filtration (0.7 µm). Total and dissolved base cations were measured by ICP-MS. Other ions (ammonium, nitrate, sulphate, chloride), dissolved organic carbon, conductivity, pH, and Gran alkalinity were measured according to standard methods. Acceptance criterion of ±15% was applied to analytical charge balance.~~

Formatted: Line spacing: single

Formatted: Font: 9 pt, Bold, English (U.S.)

Formatted: English (U.S.)

Formatted: Font: Bold

Formatted: Left, Line spacing: single

3. Results

3.1 GEM-MACH estimates of annual S_{dep} and N_{dep}

The model estimates of total S_{dep} and N_{dep} (eq ha^{-1} yr^{-1}), along with the percentage contribution of the different resolved components of sulphur and nitrogen deposition, are shown in Figures 5 and 6, respectively. The bulk of the relative fraction of total S_{dep} close to the sources of emissions is due to dry deposition of SO_2(g) and wet deposition of HSO_3^-, while the wet deposition of $SO_4^{(2-)}$ dominates in downwind regions. The relative fraction of N_{dep} near the sources is dominated by dry deposition of NO_2(g) and NH_3(g) near sources and dry deposition of HNO_3(g) and $NH_4^{(+)}$ further downwind. Figure 5 (b-e) and Figure 6 (b-i) show that for sites downwind of the source regions (hot-spots in panel (a) of these figures), wet deposition dominates. ~~As we discuss below, the model predictions~~We note that the mass of S_{dep} and N_{dep} deposited decreases with distance from the sources; for example, $NH_4^{(+)}$ dominates the relative fraction of N_{dep} in locations more distant from the sources, where total N_{dep} is relatively low. Air-quality models such as GEM-MACH are quite complex, with many possible sources of model error; some possibilities include but are not limited to errors in the input emissions data (as we examine below for base cation emissions and deposition), errors in the plume rise algorithms leading to potential errors in the relative distribution of deposition near versus far from the sources (Gordon *et al.*, 2018, Akingunola *et al.*, 2018), potential errors in the magnitude of N_{dep} associated with the absence of bi-directional fluxes of NH_3 (Whaley *et al.*, 2018) in the simulations carried out here, and biases within the meteorological forecast components of the model. As we discuss below, the model predictions nevertheless correlate well with wet deposition observations at precipitation-monitoring stations located downwind of emissions sources, and these relationships allow for an approximate correction of model S_{dep} and N_{dep} estimates using observations. This allows us to reduce the potential impact of sources of model error on estimates of critical load exceedances.

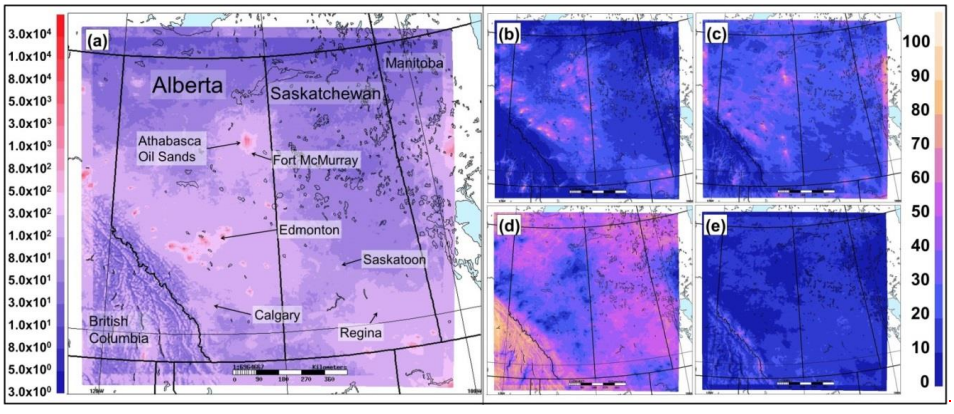

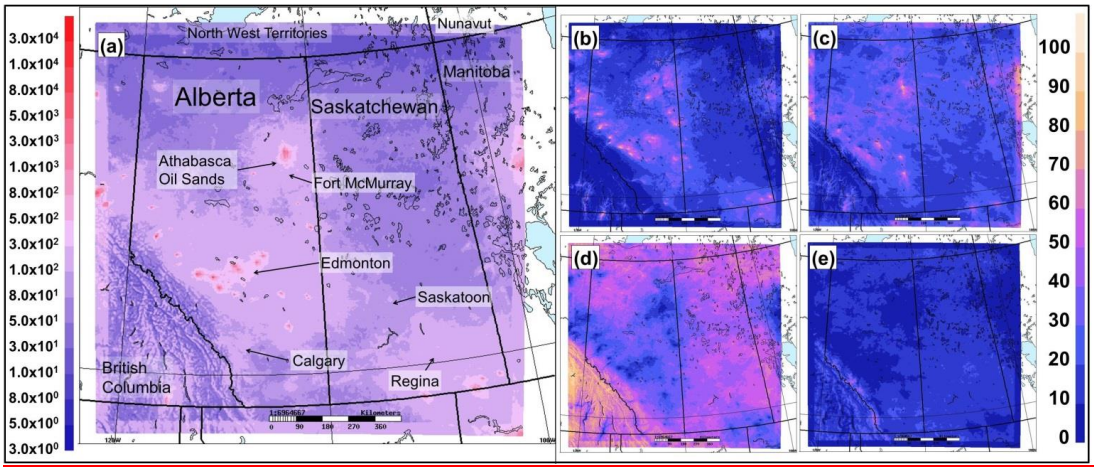

Figure 5. GEM-MACH predictions of total ~~Sulphur~~sulphur deposition and its speciation. (a) Total ~~S~~sulphur deposition (eq ha^{-1} yr^{-1}), and percentages of total ~~S~~sulphur deposition due to: (b) SO_2 (dry), (c) HSO_3^-(aq) (wet), (d) SO_4^{2-}(aq) (wet), and (e) particulate sulphate (dry).

5

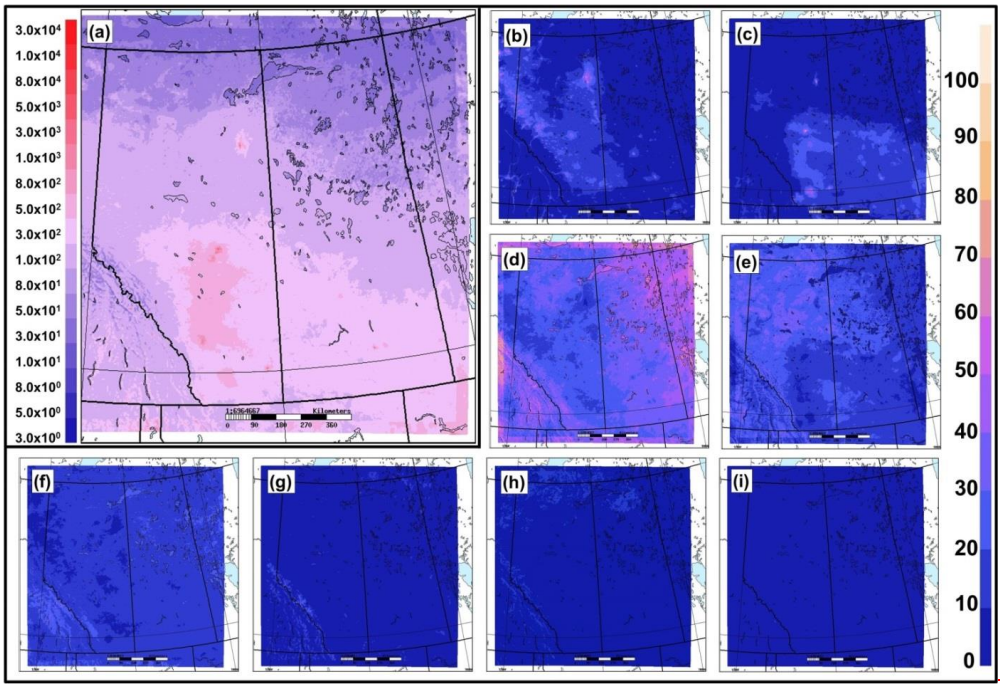

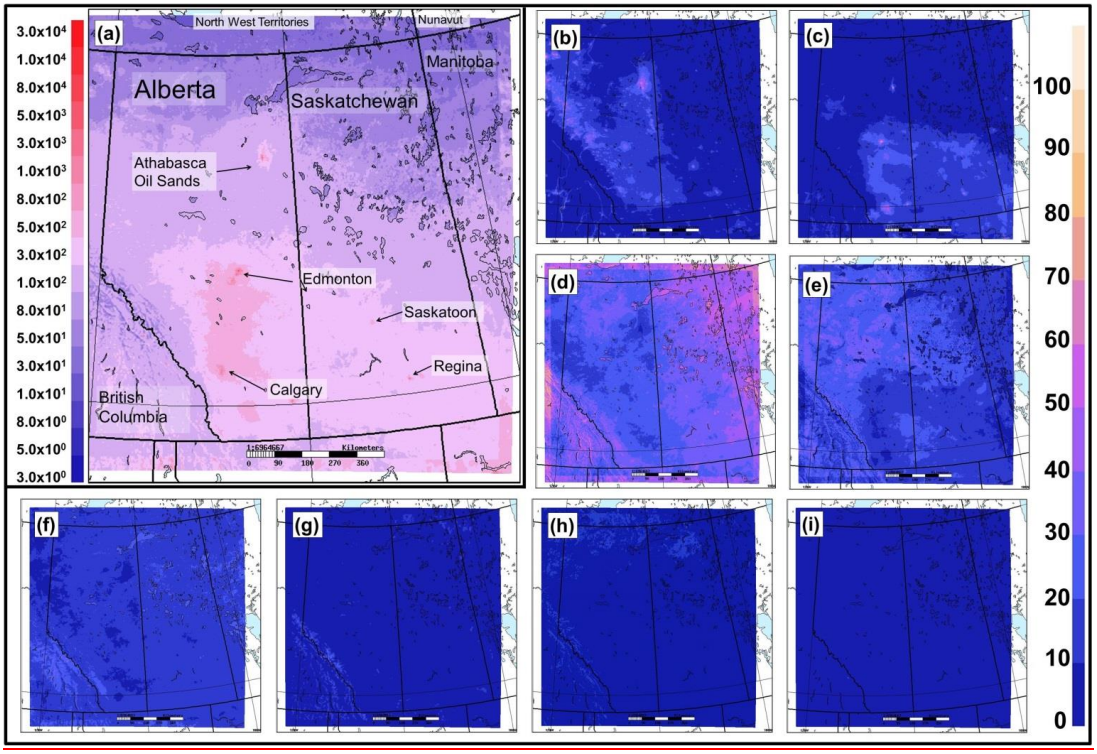

Figure 6. GEM-MACH predictions of total ~~Nitrogen~~nitrogen deposition and its speciation. (a) Total ~~N~~nitrogen deposition (eq ha^{-1} yr^{-1}), percentages of total ~~N~~nitrogen deposition due to: (b) NO_2 (dry), (c) NH_3 (dry), (d) NH_4^+(aq) (wet), (e) HNO_3 (dry), (f) NO_3^- (aq) (wet), (g) particulate ammonium (dry), (h) peroxyactylnitrate (dry). (i) each of particulate nitrate (dry), gaseous organic nitrate (dry), NO (dry) and HONO (dry) (each contribute less than 10% to N_{dep}).

3.2 Model evaluation: wet deposition

The observed wet deposition of deposited sulphur (as SO_4^{2-}), nitrogen (NH_4^+ + NO_3^-), and base cations (sum of Ca^{2+}, Mg^{2+}, Na^+, and K^+) are compared to model estimates in Figure 7 (b), (c), and (d), respectively (station locations are shown in Figure 7(a)). Note that GEM-MACH's particle speciation includes a "crustal material" component, of which base cations are a component. The model wet and dry estimates of crustal material deposition were combined, and the fraction of crustal material which is composed of base cations was estimated from the observations of surface dust collected by Wang *et al.* (2015), in the vicinity of the oil sands, in order to estimate base cation deposition. Model estimates of deposited sulphur in precipitation were biased high, with a slope of 2.2, but the model accounts for most of the observed variation with a Pearson correlation coefficient (R^2) of 0.90. Model estimates of deposited nitrogen were biased slightly low (slope = 0.89, R^2 = 0.76), and the model estimate of base cations were biased low (slope = 0.40, R^2 = 0.72).

The positive bias in simulated sulphur deposition may reflect an underestimation of the SO_2 deposition flux closer to the sources (the precipitation sites are located far from SO_2 emissions sources; a model underestimate of upwind SO_2 deposition flux may thus result in excess sulphur being transported downwind, increasing simulated wet deposition of sulphur at these downwind precipitation sites). The negative bias in simulated base cations may result from an underestimate in the model's ~~input~~ emissions inputs for the "crustal material" component of primary particulate matter from either reported anthropogenic or natural sources (and/or in the base cation fraction of these emissions). We discuss the potential impact of under-reporting to the National Pollutant Release Inventory (NPRI), below. The deposition velocity of particulate matter is a strong function of particulate size, with submicron and supermicron particles having the highest and micrometer-sized particles having the lowest deposition velocities, respectively. The size distribution of particles thus determines their residence time prior to deposition, and hence errors in the spatial pattern of estimated BC_{dep} may also reflect errors in the assumptions on the size distribution of emitted particles. Both of these possibilities are discussed further in Section 3.5.

The relatively high correlation for all three deposited quantities suggests that the linear relationships between model estimates and observed ions in precipitation may be used as a means of providing observation-corrected estimates of the S_{dep}, N_{dep} and BC_{dep} required for the critical load and critical load exceedance calculations described in Section 2.3. Therefore, critical load exceedances were calculated using the original model deposition for sulphur, nitrogen and base cations, and also using model deposition corrected using the model-observation linear relationships shown in Figure 7. We note that the resulting corrected values may underestimate exceedances near the sources of S_{dep} and N_{dep} precursor species emissions. For example, if the positive bias in wet sulphur deposition of Figure 7(b) results from a model underestimate of dry deposition of SO_2 near its sources, an overall downwind correction of SO_2 as per Figure 7(b) may underestimate sulphur deposition from SO_2 near the sources. The resulting corrected values should thus be considered a lower bound for exceedances in the near-source environment.

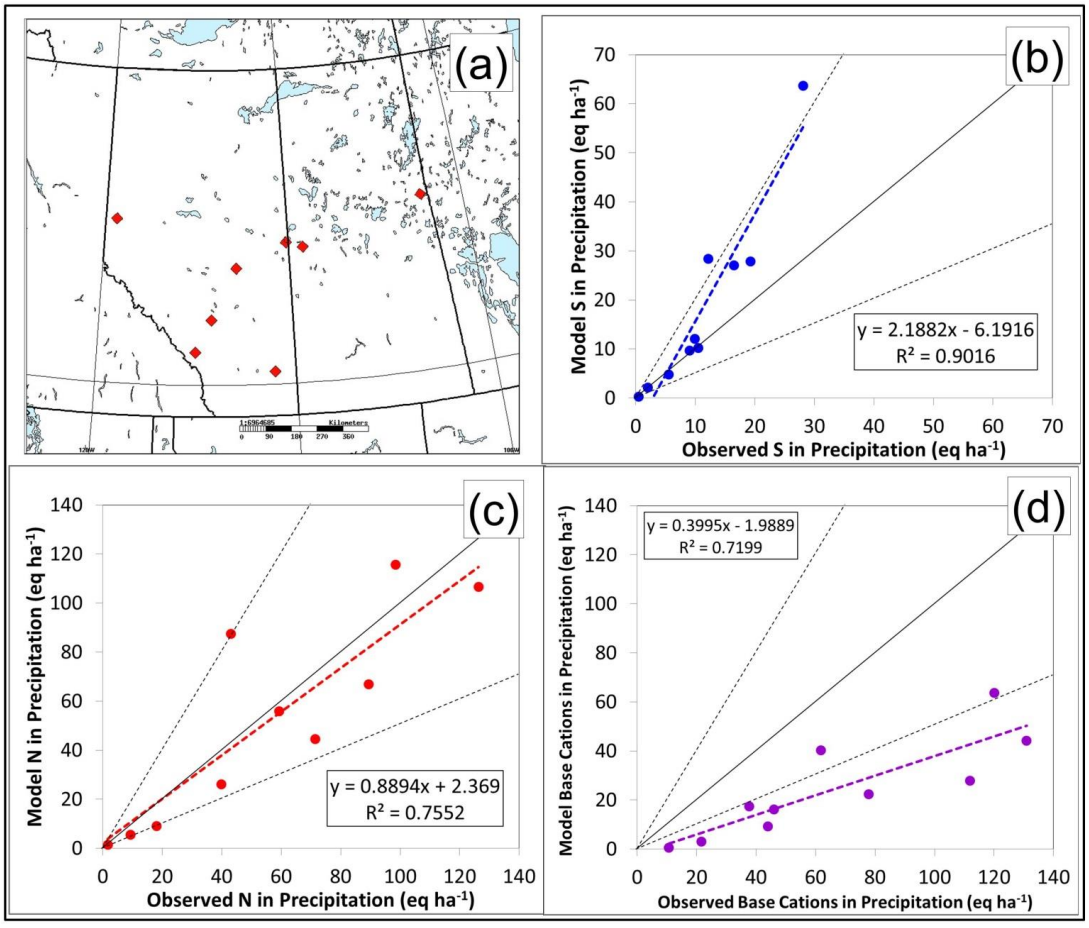
(a)
(b)
Model S in Precipitation (eq ha-1)
Observed S in Precipitation (eq ha-1)
y = 2.1882x - 6.1916
R² = 0.9016
(c)
Model N in Precipitation (eq ha-1)
Observed N in Precipitation (eq ha-1)
y = 0.8894x + 2.369
R² = 0.7552
(d)
Model Base Cations in Precipitation (eq ha-1)
Observed Base Cations in Precipitation (eq ha-1)
y = 0.3995x - 1.9889
R² = 0.7199

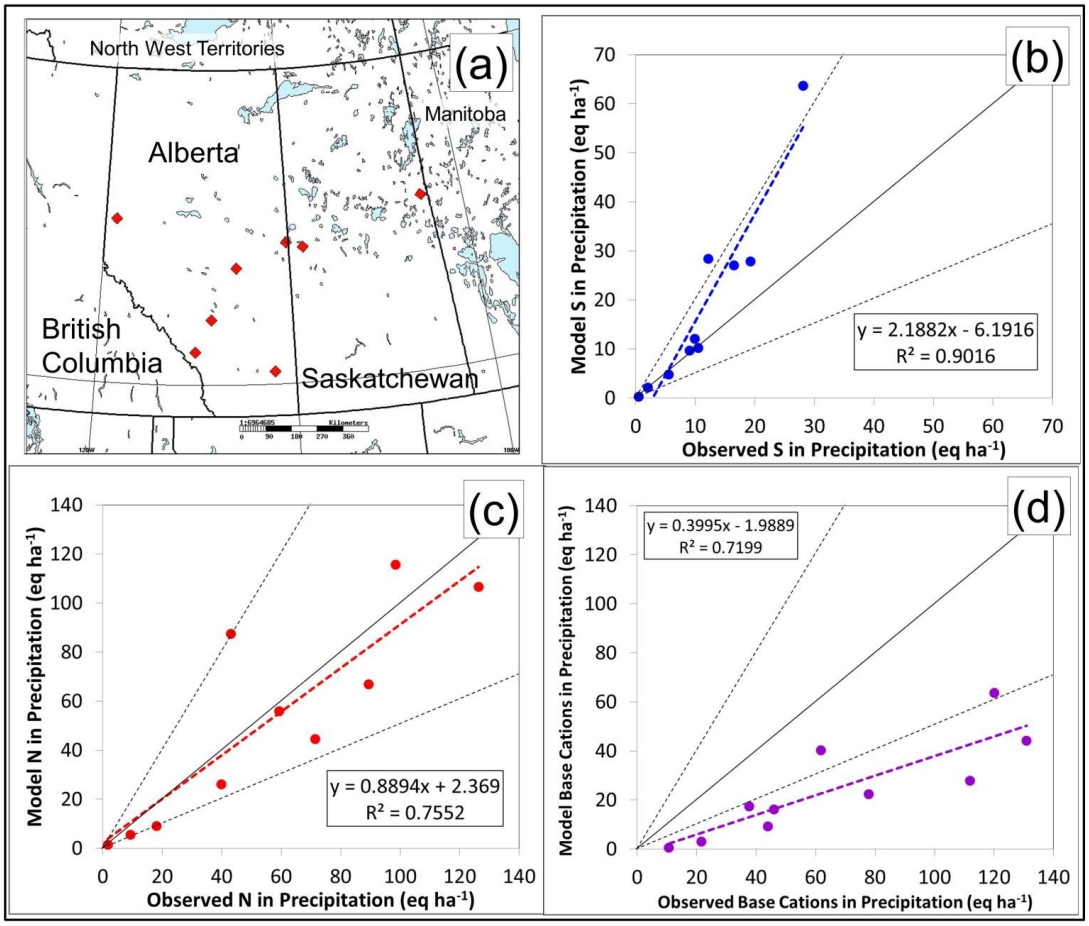

Figure 7. (a) Ions-in-total-precipitation sample collection sites. Scatterplots compare model and observed wet deposited (a) S, (b) N, and (c) base cations in precipitation (eq ha^{-1}).

3.3 Estimates of primary particulate emissions and resulting BC_{dep} from aircraft observations near the Athabasca oil sands

An airborne measurement campaign was undertaken in August and September of 2013 in the Athabasca oil sands region as part of a broader measurement plan (the Joint Oil Sands Monitoring program) to characterize emitted air pollutants, determine the extent of subsequent atmospheric transport and chemical transformation, and support the improvement of air quality models and satellite column retrieval algorithms. "Enclosure" (box) flights were carried out around individual emitting facilities, in order to characterize their emissions fluxes. As part of that work, a mass balance model was developed

(the Top-down Emission Rate Retrieval Algorithm, TERRA, Gordon *et al.*, 2015). TERRA makes use of aircraft flux data and mass conservation equations to estimate emissions from facilities, and was shown to produce SO_2 emissions estimates which were within 5% of direct within-stack estimates from Continuous Emissions Monitoring. The algorithm has more recently been used to estimate the emissions fluxes of intermediate volatility organic compounds (Liggio *et al.*, 2016), volatile organic compounds (Li *et al.*, 2017) and the primary emissions of gaseous organic acids from these facilities (Liggio *et al.*, 2017).

The TERRA algorithm, aircraft observations of total particulate matter number concentration and size close to the sources, and the fugitive dust speciation reported in Wang *et al.* (2015) were used to estimate fugitive dust emissions for six oil sands facilities, for the 12 particle bin version of the GEM-MACH model (Zhang *et al.*, 2017). We refer to these emissions and corrections to deposition based on them hereafter as "aircraft-~~observation~~ based". As shown in Zhang *et al.* (2017), the aircraft-~~observation~~ based primary particulate emissions estimates are much higher (on average, by a factor of ten) than the values reported to the National Pollutant Release Inventory by the facilities, with 96% of the primary particulate emissions being associated with fugitive dust, and 68% of this mass being at particle sizes greater than 2.5 μm diameter. ~~This in turn suggests that the~~Larger particles have higher deposition velocities compared to particles with diameters of 1μm (c.f. Zhang et al., 2001), and hence these larger, "coarse mode" primary particles ~~may~~would be expected to rapidly deposit with increasing distance from the emissions sources. This in turn implies a reduction in BC_{dep} with increasing distance from the sources, associated with this differential deposition of the larger fugitive dust particles earlier in the transportation process.

The mean Wang *et al.* (2015) base cation fractions of primary particulate matter in the 0 to 2.5 μm particle diameter size range and the 2.5 μm to 10 μm particle size ranges were found to be quite similar; we have used the former here, to describe the mass fraction of the aircraft primary particulate emissions assumed to be composed of base cations. While we have used the reported emissions inventory in annual acid deposition modelling, this comparison between the inventory and the aircraft emissions estimates suggests that former may significantly underestimate the BC_{dep} and Bc_{dep} terms used in critical load and critical load exceedance estimates.

The potential impact of higher-than-reported primary particulate emissions on the estimation of base cation deposition was investigated here via two 29 day simulations of the 12-bin version of GEM-MACH, employing the reported emissions versus the aircraft-~~observation~~ based estimates. The ratio of gridded net model wet and dry deposition of "crustal material" between the two simulations was calculated. Figure 8 shows the average value of this ratio, derived from sampling the resulting gridded field at 10 km distance and 20 degree angles about a reference point within the oil sands emissions area, out to 600km distance. As noted above, most of the primary particulate matter in the aircraft-~~observation~~ based emissions resides in the coarse mode (particle sizes greater than 2.5 μm). These larger particles have higher deposition velocities and consequently undergo rapid deposition close to the sources. The use of the aircraft-~~observation~~ based emissions thus results in enhancements in crustal material deposition relative to the reported emissions simulation~~, of~~ by a factor of 11 close to the sources. The ratio drops exponentially with distance from the sources, and shows the impact of the size fractionation

observed from the aircraft data. A combination of exponential decay functions (see Figure 8) was found to fit the average ratio to a very high correlation (r^2=0.998). Zhang *et al.* (2017) used the observations of Wang *et al.* (2015) to show that 93% of the primary particulate matter emissions were composed of crustal material. Wang *et al.* (2015) also includes the relative fraction of base cations within these particles. The exponential decay function thus describes the average relative enhancement of crustal material (and hence base cation) deposition, associated with the use of the aircraft-~~observation~~-based primary particulate emissions, relative to the reported values.

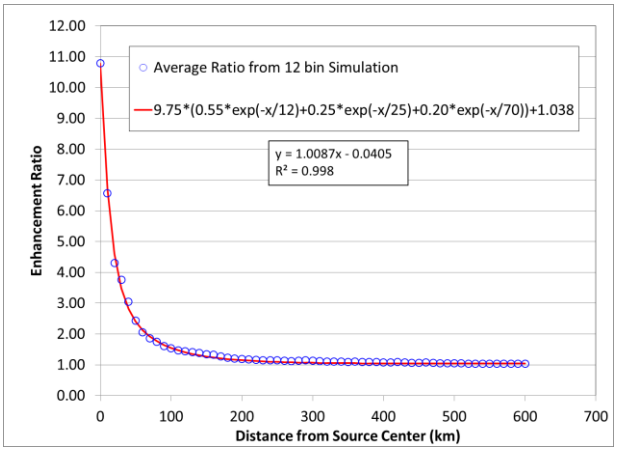

Figure 8. Temporal and spatial average ratio of total deposited crustal material as a function of distance from a reference point within the oil sands emissions region: ratio of deposition from the model simulation using aircraft-~~observation~~-based primary particulate emissions to the model simulation using reported fugitive dust emissions.

Figure 8 shows that the additional fugitive dust emissions result in a substantial enhancement in crustal material (hence base cation) deposition close to the sources, but this enhancement approaches only 3.8% further downwind due to size-segregated particle deposition en-route, with the more rapid deposition of super-micron sized particles. This result was expected, given that the aircraft observations showed that 93% of the emitted primary PM_{10} mass resides in particle sizes greater than 2 μm diameter. Particle deposition velocities have a well-established size-dependence (cf. Wesely *et al.*, 1985; Zhang *et al.*, 2001), with a rapid increase in deposition velocities occurring for particles with diameters between 1 and 10 um (a factor of 28.6 between these two particle diameters, for particle deposition to Needle-leaf trees and a wind speed of 2 m s^{-1}, Zhang *et al.*, 2001).

While the reported fugitive dust emissions in the reported inventory were used in the 2-bin annual GEM-MACH simulations carried out here, the aircraft-~~observation~~-based emission estimates and the shorter duration model simulation described above suggest that the primary particulate emissions in the reported inventory may greatly underestimate the base cation deposition. The scaling function shown in Figure 8 along with the correction to downwind base cation observations from the

precipitation data shown in Figure 5(d) were therefore used to create a combined corrected estimate of base cation deposition. We note that this combined estimate would increase base cation deposition by a factor of ~25 in the immediate vicinity of the oil sands operations, and drop off to a factor of 2.5 further downwind. However, as is shown in the next section, the use of this ~~correction~~and other observation-based corrections on the original model estimates improves both the correlation and the slope of the model-derived estimates of S_{dep}, N_{dep} and BC_{dep} relative to observations of winter deposition to snow.

3.4 Comparison of model and observed snowpack deposition

The observed snowpack-derived deposition fluxes are compared to the modelled values for total sulphur, nitrogen and base cations in Figure 9 (b), (c), and (d), respectively (site locations are shown in Figure 9(a)). The uncorrected model and observation pairs for each site are shown in blue for each of these figures. The model slopes for sulphur and nitrogen are relatively high and correlations relatively low in comparison to the total deposition in precipitation comparisons carried out at stations further downwind (compares Figures 7 and 9). The model values however represent the total deposition to all surface types within each model grid-square, while the snowpack observations correspond to values in forested clearings; thus, as noted in Section 2.~~3~~2.2, the snowpack observations may underestimate the total deposition by a factor of 2.6 (S_{dep}) and 2.0 (N_{dep}).

~~The nitrogen deposition (Figure 9(b)) is dominated by deposition of ammonium, and other work (Whaley *et al.*, 2017~~The nitrogen deposition (Figure 9(b)) is dominated by deposition of ammonium, and other work (Whaley *et al.*, 2018), has found that model overestimates of surface concentrations of ammonia in the immediate vicinity of oil sands emissions sources likely result from incomplete stack information for the relevant facilities' ammonia emissions records (missing volume flow rates, temperatures). In the absence of this information, default EPA values for stacks are used in the emissions processing, which likely underestimates the vertical dispersion of emitted ammonia; see Whaley *et al.* (~~2017~~2018), Zhang *et al.* (2017)).

The model estimates of base cation deposition to snowpack have a strong negative bias (slope = 0.05, R^2 = 0.22). This bias is considerably stronger than noted for the precipitation sites further downwind (compare Figure 9(d) to Figure 7(d)). The additional bias is likely due to the under-reporting of primary particulate emissions in the emissions inventories.

Purple lines and symbols on Figures 9(b), and 9(c) depict the relationships between modelled and open snowpack S_{dep} and N_{dep} loads, when the latter are corrected to approximate throughfall values using the model-derived SO_2 and NH_3 deposition velocity ratios for needle-leaf forest to open snow-covered surfaces. These corrections result in a considerable improvement to the slope between model-derived and snowpack S_{dep}, fluxes, and the apparent N_{dep} overestimate is halved.

Green lines and symbols on Figure 9(d) compare model values of BC_{dep} corrected by the combination of precipitation and aircraft ~~observation~~ based scaling factors described earlier, to the observations, which are also corrected using the expected ratio of needle-leaf forest to open snow covered particle deposition velocities. Red symbols and lines indicate the fit occurring when only the model values are corrected. The correction of modelled values improves both the slope and correlation coefficient of the best fit line, while correction of observations for the expected influence of snowfall versus snowpack further improves the slope. We note that the combination of precipitation and aircraft ~~observation~~ based correction factors on the model's original estimates of base cation deposition increase that estimate by a factor of 25, yet result in a substantial improvement to the fit and slope relative to observations. These results suggest that the primary particulate emissions resulting from aircraft observations is an underestimate, and/or that the base cation mass fraction derived from collection of deposited surface dust (Wang *et al.*, 2015) is biased low relative to fugitive dust in the atmosphere in this region. Further observation flights are planned for the spring and summer of 2018 to sample both base cation mass fractionation and particulate size distribution in order to further improve estimates of base cation emissions from oil sands operations and other sources.

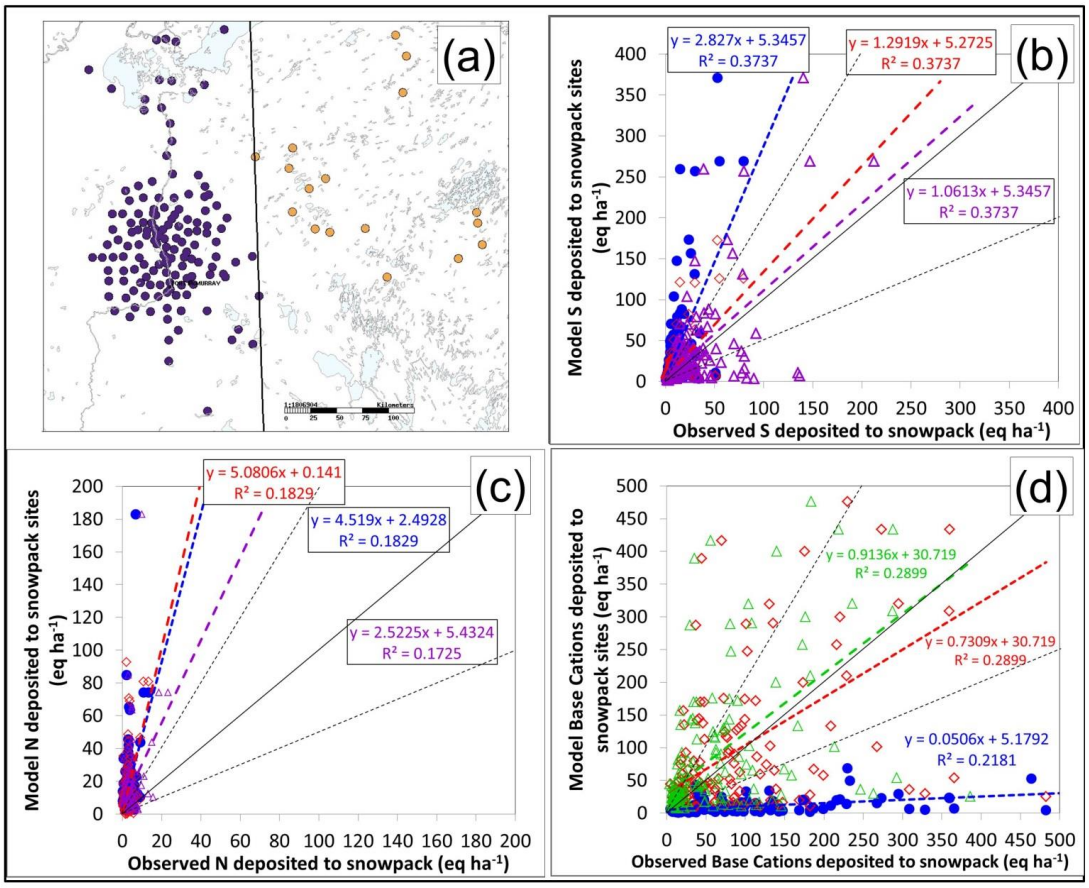
(a)
(b)
y = 2.827x + 5.3457
R² = 0.3737
y = 1.2919x + 5.2725
R² = 0.3737
y = 1.0613x + 5.3457
R² = 0.3737
Model S deposited to snowpack sites (eq ha-1)
Observed S deposited to snowpack (eq ha-1)
(c)
y = 5.0806x + 0.141
R² = 0.1829
y = 4.519x + 2.4928
R² = 0.1829
y = 2.5225x + 5.4324
R² = 0.1725
Model N deposited to snowpack sites (eq ha-1)
Observed N deposited to snowpack (eq ha-1)
(d)
y = 0.9136x + 30.719
R² = 0.2899
y = 0.7309x + 30.719
R² = 0.2899
y = 0.0506x + 5.1792
R² = 0.2181
Model Base Cations deposited to snowpack sites (eq ha-1)
Observed Base Cations deposited to snowpack (eq ha-1)

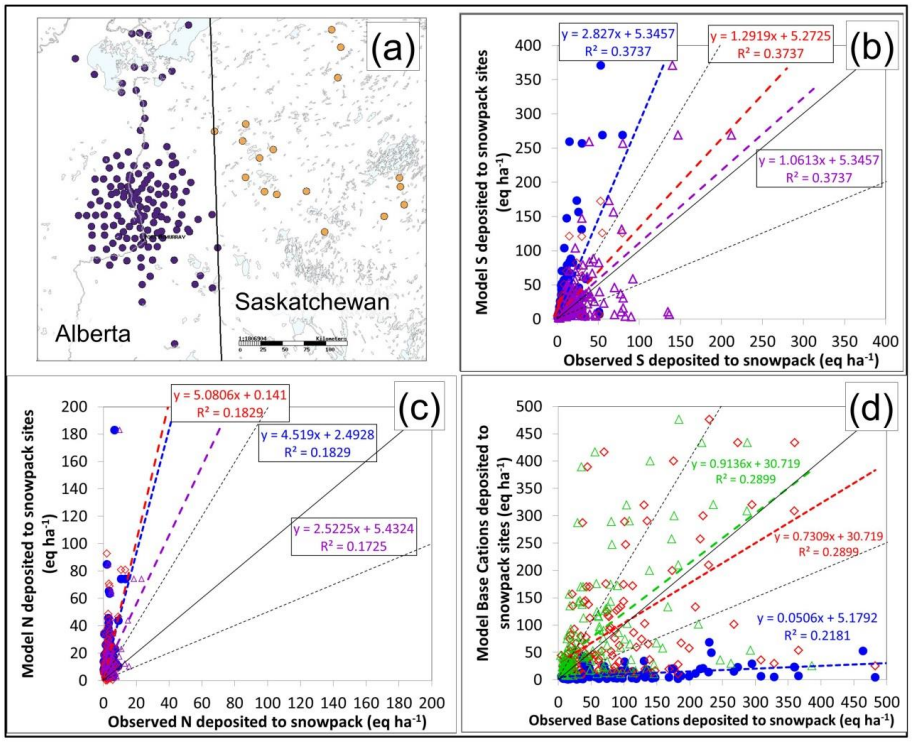

Figure 9 (a) Snowpack sample collection sites (purple: Environment and Climate Change Canada sampling sites; orange: Saskatchewan Environment sampling sites). (b), (c), (d): Relationships between modelled and snowpack-derived S_{dep}, N_{dep} and BC_{dep}, fluxes, respectively. Blue lines: uncorrected model estimates compared to uncorrected snowpack observations. Red lines: Model estimates corrected using downwind precipitation observations (b,c,d) and aircraft-obervation-based fugitive dust emissions estimates (d). Purple lines: original model values compared to snowpack-derived loads corrected by the expected ratios of throughfall to open surface collection for S_{dep} (b) and N_{dep} (c). Green line (d): model BC_{dep} estimates scaled using precipitation and aircraft observations paired with observations corrected by the expected ratio of throughfall to open surface collection for $PM_{2.5}$. Units are eq ha^{-1} for the snowpack sampling periods; model values are the sum of hourly values during snowpack sampling times.

3.5 Comparison of base cation fluxes

Given the dependence of critical loads on base cation levels in both terrestrial and aquatic ecosystems, we compare the observation-based base cation catchment export from aquatic ecosystems (Figure 10(a)) to three different estimates of base cation fluxes used in the subsequent critical load exceedance calculations. Figure 10(a) is equivalent to the sum of

atmospheric deposition, soil weathering, soil cation exchange and groundwater contributions within catchment water, and consequently has larger values than the remaining three estimates, which depict different estimates of the atmospheric component (BC_{dep}). Figure 10(b) shows the BC_{dep} values estimated via interpolation and extrapolation of Canada-wide observation station data collected between 1994 through 1998, with the observation stations within GEM-MACH's 2.5km domain shown as diamond symbols. Figure 10(c) shows the original GEM-MACH-derived base cation deposition (using the reported fugitive dust emissions, the model's summed wet and dry crustal material deposition, and the Wang *et al.* (2015) base cation fractionation reported above). Figure 10(d) shows the base cation deposition fields resulting from correcting the model values of Figure 10(c) with the precipitation-observation-based and aircraft-~~observation~~ based emission scaling factors of Figures 7(c) and 8, and represent an observation-corrected estimate of base cation deposition. We note that the observation stations of Figure 10(c) measure only the wet component of base cation deposition. However, model calculations show that the dry particulate matter flux of base cations drops off rapidly with distance from the sources. The precipitation sites are intended as background sites, located far from sources, and the bulk of base cation deposition at these locations is expected to be via wet deposition.

Three important features should be noted from Figure 10.

First, the net base cation flux exported from aquatic ecosystem catchments (Figure 10(a), data described in Section 2.~~1~~3.4) is usually much larger than any of the three estimates of BC_{dep} in the remaining panels of the Figure. This implies that the aquatic ecosystem base cation load is usually dominated by soil weathering, soil cation exchange and groundwater inputs. The area of lowest cation flux exported from aquatic systems is observed in north-west Saskatchewan,

Second, the observation-derived estimates of BC_{dep} derived from sparse measurement station data, at station locations designed to be relatively remote from sources (Figure 10(b)) are relatively spatially homogeneous compared to the two remaining BC_{dep} estimates, which are derived from model estimates of crustal material emissions. However, the model results suggest that these station locations may consequently miss much of the base cation deposition associated with large sources of fugitive dust emissions, which is highly localized. The largest values in the model estimates are in close proximity to the anthropogenic sources (Figure 10(c,d)). The latter show a rapid drop-off of estimated base cations with distance from the sources, as was expected from Figure 8. Within these anthropogenic emission "hot-spots" of Figure 10(c,d), BC_{dep} estimates reach as high as $3x10^4$ eq $ha^{-1}yr^{-1}$, compared to background levels in the 10's of eq ha^{-1} yr^{-1} (note that the colour scale on Figure 10 is logarithmic).

Third, the corrections applied to Figure 10(c), to create the combined aircraft-~~observation~~ based and precipitation-observation based corrected field of Figure 10(d), are in reasonable agreement with the 1994-1998 observation station values at the remote-from-sources observation station locations (diamond symbols, Figure 10(b)), and also reflect the increases of

base cation deposition expected from the aircraft-~~observation~~-based fugitive dust emissions estimates in the immediate vicinity of the oil sands. As noted in the previous section, these final estimates of BC_{dep} also have a greater degree of agreement with snowpack observations of base cations in the immediate vicinity of the oil sands (Figure 9 (d)).

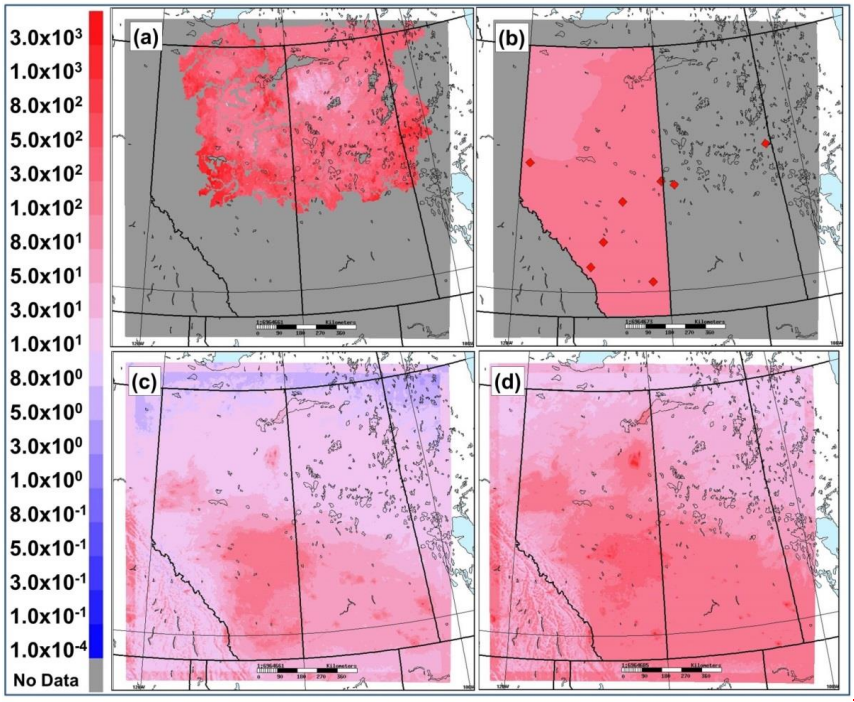

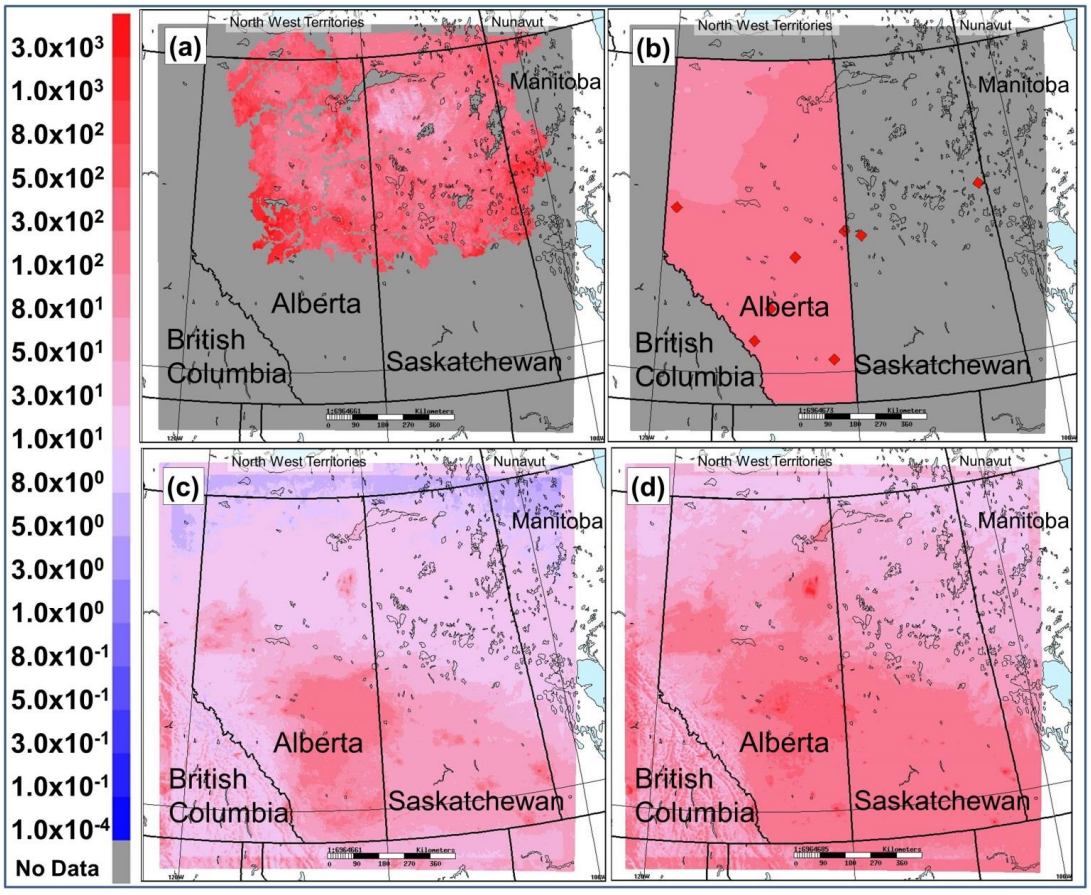

Figure 10. Base cation fluxes (eq ha^{-1} yr^{-1}). (a) Total export flux of base cations from aquatic ecosystem catchments. (b) Atmospheric deposition flux of base cations from surface data collected between 1994 through 1998, monitoring station locations shown as red diamonds, (c) base cation deposition from GEM-MACH, making use of Wang *et al.* (2015) speciation, (d) GEM-MACH BC_{dep} corrected using and precipitation measurements and aircraft observations of fugitive dust.

Watmough *et al.* (2014) presented observations within 135 km of the oil sands which compared $S_{dep}+N_{dep}$ to BC_{dep}. The base cations were found to be in excess of the S_{dep} and N_{dep}, and hence one of their conclusions was that "despite extremely low soil base cation weathering rates in the region, the risk of soil acidification is mitigated to a large extent by high base cation deposition". However, the rapid decrease in base cation deposition with distance from the sources in Figures 10(c,d) and Figure 8 suggest that this neutralization effect may be limited with increasing distance from the sources of base cation emissions. We re-examined the summer throughfall data presented in Watmough *et al.* (2014), and show the excess in base

cation deposition (i.e. $BC_{dep} - N_{dep} - S_{dep}$) as a function of distance from the oil sands emissions region in Figure 11. The data show a rapid decrease in neutralization with distance from sources in the oil sands region, with a linear best fit crossing the intercept, from neutralizing to non-neutralizing conditions, at a distance of 142 km. The data also show a wide variation within the 30 km central region, suggesting neutralization is not uniform. Both these observations (Figure 11) and the model estimates of BC_{dep} (Figure 10(c,d)) thus suggest the neutralization impact of base cation deposition from oil sands sources will be limited in spatial extent. A circle with radius 140 km around the oil sands emissions region appears on the maps of critical load exceedance in Section 3.6, to serve as a visual guideline of this observation-based cross-over distance between base cation neutralization and acidification.

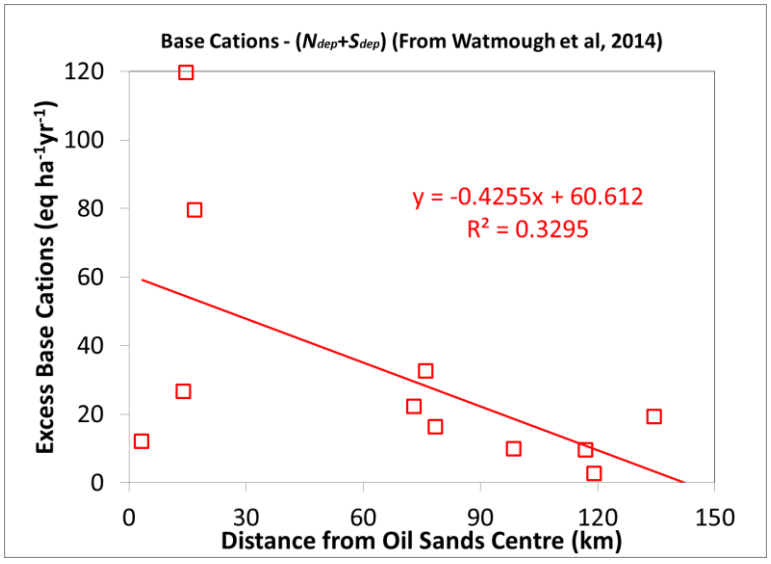

Figure 11. ***BC*$_{dep}$ – *N*$_{dep}$ – *S*$_{dep}$, using the data of Watmough *et al.* (2014).**

The estimates of BC_{dep} from Figure 10 (b) and (d) are shown as ratios to the base cation catchment export flux (Figure 10(a)) in Figure 12 (a,b) respectively. The ratios are usually less than unity (blue shades) indicating that contributions aside from BC_{dep} control the base cation budget, while regions where BC_{dep} is greater than the observation-based total base cation export in catchment water (red shades) occur in the center of the oil sands region and in part of northern Saskatchewan. The latter indicate regions where atmospheric base cation deposition is expected to exceed catchment export in surface water, and hence where accumulation of base cations may occur over time, resulting in neutralization. The measured in-situ concentrations in surface water (cf. Cathcart *et al.*, 2016), combined with our model estimates of S_{dep} and N_{dep}, indicate that at the current time this potential accumulation is insufficient to counteract much of the exceedances of critical loads (see

following sections). However, we note that these regions may warrant further future water sampling ~~for~~to monitor changes in base cation concentrations, due to their potential for future neutralization.

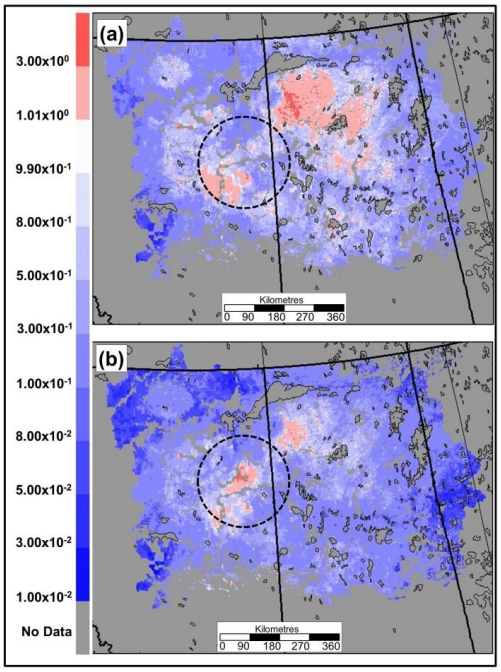
(a)
(b)
3.00x10^0
1.01x10^0
9.90x10^-1
8.00x10^-1
5.00x10^-1
3.00x10^-1
1.00x10^-1
8.00x10^-2
5.00x10^-2
3.00x10^-2
1.00x10^-2
No Data
Kilometres
0 90 180 270 360
Kilometres
0 90 180 270 360

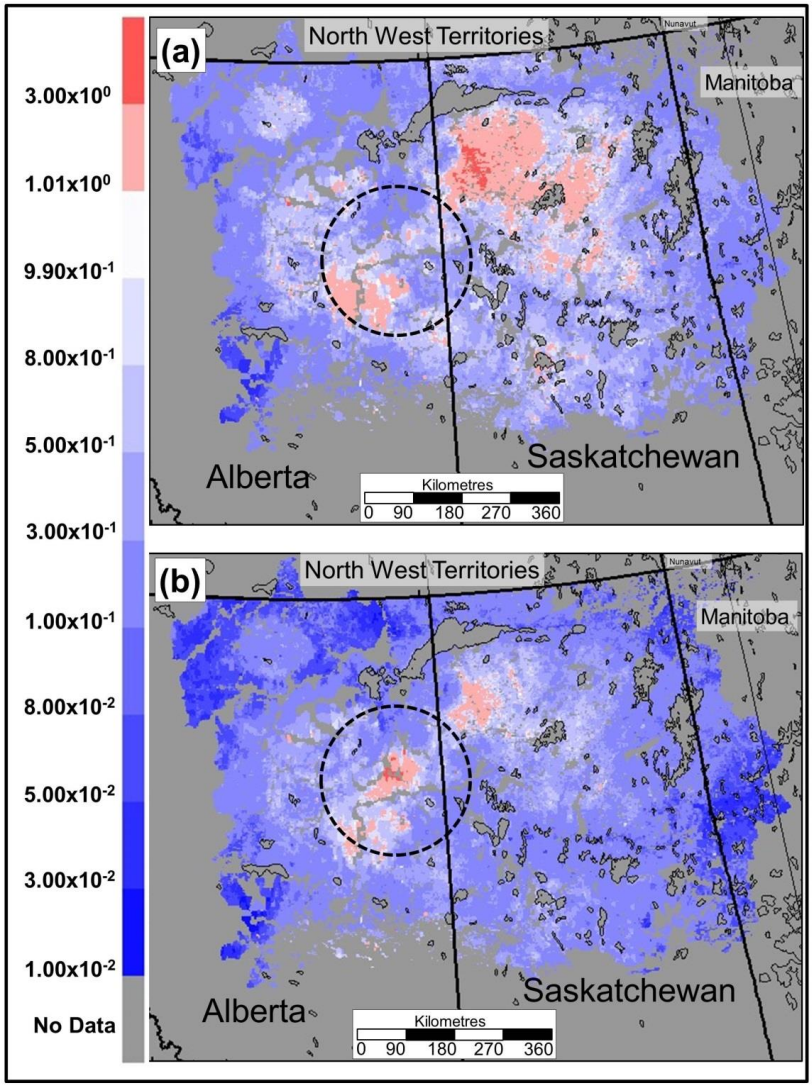

Figure 12. Ratio of estimates of base cation deposition to base cation fluxes exiting aquatic ecosystems. (a) Ratio of interpolated/extrapolated base cation flux from 1994 to 1998 observations to aquatic base cation flux. (b) Ratio of model-generated and precipitation and aircraft-~~observation~~based corrected base cation flux to aquatic base cation flux. Circled region: 140 km radius diameter circle around the Athabasca oil sands.

3.6 Estimates of Critical Load Exceedances

We now estimate critical ~~load~~loads and their exceedances, using both uncorrected and observation-corrected model estimates of S_{dep}, N_{dep} and BC_{dep}, along with the different sources of critical load data and methodologies described above. The data of Wang *et al.* (2015) showed that the equivalent units sodium fraction of BC_{dep} was 4.3%, so we assumed Bc_{dep} = 0.957 BC_{dep}, in the work which follows.

3.6.1 Exceedances ~~with respect to~~of Forest and Terrestrial Ecosystem Critical Loads

The forest critical load exceedances for S_{dep}+N_{dep} calculated using the upper limit NGE-ECP (2001) critical load estimates (Canada-wide data, equations (16) and (17)), and the full CLRTAP (~~2004, 2016,~~ 2017) calculation ~~protocol~~methodology (Alberta data), are shown in Figures 13 and 14 respectively. All critical load exceedances in this section are depicted using the same logarithmic colour scale for easy cross-comparison: red regions represent exceedances, and blue regions are below exceedance. Lighter coloured shades are closer to net neutral conditions. Each critical load exceedance figure includes the total area in exceedance, and its percentage compared to the area of available critical load data. The portions of the model domain which do not coincide with the given dataset are depicted as "no data", in gray.

Figure 13 shows the predicted levels of exceedance using different S_{dep}, N_{dep} and BC_{dep} estimates. Figure 13(a) shows the predicted exceedances when the 1994-1998 BC_{dep} values inferred from Canada-wide station observations are used (those stations within the 2.5km model domain appear as yellow diamonds). Figure 13(b) shows the predicted exceedances using the model's uncorrected values of BC_{dep}, S_{dep} and $N_{dep.}$ Figure 13(c) shows the predicted exceedances using precipitation and aircraft-~~observation corrected~~based deposition fluxes. The different deposition estimates result in a factor of 7 variation in the predicted area of exceedance, with the observation-corrected values having the smallest area at 1.~~15x10~~^{4}20x10^{4} km^2 in exceedance, or about 1% of the total (coloured) area of available critical load data. The strong impact of the model's spatially distributed base cation field and the precipitation-observation reduction in S_{dep} may be seen by comparing Figures 13(b) and (c). The 140 km radius circule is around the Athabasca oil sands– acidification is predicted by the original model fields constructed using the reported emissions (Figure 13(b)), while most of this region is neutralized with the scaling of model values to match observations (Figure 13(c)). Many of the other exceedance regions of Figure 13(b) are greatly reduced in size with the scaled information (Figure 13(c)). Nevertheless, the size of the total region in exceedance of critical loads for forest ecosystems across the entire domain using the NGE-ECP (2001) ~~protocol~~methodology, designed to create a lower estimate of critical load exceedances, is still considerable, about the size of ~~Columbia~~Qatar (1.14x10^4 km^2).

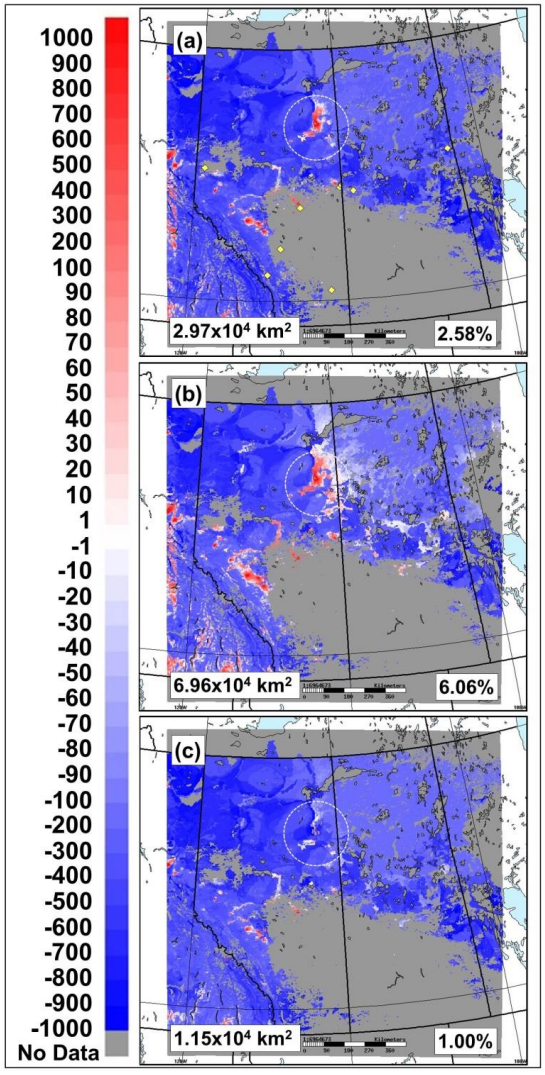
1000
900
800
700
600
500
400
300
200
100
90
80
70
60
50
40
30
20
10
1
-1
-10
-20
-30
-40
-50
-60
-70
-80
-90
-100
-200
-300
-400
-500
-600
-700
-800
-900
-1000
No Data
(a)
2.97x10⁴ km²
2.58%
(b)
6.96x10⁴ km²
6.06%
(c)
1.15x10⁴ km²
1.00%

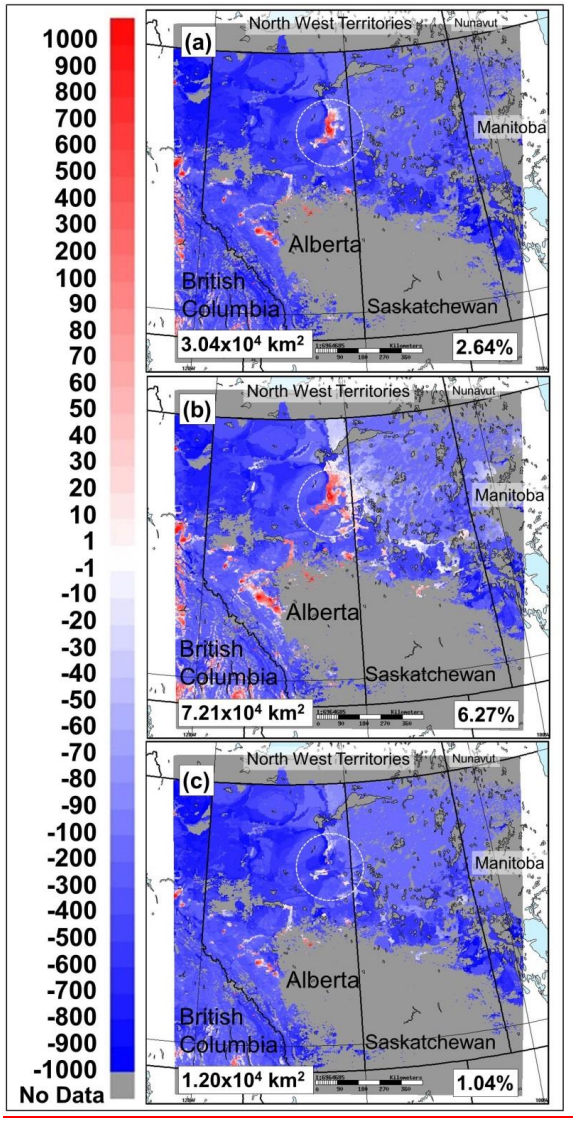

Figure 13. Predicted forest ecosystem critical load exceedances with respect to acidity (S + N deposition), using NEG-ECP (2001) ~~protocols~~methodologies (eq ha^{-1} yr^{-1}). White to red regions: exceedance, white to blue regions: below exceedance. (a) GEM-MACH S+N deposition, interpolated and extrapolated base cation deposition from 1994-1998 observations. Station locations for base cation observations are shown as yellow diamonds. (b) GEM-MACH S+N deposition, model base cations from reported emissions of crustal material and Wang *et al* (2015) cation fractionation. (c) GEM-MACH S+N deposition scaled according to precipitation observations, base cations *scaled* using precipitation and aircraft data Lower left of each panel: total area in

exceedance, in km^2. Lower right of each panel: percentage of the entire critical load data area which is in exceedance. Circled region: 140 km radius diameter circle around the Athabasca oil sands.

The terrestrial ecosystem critical load exceedances for the same estimates of BC_{dep}, N_{dep}, and S_{dep}, for the Alberta data using the full CLRTAP (~~2004, 2016,~~ 2017) ~~protocol~~methodology appear in Figure 14 (a, b, c). While the critical load data in this case are only available for the province of Alberta itself, the regions of exceedance within that province ~~have increased in size relative to~~are larger than the estimates of the NGE-ECP(2001) ~~protocol~~methodology. The influence of the precipitation observation and aircraft-~~observation~~based corrections on model-estimated deposition are evident, comparing Figure 14(c) to Figure 14 (a,b), particularly within 140 km distance of the oil sands. The increases in BC_{dep} and decreases in S_{dep} result in exceedances falling below zero in the central part of the circled region within the province of Alberta, and being reduced in magnitude elsewhere. However, it is important to note that despite these corrections, predicted exceeded areas nevertheless have a significant spatial extent, within some parts of the 140km radius, and remain spatially significant outside of that zone (Figure 14(c)). The total within-Alberta area in exceedance for terrestrial ecosystem critical loads using the corrected fields is $7x10^4$ km^2 (roughly equivalent in spatial extent to Ireland, and accounting for about 10% of the area of the province of Alberta).

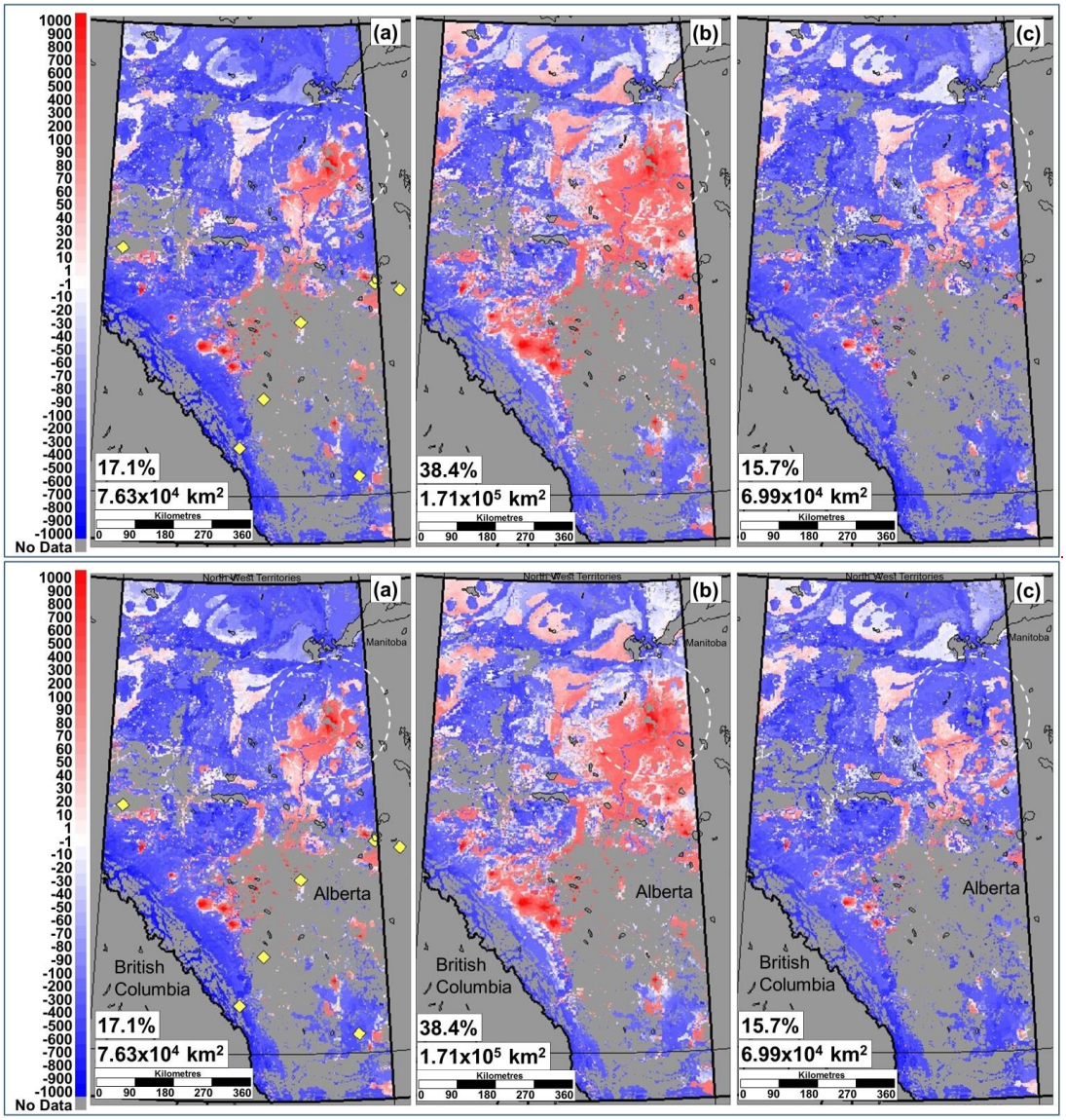

Figure 14. Predicted terrestrial ecosystem critical load exceedances with respect to sulphur and nitrogen (eq ha^{-1} yr^{-1}), Alberta Environment and Parks data. (a) GEM-MACH S and N deposition, 1994-1998 observed base cation deposition. Observation stations shown as yellow diamonds. (b) GEM-MACH S and N deposition, NPRI/Wang *et al.* (2015) base cation deposition. (c) GEM-MACH S and N deposition, base cation deposition scaled according to aircraft and precipitation-based corrections. Circled region: 140 km radius diameter circle around the Athabasca oil sands.

The total area of exceedance falling within each of the four regions described in Section 2.~~1~~3.1 and Figure 1, along with the percentage of the total area in exceedance, are shown in the boxed portion of each panel of Figure 15. Exceedances predominantly occur in Region 2 in all cases, suggesting that both S_{dep} and N_{dep} are contributing most frequently to the total exceedance. The BC_{dep} field in Figure 15(b) is in general lower than for Figure 15(a), resulting in lower values of $CL_{max}(N)$, and a greater proportion of Region 1 exceedances in Figure 15(b) compared to Figure 15(a). In Figure 15(c), both BC_{dep} and N_{dep} have increased; while the total region in exceedance has decreased, the relative proportion within Region 1 between Figure 15 (b) and (c) therefore remains almost unchanged. The proportion of the terrestrial ecosystems where exceedances are with respect to S_{dep} alone (Region 4) is the smallest for the exceedance estimate using observation-based corrections of S_{dep}, N_{dep}, and BC_{dep} (Figure 15(c)).

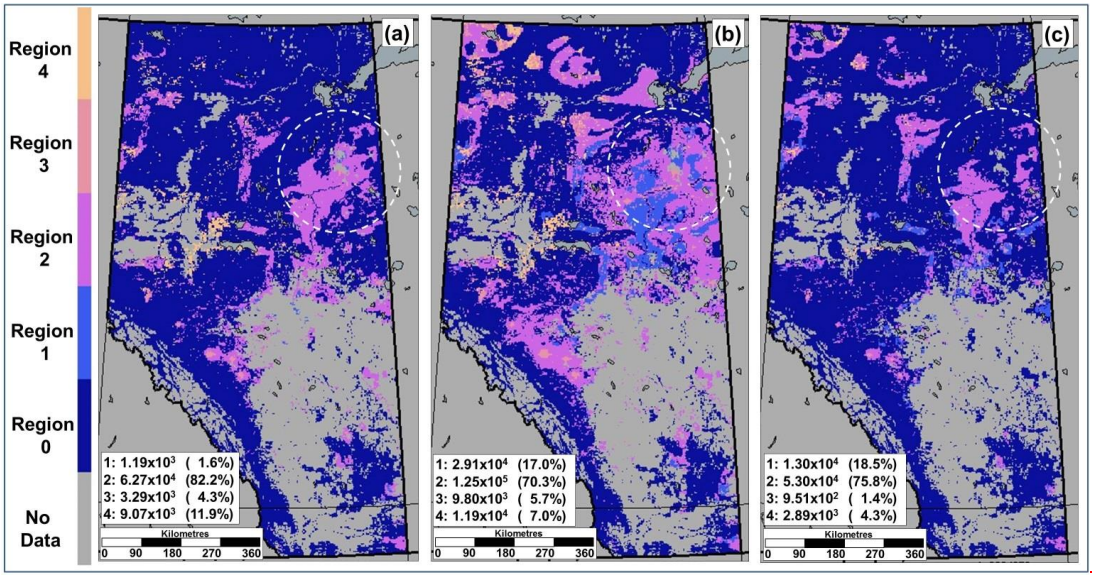

Figure 15. presents possible avenues to reduce the impacts of deposition. Areas within Regions 1,2, and 3 with respect to Figure 1 may be brought below exceedance levels through a combination of reductions in S_{dep} and N_{dep}, the relative magnitude of each depending on the location of the current N_{dep},S_{dep} on Figure 1, with more than one reduction strategy often possible. However, areas within region 4 may only be brought below exceedance by reductions in S_{dep}. Figure 15 thus may be of use to policy-makers in determining strategies to reduce deposition to levels below critical load exceedance.

Formatted: Font: 10 pt, Not Bold, English (U.K.)

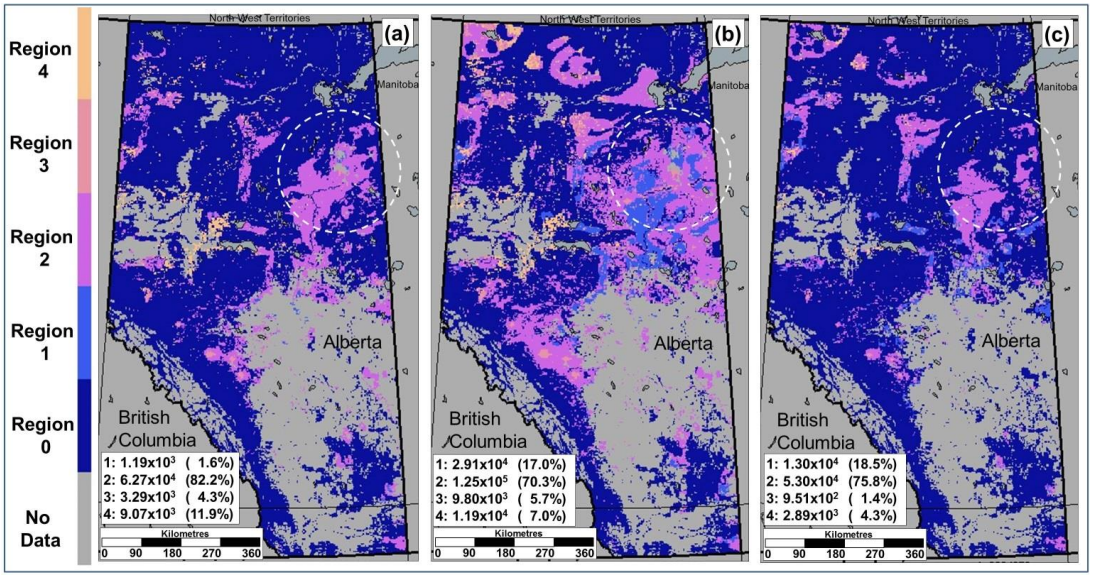

Figure 15. Predicted ~~regions~~sub-types of terrestrial ecosystem critical load exceedance~~,~~ (see Figure 1), with panels arranged as in Figure 14. Inset information shows the area within S + N exceedance ~~regions~~sub-types 1, 2, 3, and 4 (km^2) and the corresponding percentage of the total area of exceedance. Circled region: 140 km radius diameter circle around the Athabasca oil sands.

3.6.2 Exceedances ~~with respect to~~of Aquatic Ecosystem Critical Loads

3.6.2.1 SSWC model: Canada-wide versus Alberta and Saskatchewan critical load datasets.

As noted earlier, aquatic ecosystems tend to be more sensitive to acidifying precipitation (i.e. have lower critical loads) than the forest / terrestrial ecosystems. Exceedances with respect to S_{dep}, calculated using equation (~~7~~5), for the Canada-Wide and the Alberta and Saskatchewan critical load data, are shown in Figures 16 and 17, respectively. Unlike the forest and terrestrial ecosystem critical loads, the base cations of the SSWC model are derived from observations of surface water, hence only the observation-based corrections to S_{dep} are applied to these figures (Figure 16 and 17 (a) are using the uncorrected model S_{dep}, while (b) of each figure uses the precipitation-observation-based S_{dep} correction discussed earlier.

The Canada-Wide data (Figure 16) covers a smaller spatial extent, and utilizes a coarse 45km resolution superimposed ~~in~~on the 2.5km resolution of GEM-MACH; spatial variation of the exceedances within the 45km squares are thus the result of variations in the 2.5km S_{dep} values. The S_{dep} correction reduces the critical load exceedance percentage area in both cases (from 24.9% to 15.9% for Figure 16, and from 79.6% to 47.1% in Figure 17). Aquatic ecosystems in the more recent of the two datasets (Figure 17) are clearly more sensitive than the older data (Figure 16); the use of more recent water sampling observations, and georeferenced soil and other data, have resulted in critical load estimates being somewhat lower than the earlier data (compare also Figure 2(a) and Figure 4(b)). The georeferenced data (Figure 17) also gives a more complete spatial coverage for the region, allowing greater local detail, but also showing that portions of the region for which no data were previously available (e.g. grey areas in Northern Saskatchewan, Figure 16) are likely to be in exceedance of critical loads for S_{dep} (corresponding regions in Figure 17).

The lower estimates of the net area of the exceedance region in these two figures is 7.8×10^4 km^2 for the older critical load data, and 3.3×10^5 km^2 for the new georeferenced critical load data. The former area is roughly equivalent to that of the Czech Republic (7.9×10^4 km^2), the latter that of Germany (3.6×10^5 km^2).

It is worth noting here that the extent of neutralization implied by comparing the atmospheric deposition of base cations (BC_{dep}) to S_{dep} and N_{dep} does not seem to be reflected in the lake water samples used to create the critical loads used in Figures 16 and 17, although some effects due to oil sands fugitive dust deposition may be seen in the observation-corrected exceedance estimates for the areas on the northern side of the oil sands (blue regions Figures 16(b) and 17(b), northern end of the circled region on each Figure). The estimated export of base cations from catchments is usually higher than the BC_{dep} values (see Figures 10 and 11 and related discussion), implying a net loss of deposited base cations. However, some areas within the domain have higher predicted base cation deposition than observed export in surface waters, indicating the potential for an accumulation of base cations over time. This implies a potential lag time between atmospheric deposition and surface water response.

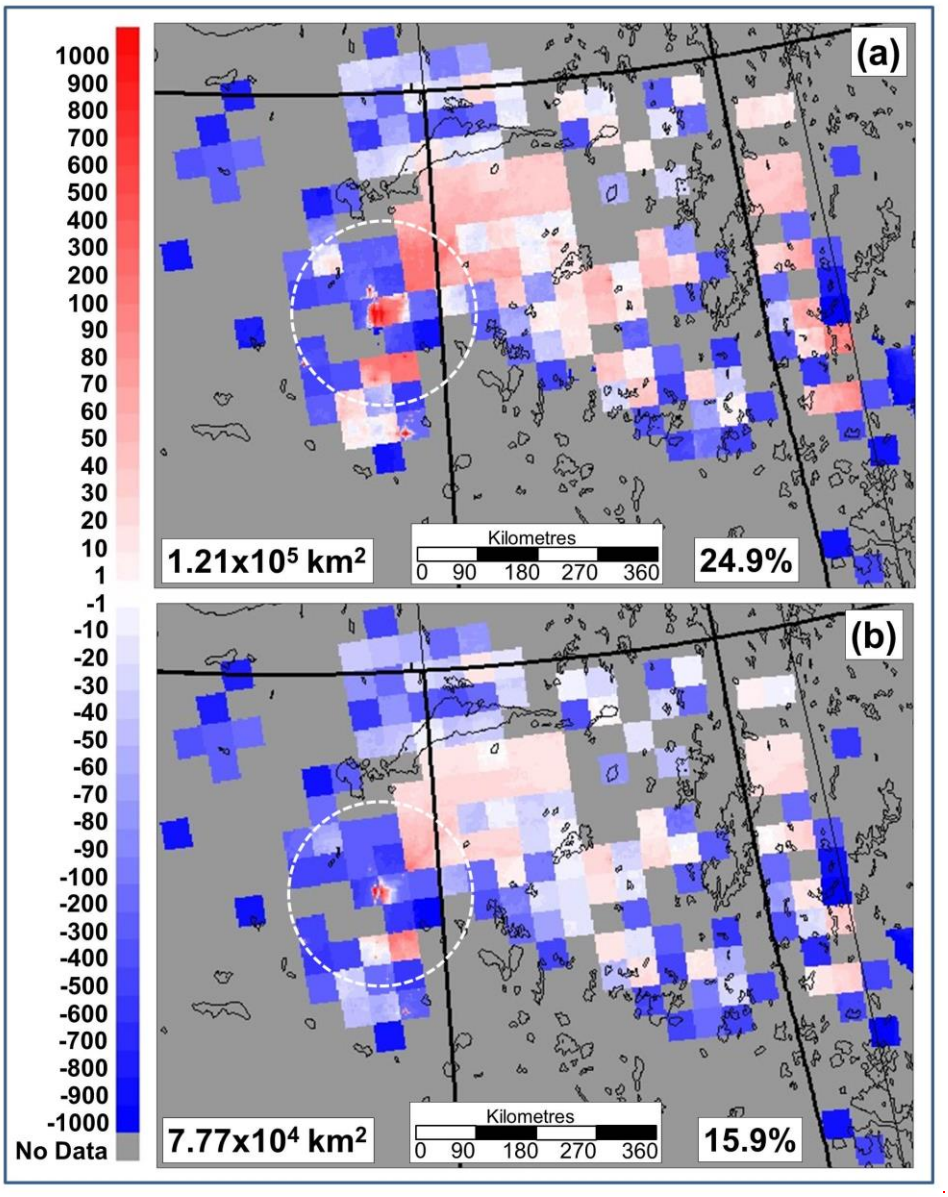
1000
900
800
700
600
500
400
300
200
100
90
80
70
60
50
40
30
20
10
1
-1
-10
-20
-30
-40
-50
-60
-70
-80
-90
-100
-200
-300
-400
-500
-600
-700
-800
-900
-1000
No Data
(a)
1.21x10⁵ km²
Kilometres
0 90 180 270 360
24.9%
(b)
7.77x10⁴ km²
Kilometres
0 90 180 270 360
15.9%

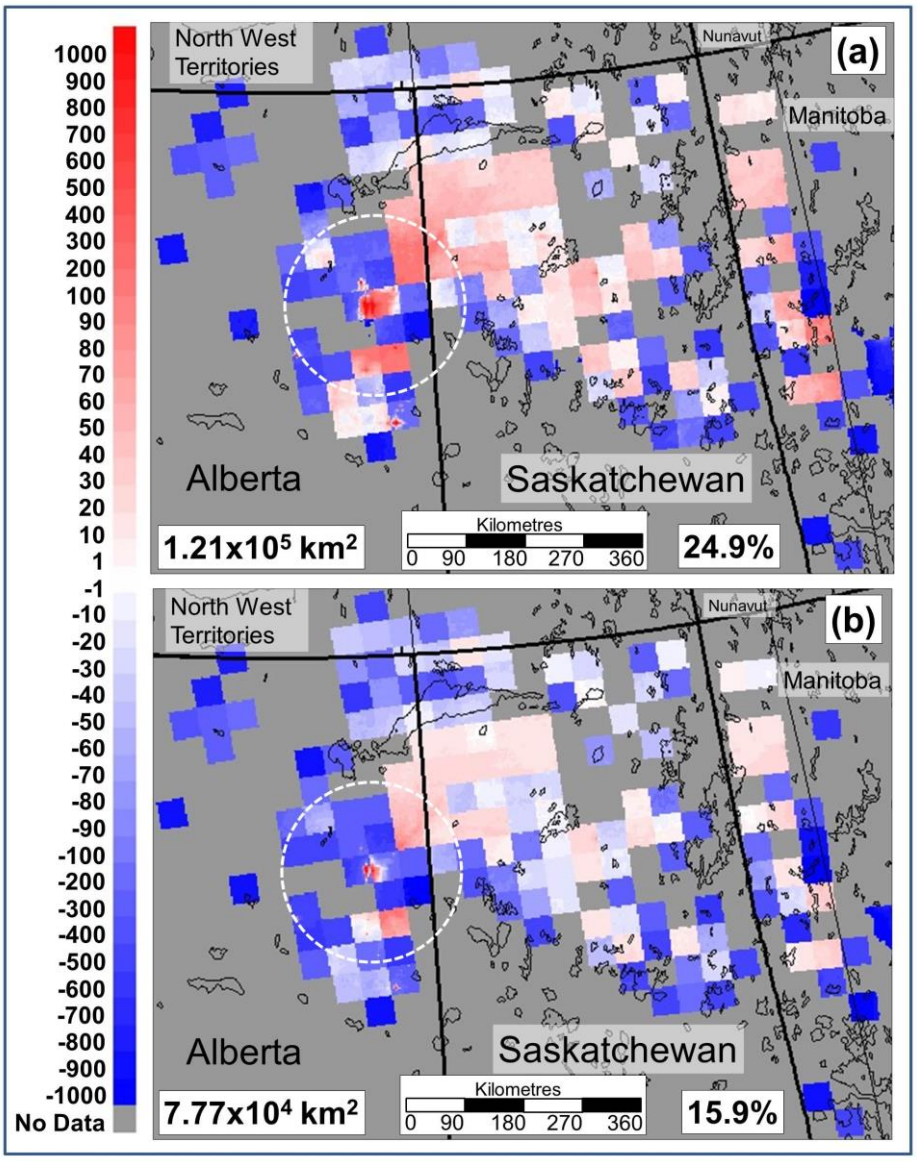

Figure 16. Predicted lake ecosystem critical load exceedances with respect to S_{dep}, NEG-ECP (2001) ~~protocol~~methodology (eq ha^{-1} yr^{-1}). (a) Exceedances calculated using original GEM-MACH S_{dep}. (b) Predicted exceedances calculated using GEM-MACH S_{dep} scaled using precipitation deposition observations. Circled region: 140 km radius diameter circle around the Athabasca oil sands.

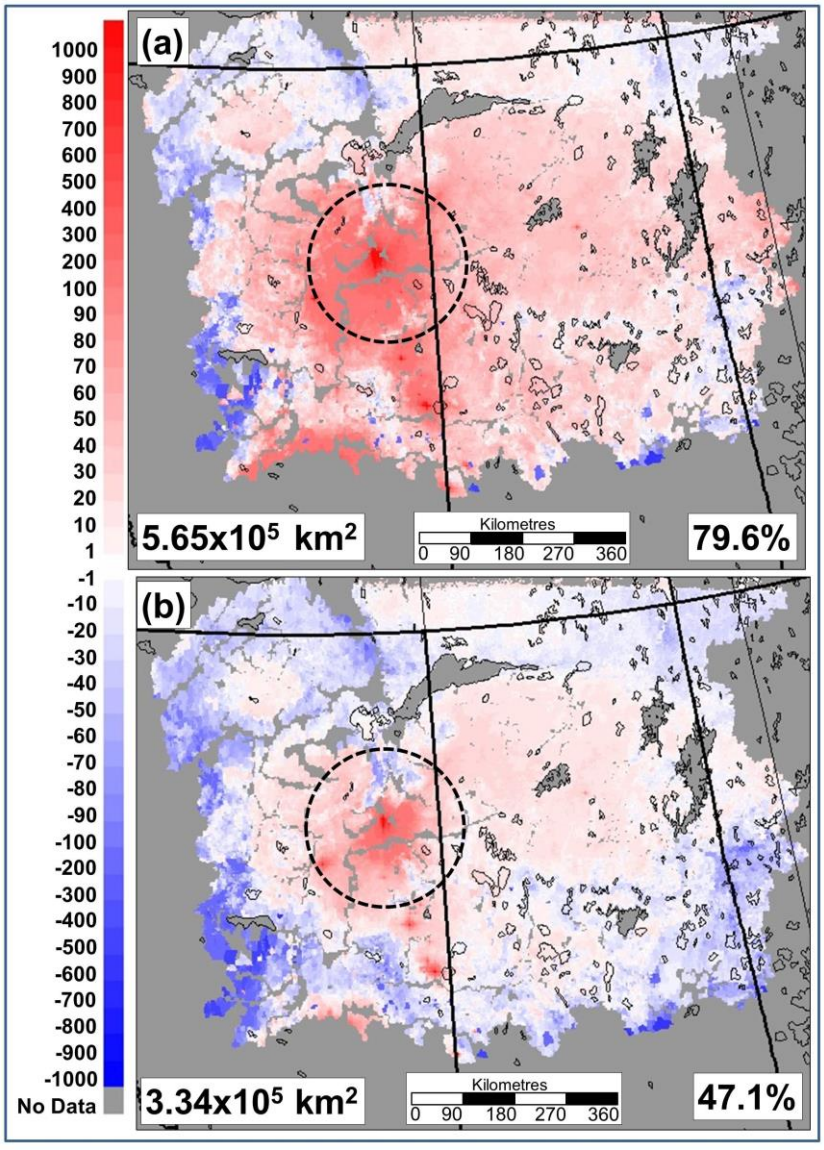
1000
900
800
700
600
500
400
300
200
100
90
80
70
60
50
40
30
20
10
1
-1
-10
-20
-30
-40
-50
-60
-70
-80
-90
-100
-200
-300
-400
-500
-600
-700
-800
-900
-1000
No Data
(a)
5.65x10⁵ km²
Kilometres
0 90 180 270 360
79.6%
(b)
3.34x10⁵ km²
Kilometres
0 90 180 270 360
47.1%

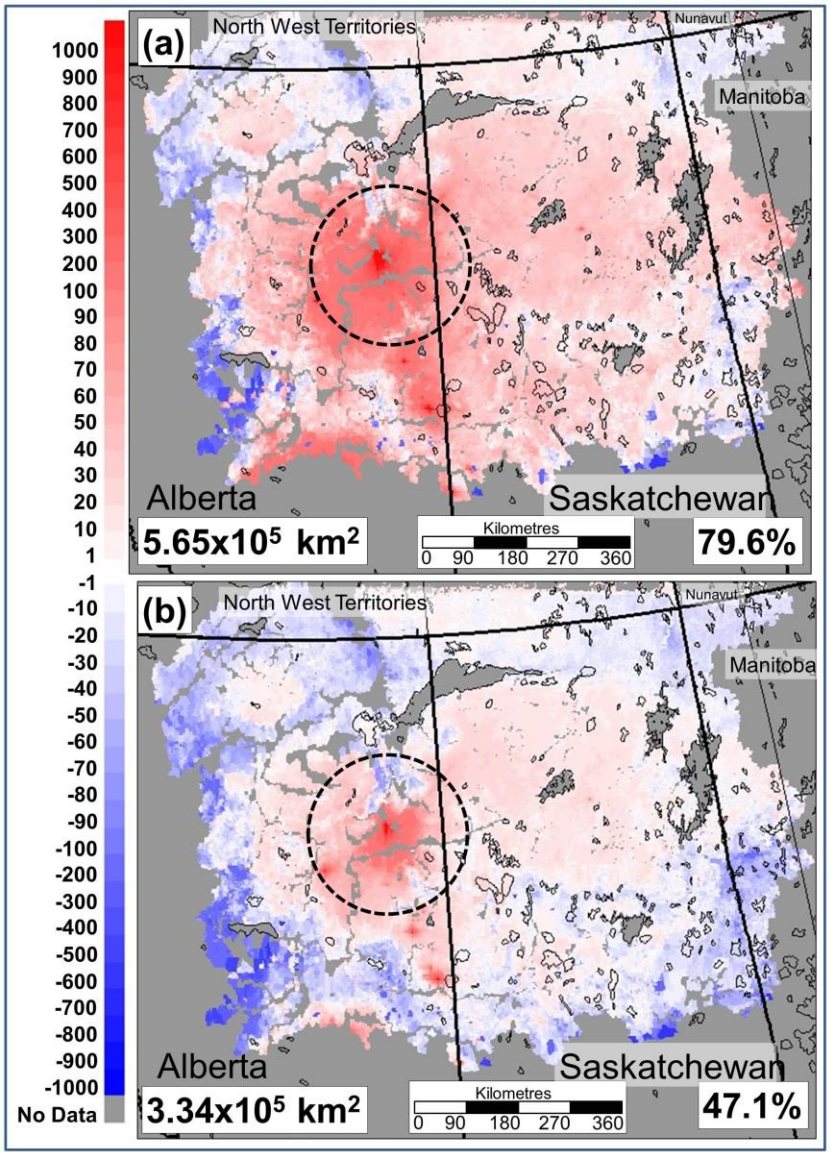

Figure 17. Predicted aquatic ecosystem critical load exceedances with respect to S_{dep}, CLRTAP (~~2016,~~ 2017) ~~protocol~~methodology (eq ha^{-1} yr^{-1}). (a) Exceedances with uncorrected model S_{dep}. (b) Predicted exceedances with model S_{dep} corrected to match precipitation observations. Circled region: 140 km radius diameter circle around the Athabasca oil sands.

Formatted: Font: Italic

Formatted: Font: Italic

Formatted: Font: Italic

3.6.2.2 FAB model: exceedances with respect to N_{dep}+S_{dep} for Aquatic Ecosystem Critical Loads

The exceedances for aquatic ecosystems with respect to both N_{dep} and S_{dep} are shown in Figure 18, using the original (Figure 18(a)) and precipitation-observation-corrected (Figure 18(b)) model fields for N_{dep} and S_{dep}. The total area of exceedance again decreases with use of the observation-corrected fields (though not to the same degree as Figure 17, probably due to the increases resulting with the N_{dep} correction offsetting some of the decreases associated with the S_{dep} correction). The total area in exceedance is similar to the SSWC results (decreasing slightly for the original model S_{dep} and N_{dep}, increasing slightly for the corrected fields: compare panels (a) and (b) between Figures 17 and 18). The FAB model critical loads suggest deposition significantly below exceedance takes place in specific lakes (dark blue, Figure 18), while the SSWC model (Figure 17) suggests a more smoothly distributed variation between exceedance and non-exceedance regions.

Both the SSWC and FAB exceedance estimates show the oil sands region as a prominent "hot-spot" of aquatic critical load exceedance, with an influence extending far beyond the 140 km circle shown on Figures 17 and 18. Exceedances to aquatic ecosystem critical loads are predicted as far east as northern Manitoba, and into the North-West Territories on the northern end of the data region. The exceedances using the uncorrected model deposition estimates are roughly equivalent in size to Spain (5.0×10^5 km^2), while the exceedances using the observation-corrected model deposition are closer to the size of Germany (3.6×10^5 km^2). By comparison, Alberta and Saskatchewan have areas of 6.6×10^5 and 6.5×10^5 km^2, respectively: the predicted area in exceedance of aquatic ecosystem critical loads is a significant fraction of the spatial extent of these provinces.

~~Figure 19 shows the shift in exceedance regions resulting between the original (a) and observation corrected (b) N_{dep} and S_{dep} model fields; with the reduced S_{dep} and increased N_{dep} resulting from the corrections to observations, a greater proportion of the exceedance regions fall within Region 1, and the totals within Region 1 increase. The totals within the remaining regions decrease, reflecting the drop in S_{dep} with the precipitation-observation-based corrections.~~

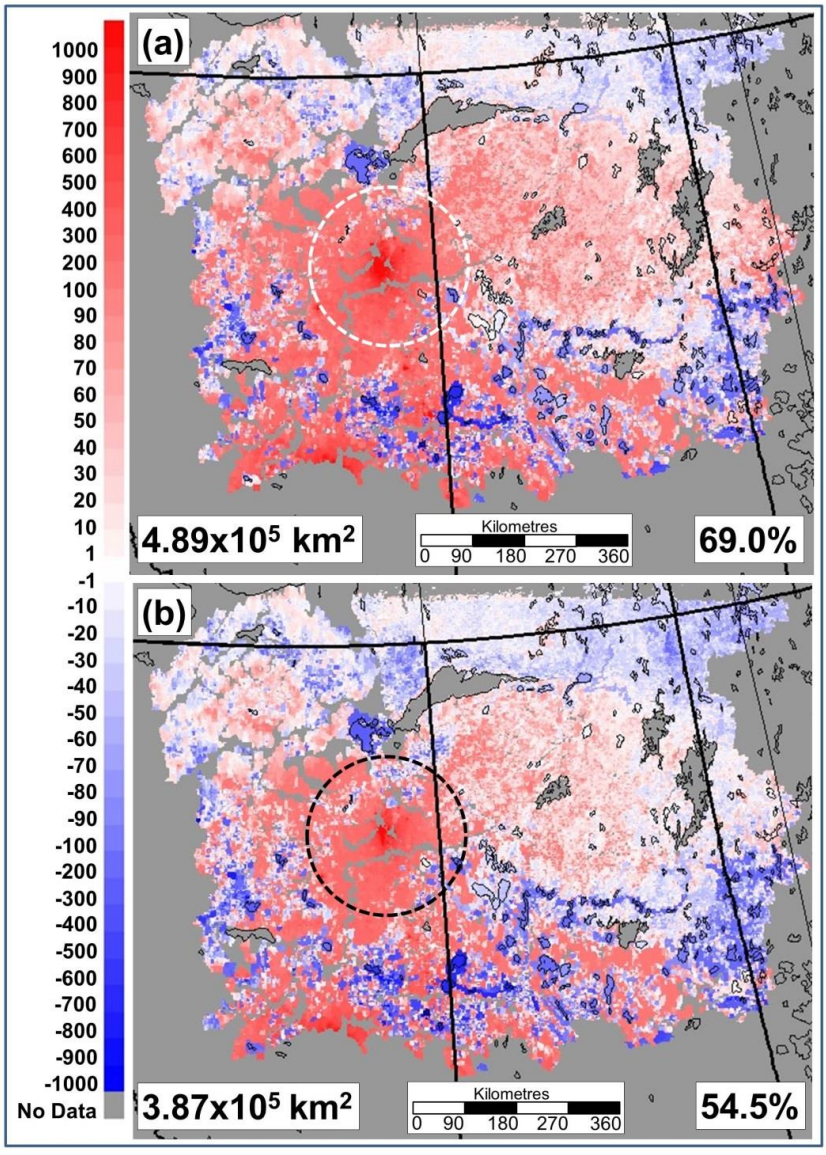
1000
900
800
700
600
500
400
300
200
100
90
80
70
60
50
40
30
20
10
1
-1
-10
-20
-30
-40
-50
-60
-70
-80
-90
-100
-200
-300
-400
-500
-600
-700
-800
-900
-1000
No Data
(a)
4.89x10⁵ km²
Kilometres
0 90 180 270 360
69.0%
(b)
3.87x10⁵ km²
Kilometres
0 90 180 270 360
54.5%

Figure 19 shows that most of the exceedances for aquatic ecosystems reside within Regions 1 or 2 with respect to the regions shown in Figure 1, and thus may be brought to below exceedance conditions by different combinations of reductions in S_{dep} and N_{dep}, depending on the location of the current N_{dep},S_{dep} on Figure 1.

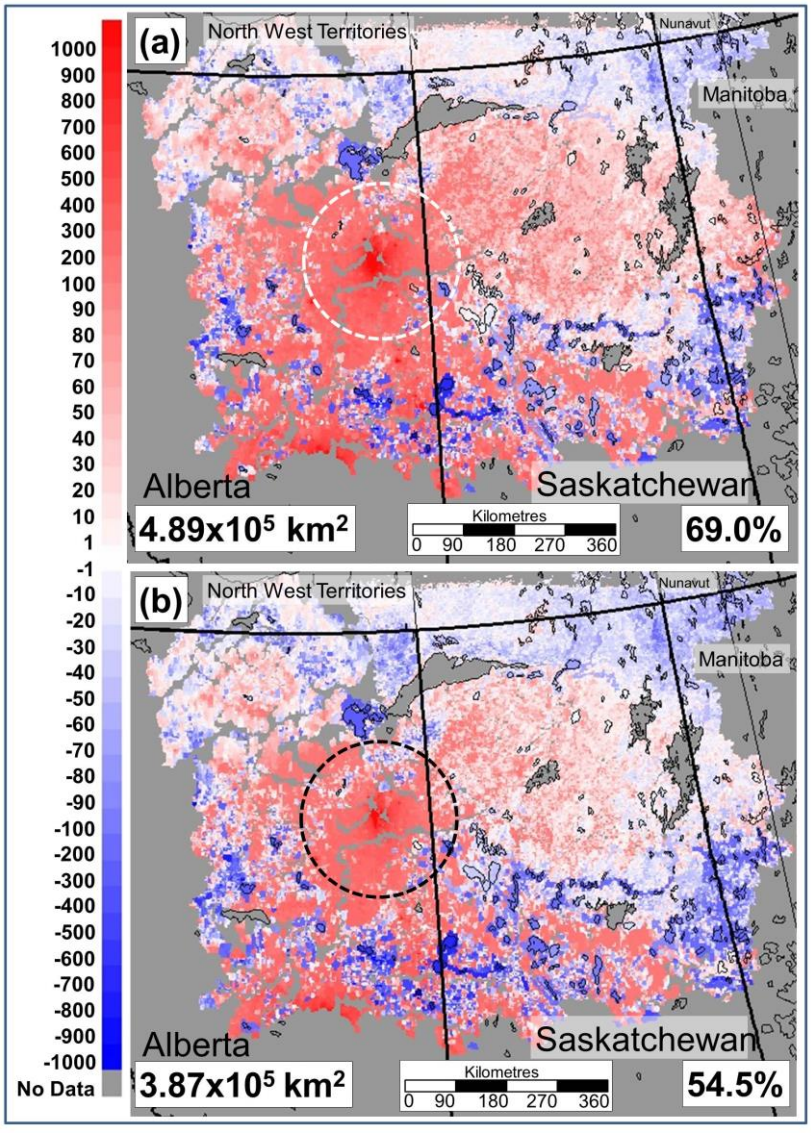

Figure 18. Predicted aquatic ecosystem critical load exceedances with respect to sulphur and nitrogen deposition, (eq ha^{-1} yr^{-1}). Boxed numbers are the area in exceedance and the percent of the total area for which critical loads are available which is in exceedance. (a) Calculated using original model sulphur and nitrogen deposition. (b) Calculated using model sulphur and nitrogen deposition corrected to match precipitation observations. Circled region: 140 km radius diameter circle around the Athabasca oil sands.

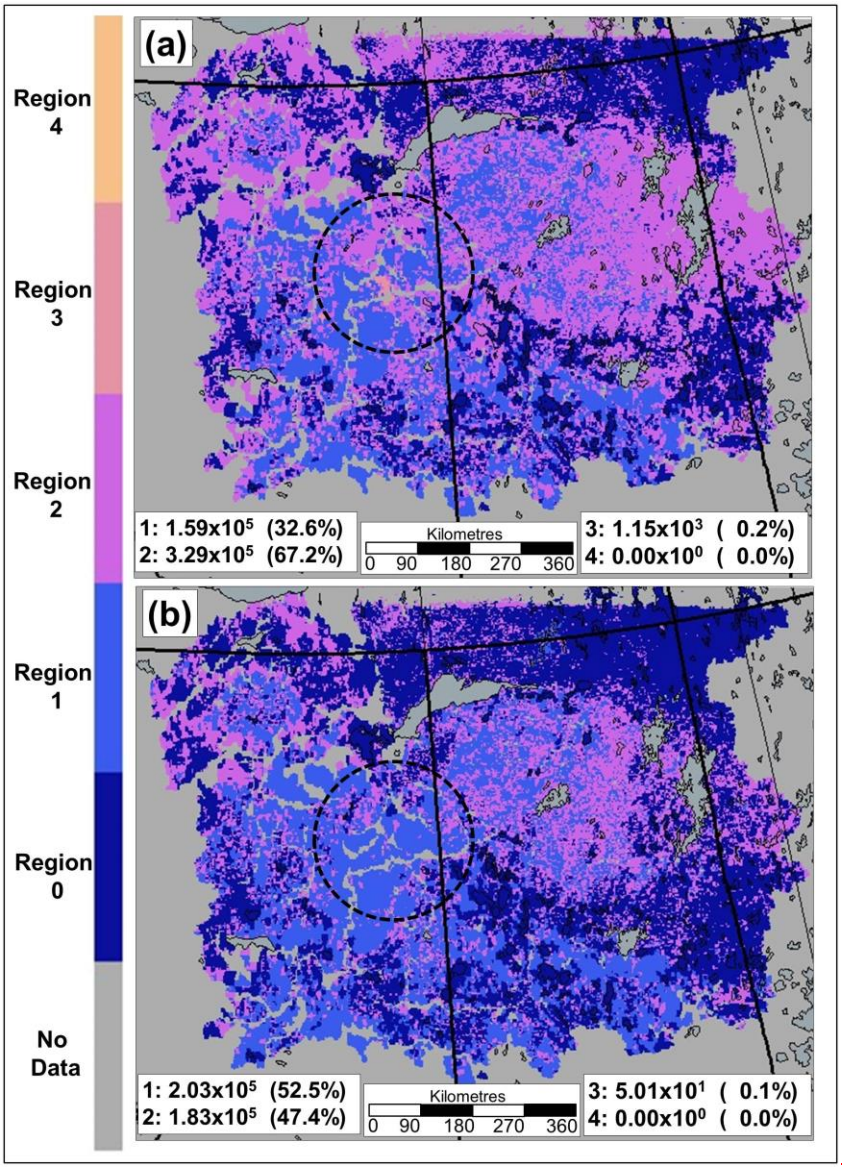
Region 4
Region 3
Region 2
Region 1
Region 0
No Data
(a)
1: 1.59x10^5 (32.6%)
2: 3.29x10^5 (67.2%)
Kilometres
0 90 180 270 360
3: 1.15x10^3 (0.2%)
4: 0.00x10^0 (0.0%)
(b)
1: 2.03x10^5 (52.5%)
2: 1.83x10^5 (47.4%)
Kilometres
0 90 180 270 360
3: 5.01x10^1 (0.1%)
4: 0.00x10^0 (0.0%)

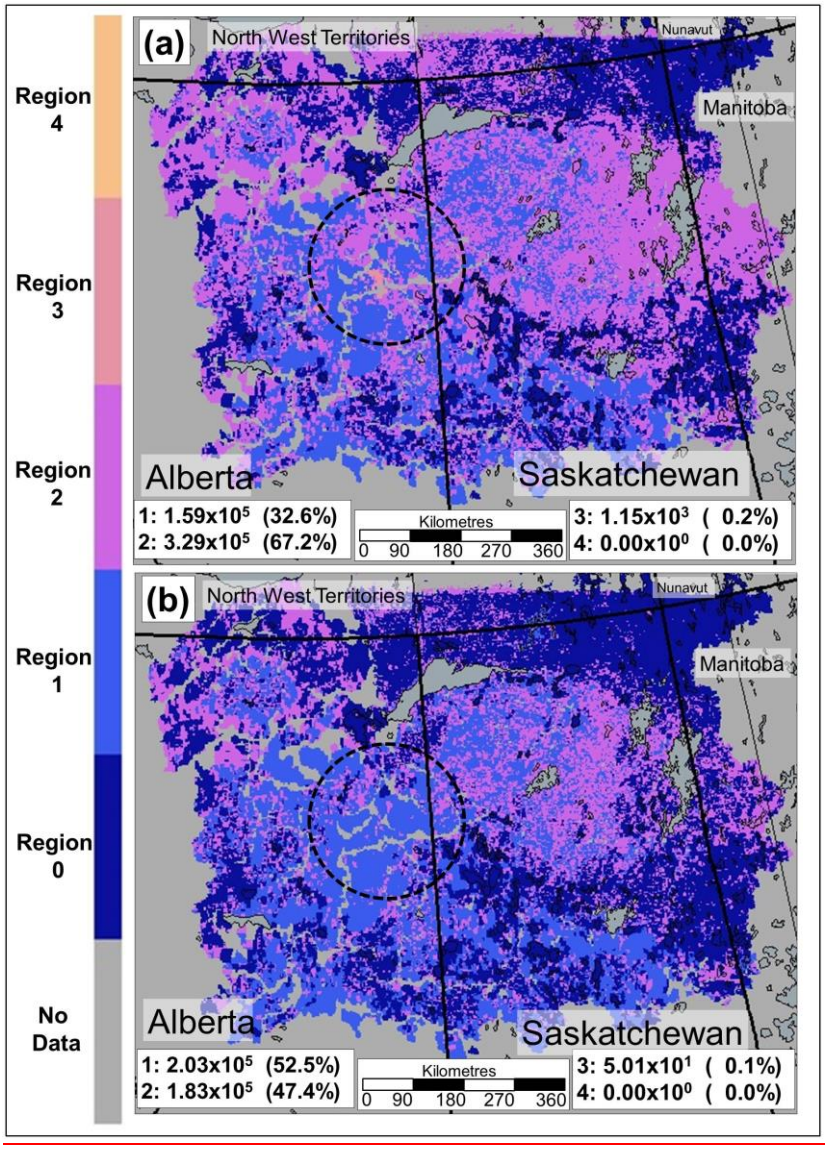

Figure 19. Predicted ~~regions~~sub-types of aquatic ecosystem critical load exceedance (see Figure 1), with respect to deposition of sulphur and nitrogen~~, aquatic ecosystems.~~ deposition.. Boxed numbers give the area in exceedance within each ~~region~~of exceedance sub-types 1, 2, 3 and 4 (km^2) and the corresponding percentage of the total area in exceedance. (a) Calculated using original model sulphur and nitrogen deposition estimates. (b) Calculated using model S_{dep} and N_{dep} estimates corrected to match precipitation observations. Circled region: 140 km radius diameter circle around the Athabasca oil sands.

4 Discussion

The critical load exceedance calculations described in the previous section were carried out with the best currently available datasets and modelling tools. However, the work has also identified limitations of those sources of information, which, if improved, would lead to improved critical load exceedance predictions. In addition, while the calculations identify the potential for ecosystem damage to be taking place now or at some point in the future, additional analysis would be required to estimate the time span to the occurrence of that damage, or to subsequent recovery. We discuss these issues, and make specific recommendations for future work, below.

(1) Clearly, better estimates of the emissions of primary particulate matter and their base cation fractionation are needed, as well as additional ambient concentration and deposition observations of the species contributing to S_{dep}, N_{dep} and BC_{dep} in sensitive regions. We have attempted to correct model results using the available data: comparisons between modelled and observed deposition, and the impact of aircraft-~~observation~~-based estimates of base cation emissions on deposition. Combined, these corrections greatly reduce the bias and improve the ~~bias and~~ correlation fit between observed and estimated base cation deposition to snowpack in the vicinity of the oil sands in winter. Observation-corrected model BC_{dep} values are therefore recommended for future critical load exceedance work. However, in the region examined here, this combined correction amounts to a twenty-five fold increase in base cation emissions relative to the reported values for oil sands sources. We note that the increase may represent underestimates of primary particulate matter emissions by mass, and/or a higher base cation fractionation of that mass than was observed in surface dust collected by Wang *et al.* (2015). Additional measurement-based estimates of speciated primary particulate emissions and ambient concentrations are required to carry out exceedance calculations with improved model performance.

(2) Other work (Whaley *et al.*, ~~2017~~2018) has suggested that bidirectional fluxes of ammonia in the boreal forest region may be taking place, and would account for GEM-MACH underestimates in the column ammonia concentration relative to satellite and aircraft observations. Further research is needed to improve bi-directional flux parameterizations (the parameterization used in the given case improved ammonia performance for the boreal forest, but decreased it for agricultural regions). However, we also note that the bidirectional flux system will result in increased "natural" ammonia fluxes from land, but will not result in upward fluxes of ammonia over water. We have carried out tests which suggest that bidirectional fluxes of ammonia will increase the net flux of ammonia to water-covered surfaces, and hence the net N_{dep} to aquatic ecosystems calculated in the current work should be considered a lower estimate.

(3) As noted earlier, exceedances to critical loads indicate the *potential* for ecosystem damage, but not the timeline over which damage may be expected to occur~~,~~ or has occurred, the time to ecosystem recovery~~,~~ (if acidifying deposition is reduced~~.~~), or the magnitude of the ecosystem impacts of exceedance. These time estimates may be obtained with the use of dynamic models (CLRTAP, ~~2015~~2017), and their use is recommended for targeted studies in the areas we

have predicted to be in exceedance of critical loads. These dynamical modelling studies should be accompanied by measurements in the same specific exceedance areas. In past observational studies of lakes in the environs of the Athabasca oil sands (Hazewinkel *et al.*, 2008; Curtis *et al.*, 2010; Laird *et al.*, 2013), two out of twenty lakes were found to show signs of acidification. These observation locations are depicted in Figure 20, overlaid on the map of exceedances for aquatic ecosystems with respect to S_{dep} of Figure 17(b). Lake sediments from four locations (white symbols, Figure 20) were found to have increasing levels of acidity, but within natural variability (Hazewinkel *et al.*, 2008), two lakes (red symbols, Figure 20) were found to have undergone recent acidification (Curtis *et al.*, 2010; Laird *et al.*, 2013), and the remaining locations (blue symbols, Figure 20) were not found to be acidifying. However, the sediment core stratigraphy within the region was found to be "broadly consistent with increased anthropogenic pressures in the region" (Hazewinkel *et al.*, 2008), and an examination of fifty years of six lake sediment cores found evidence for a factor of 2.5 to 23 increase in the flux of polycyclic aromatic hydrocarbons since the 1960s (Kurek *et al.*, 2013) . One of the acidifying lakes was noted to be relatively shallow and in peaty soil, with the implication that similar lakes may show the effects of acidification first (Curtis *et al.*, 2010). Twelve lake sediment cores showed that the signs of ecological changes such as sediment enrichment have been increasing over the last three decades, and increased phosphorus concentrations in several lakes were attributed to the dry deposition of NO_x (=NO + NO_2) and other forms of N_{dep} (Curtis *et al.*, 2010). However, a study of sediment cores from 15 non-acid-sensitive lakes in northern Saskatchewan did not show evidence of lake enrichment by N_{dep}, based on analysis of algal communities (Laird *et al*, 2017, Mushet *et al*, 2017). Our calculations of aquatic critical load exceedances imply that acidification will eventually occur; Figure 20 highlights the need for ongoing monitoring of aquatic ecosystems in this region. Dynamical modelling (CLRTAP, ~~2015~~2017) would ~~further~~also aid in prioritizing locations for further studies to quantify acidifying effects.

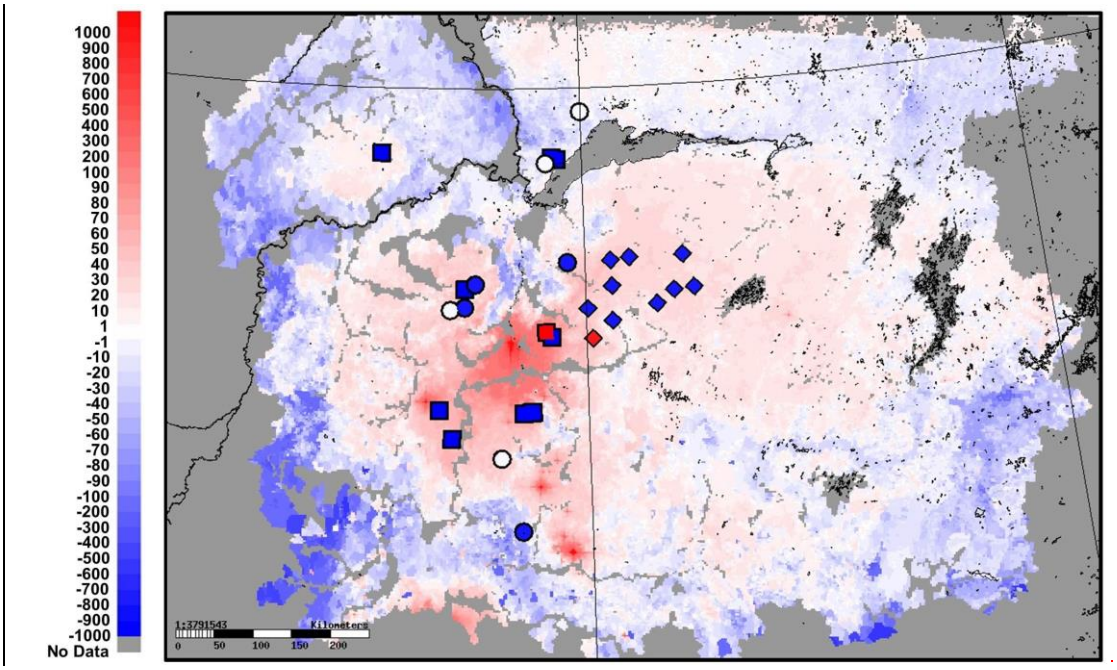
1000
900
800
700
600
500
400
300
200
100
90
80
70
60
50
40
30
20
10
1
-1
-10
-20
-30
-40
-50
-60
-70
-80
-90
-100
-200
-300
-400
-500
-600
-700
-800
-900
-1000
No Data
1:3791543
Kilometers
0 50 100 150 200

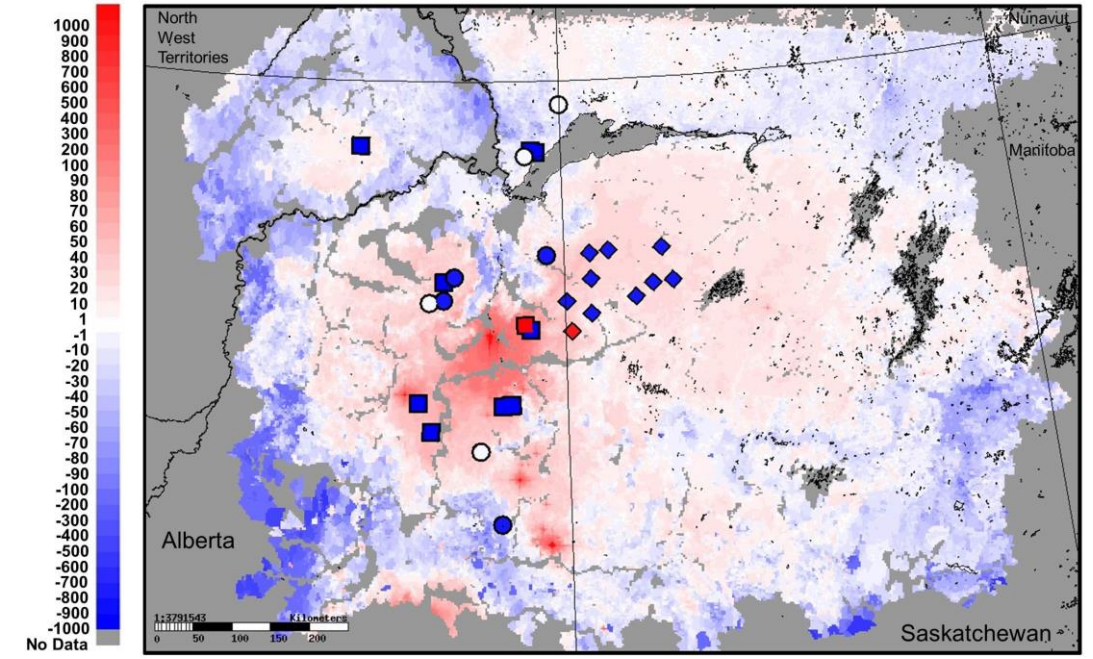

Figure 20. Comparison of predicted exceedances with model S_{dep} corrected to match precipitation observations (Figure ~~18b~~17b, units eq ha^{-1} yr^{-1}) with lake observation data of Hazewinkel *et al.*, 2008 (circles), Curtis *et al.*, 2010 (squares) and Laird *et al.*, 2013 (diamonds). Blue symbols: sample locations showing no acidification at the current time, white symbols: locations with decreasing pH, but within natural variability; red symbols: locations where signs of acidification were detected. Note that the colour of the symbols, which are for illustration purposes only, does not correspond to numerical exceedance values on the colour scale~~, which refers only~~.

Formatted: Font: Italic

(4) Future GEM-MACH simulations should include the full twelve-bin particle size distribution rather than the more computationally efficient operational forecast two-bin particle size distribution used here for the annual simulation, in order to better capture the variation in base cation particle deposition with distance as a function of particle size. We also note that the 142 km drop-off distance associated with BC_{dep} shown here is a function of the size distribution of the emitted fugitive dust particles – while our expectation is that the bulk of fugitive dust emissions are likely to be in the coarse mode (sizes greater than 2.5 mm diameter) as they are here, differences in the initial size distribution may lead to different decrease functions with distance from fugitive dust sources. However, a general result from our findings is that fugitive dust base cation neutralization will be limited in spatial scope, due to the effect of particle deposition increasing with increasing size in the coarse mode.

(5) New measurement studies are needed in order to acquire the data to improve the current parameterizations used for estimating deposition velocities, particularly for gas-phase dry deposition. For example, most current

parameterizations are based on direct observations of SO_2 and O_3, with deposition parameters for other gases being inferred by indirect means, and the temperature dependence of deposition to snowpack has been measured directly for only two species, SO_2 and HNO_3 (see Supplementary Information). ~~-~~Future work to characterize gas deposition, particularly under cold conditions, is therefore recommended. Snowpack deposition observations should attempt to measure both "throughfall" and "open" deposition, in order to more accurately estimate total deposition to snow-covered vegetation.

5 Summary and Conclusions

Our work has predicted that critical loads for acidifying deposition are being exceeded in the provinces of Alberta and Saskatchewan, for both terrestrial and aquatic ecosystems. Model predictions indicate that that total deposition downwind of sources is dominated by the wet component. Model comparisons of sulphur, nitrogen and base cation deposition with observations indicate that the model has some skill in accounting for the observed variability in wet deposition (R^2 of 0.90, 0.76, and 0.72, respectively). We therefore used the model versus observation linear relationships from wet deposition to provide a correction to model values for total deposition of sulphur, nitrogen and base cations. Aircraft ~~observation~~-based estimates of primary particulate matter emissions were shown to result in a factor of 10 increase in atmospheric base cation deposition close to the oil sands emissions regions, and corrections for base cation deposition based on these estimates were also incorporated into our investigation of exceedances. Making use of both the original model predictions and the corrected fields, exceedances of critical loads were calculated using simplified methodologies designed to provide lower limit estimates of exceedances (NEG-ECP, 2001), and more rigorous methodologies to take into account additional factors such as ecosystem buffering capacity (CLRTAP, ~~2004, 2016,~~ 2017). While atmospheric base cation deposition was shown to have a significant neutralizing impact for terrestrial ecosystems close to the sources of fugitive dust emissions, this effect was shown in both observations and model results to drop off rapidly with distance in comparison to the size of the predicted areas of aquatic critical load exceedance, in accord with well-known physics controlling the deposition velocities of atmospheric particles as a function of their size. Exceedances were predicted further downwind, despite these corrections to the original model estimates (which include an assumed factor of twenty-five increase in primary particulate matter emissions from oil sands sources, relative to reported emissions). Aquatic ecosystem critical load data suggest that the base cation loading within catchment waters is insufficient to counteract much of the atmospheric deposition of sulphur and nitrogen. The results thus indicate that potential ecosystem damage may be taking place, due to acidifying deposition in the provinces of Alberta and Saskatchewan. The use of dynamic models to determine the timelines until damage occurs and/or recovery may take place, and observational studies for the presence of ecosystem damage, are recommended for future work, with a focus on the highest exceedance regions predicted here. Further observations of deposition of sulphur, nitrogen and size-resolved base cations are also recommended, at distances greater than 140 km from the sources, to further evaluate and improve on our findings.

Specific results of our work include:

(1) The spatial extent of predicted exceedances of forest and terrestrial ecosystem critical loads range from $1x10^4$ km^2 to $6.69x10^4$ km^2 (10% of the area of the province of Alberta), with the latter estimate based on the more comprehensive critical load calculation ~~protocol~~methodology.

(2) The spatial extent of predicted exceedances of aquatic ecosystem critical loads in the region studied is larger than that of forest and terrestrial ecosystem critical loads. Estimates using both earlier lake observation data and more recent georeferenced data indicate that a significant fraction of northern Alberta and Saskatchewan lakes are predicted to be in exceedance. Some neutralization due to base cation levels in water observations may be occurring immediately to the north of the oil sands, but overall, exceedances are predicted over much of the north of the two provinces, and extend eastwards into Manitoba, for all three of the critical load datasets and ~~protocols~~methodologies employed here.

(3) Our work suggests that other sources of base cations, aside from atmospheric deposition, usually controls the surface water base cation concentration. Our model results and our re-examination of the throughfall data of Watmough *et al.* (2014) suggests that the neutralization associated with base cation deposition from sources of fugitive dust in the oil sands area will be limited in spatial extent. Despite this near-source neutralizing effect, potential ecosystem damage associated with acidifying precipitation may take place further downwind. Nevertheless, our work demonstrates that both natural and anthropogenic base cation emissions may have a significant impact on, and should be included in, critical load exceedance calculations.

(4) We predict that in some portions of the study region, base cation deposition from the atmosphere may exceed the estimated removal of base cations from catchments in water. While the observations of surface water ion content and estimates of the export of water from catchments used to create the critical loads employed here indicate that the base cation level in surface water is insufficient to counteract acidification, there exists the potential for this to change over time. Repeat measurements of catchment water in these regions of potential base cation buildup, and follow-up work to improve and evaluate catchment water export rates, are therefore recommended. Strategies to measure deposition to very acid-sensitive regions (e.g., exceedance (red) regions in Figure 14(c), Figure 17(b), and Figure 18(b)), which are distant from existing conventional deposition monitoring sites, should be considered.

(5) We have found that corrections of model estimates of S_{dep}, N_{dep} and BC_{dep} using observations, and using direct observation-based emissions data for base cations, have a significant impact on model estimates of critical load exceedances. Here, relatively simple corrections using model-observation relationships were employed. We note that other means of model-measurement fusion for acidifying pollutants are under investigation, and show great promise for creating observation-corrected air-quality model deposition fields (e.g. Robichaud *et al.*, 2018).

6 Author Contribution

P.A.M: Study concept and design, analysis of model output and critical load exceedances, writing of manuscript and modifications of same; A.A.: GEM-MACH simulations, assistance with model evaluation and analysis; J.A.: critical load data section of text, provision of aquatic ecosystem critical loads; A.S.C: preparation of precipitation deposition data, assistance with new and historical aquatic critical load data sections of manuscript; Y.A.: AEP terrestrial ecosystem critical load data and description and AEP precipitation data; J.Z: creation of emissions files used in the model,; I. Wong: provision of ECCC ~~Lakes~~lakes and ~~Forest~~forest critical load data; K.H. and S-M.L.: provision of aircraft data; J.K.: provision of ECCC snowpack data and text on same; K.S.: provision of Saskatchewan Environment snowpack data and text on same; M.D.M: assistance with emissions data for model; A.R.: creator of the gas-phase dry deposition module in GEM-MACH, and assistance with Supplement 1 text; H.C: creation and provision of aquatic critical load data; P.B.: assistance with generation of emissions data; B.P. and P.C.: assistance with GEM-MACH setup, model simulations; Q. Zheng: assistance with emissions generation. In addition, the first author would like to thank all co-authors for extensive comments on different versions of the manuscript.

7 Acknowledgements

This project was jointly supported by the Climate Change and Air Quality Program of Environment and Climate Change Canada, Alberta Environment and Parks, and the Joint Oil Sands Monitoring program.

8 References

AAF, 2017:— Alberta Agriculture and Forestry, Alberta Climate Information Service (ACIS), https://agriculture.alberta.ca/acis (last accessed May 2017)

AAF, 2015: Alberta Agriculture and Forestry, Forest Resource Analysis Section, Forest Management Branch, (*personal communication*).

AAFC, 2010: Soil Landscapes of Canada version 3.2., Soil Landscapes of Canada Working Group, Agriculture and Agri-Food Canada (digital map and database at 1:1 million scale), 2010. http://sis.agr.gc.ca/cansis/nsdb/slc/v3.2/index.html. Last accessed August 25, 2017.

ABMI, 2010:— Alberta Biodiversity Monitoring Institute, Wall-to-wall land cover map version 2.1 (ABMIw2wLCV2010v1.0), 2010. http://www.abmi.ca/home/data/gis-data/land-cover-inventory.html. Last accessed August 25, 2017.

Aherne, J, Uncertainty in critical load exceedance (UNCLE): critical loads uncertainty and risk analysis for Canadian forest ecosystems, 22pp, Canadian Council of Ministers of the Environment, report PN XXXX, 2011.

Aherne J. & Posch M. Impacts of nitrogen and sulphur deposition on forest ecosystem services in Canada. *Current Opinion in Environmental Sustainability*, 5, 108-115, 2013.

Akingunola , A., Makar, P.A., Zhang, J., Darlington, A., Li, S.-M., Gordon, M., Moran, M.D., and Zheng, Q., A chemical transport model study of plume rise and particle size distribution for the Athabasca oil sands, accepted, Atmos. Chem. Phys., https://doi.org/10.5194/acp-2018-15, 2018.

Aklilu, Y.-a., Blair, L., Aherne, J., & Dinwoodie, G., *Determining Critical Loads of Acidity for Terrestrial Ecosystems in Alberta*. Alberta Environment and Parks, 2018.

Alberta, 2016: Government of Alberta. Extended Alberta Vegetation Index, Dominant Forest Cover, 2016, http://aep.alberta.ca/forms-maps-services/maps/resource-data-product-catalogue/forest-vegetation-inventories.aspx, last accessed October 23, 2017.

Alberta Environment and Parks, 2016. Surface water quality database. URL: aep.alberta.ca/water/reports-data/surface-water-quality-data/default.aspx.

Baldocchi, D.D., Hicks, B.B., Camara, P., A canopy stomatal resistance model for gaseous deposition to vegetated surfaces, Atm. Env., 21, 91-101, 1987

Baker, L.A., Brezonik, P.L., Dynamic model of in-lake alkalinity generation. Water Resources Research, 24(1), 65–74, 1988.

Baklanov, A., Schlunzen, K., Suppan, P., Baldasano, J., Brunner, D., Aksoyoglu, S., Carmichael, G., Douros, J., Flemming, J., Forkel, R., Galmarini., S., Gauss, M., Grell, G., Hirtl, M., Joffre., S., Jorba, O., Kaas, E., Kaasik, M., Kallos, G., Kong, X., Korsholm, U., Kurganskiy, A., Kusta., J., Lohmann, U., Mahura, A., Manders-Groot, A., Maurizi, A., Moussiopoulos, N., Rao, S.T., Savage, N., Siegneur, C., Sokhi, R.S., Solazzo, E., Solomos, S., Sorensen, B., Tsegas, G., Vignati, E., Vogel, B., and Zhang, Y., Online coupled regional meteorology chemistry models in Europe: current status and prospects, Atm. Chem. and Phys., 14, 317-398, 2014.

Beaudoin, A., Bernier, P.Y., Guindon, L., Villemaire, P., Guo, X.J., Stinson, G., Bergeron, T., Magnussen, S., and Hall, R.J., Mapping attributes of Canada's forests at moderate resolution through kNN and MODIS imagery. Canadian Journal of Forest Research, 44, 521–532, 2014.

Binkowski, F.S., and Roselle, S.J., Models-3 Community Multiscale Air Quality (CMAQ) model aerosol component1. Model Description, J. Geophys. Res., 108, No. D6, 4183, doi: 10.1029/2001JD001409, 18 pp., 2003.

Binkowski, F.S., and Shankar, U., The regional particulate model, 1, Model description and preliminary results, J. Geophys. Res., 100, 26,191-26,209, 1995.

Brook, J.R., Zhang, L., Di-Giovanni, F., Padro, J., Description and evaluation of a model of deposition velocities for routine estimates of air pollutant dry deposition over North America. Part I: model development. Atm Env., 33, 5037-5051, 1999.

Calvert, J.G., and Stockwell, W.R., Acid generation in the troposphere by gas-phase chemistry, Environ. Sci. Tech., 11, 1181-1185, 1977.

Carou, S., Dennis, I. Aherne, J., Ouimet, R., Arp, P.A., Watmough, S.A., DeMerchant, I., Shaw, M., Vet, B., Bouchet, V. and Moran, M.: A national picture of acid deposition critical loads for forest soils in Canada. *Canadian Council of Ministers of the Environment, PN 1412*, 6 pp, 2008.

Cathcart H., Aherne, J., Jeffries, D., and Scott K., Critical loads of acidity for 90,000 lakes in northern Saskatchewan: A novel approach for mapping regional sensitivity to acidic deposition, Atmospheric Environment, 146, 290-299, 2016.

Chang, J.S., Brost, R.A., Isaksen, I.S.A., Madronich, S., Middleton, P., Stockwell, W.R., Walcek, C.J., A three-dimensional Eulerian acid deposition model: physical concepts and formulation, J. Geophys. Res., 92, 14,681-14,700, 1987.

CLRTAP ~~2004~~2017. Manual on methodologies and criteria for modelling and mapping critical loads and levels and air pollution effects, risks and trends. http://icpmapping.org/Latest_update_Mapping_Manual Last accessed August 15, 2017.

~~CLRTAP, 2015: Dynamic modelling, Chapter VI of Manual on methodologies and criteria for modelling and mapping critical loads and levels and air pollution effects, risks and trends. UNECE Convention on Long-range Transboundary Air Pollution, http://icpmapping.org/Latest_update_Mapping_Manual. Last accessed August 15, 2017.~~

~~CLRTAP, 2016: Guidance on mapping concentration levels and deposition levels, Chapter VII: Exceedance calculations of Manual on Methodologies and criteria for modelling and mapping critical loads and levels and air pollution effects, risks and trends. UNECE Convention on Long-range Transboundary Air Pollution, 2016. http://icpmapping.org/Latest_update_Mapping_Manual. Last accessed August 15, 2017.~~

~~CLRTAP, 2017: Guidance on mapping concentration levels and deposition levels, Chapter V, Critical Loads for Ecosystems. UNECE Convention on Long-range Transboundary Air Pollution, 2016. http://icpmapping.org/Latest_update_Mapping_Manual. Last accessed August 15, 2017.~~

Curtis, C. J., Flower, R., Rose, N., Shilland, J., Simpson, G. L., Turner, S., Yang, H., and Pla, S.: Paleolimnological assessment of lake acidification and environmental change in the Athabasca Oil Sands Region, Alberta, J. Limnol., 69, 92-104, 2010.

Dasch, J.M., and Cadle, S.H., Dry deposition to snow in an urban area, Water, Air and Soil Pollution, 29, 297-308, 1986.

de Vries, W., Hettelingh, J-P. and Posch M. (eds), Critical Loads and Dynamic Risk Assessments: Nitrogen, Acidity and Metals in Terrestrial and Aquatic Ecosystems. Springer, Dordrecht, Netherlands 647pp, 2015.

Elisassen, A., Hov, O., Isaksen, I.S.A., Saltbones, J., Stordal, F., A Lagrangian long-range transport model with atmospheric boundary layer chemistry, J. App. Met., 21, 1645-1661, 1982.

Ellsworth, D.S. and Reich, P.B., Canopy structure and vertical patterns of photosynthesis and related leaf traits in a deciduous forest, Oecologia, 96, 169-178, 1993.

Environment and Climate Change Canada. 2004: Canadian acid deposition science assessment 2004. 440 pp. http://publications.gc.ca/pub?id=9.650140&sl=0 (last accessed: May 29, 2017).

ECCC, 2017: Environment and Climate Change Canada, http://climate.weather.gc.ca/. Last accessed May, 2017.

Gong, S.L., Barrie, L.A., Lazare, M., Canadian Aerosol Module (CAM): a size-segregated simulation of atmospheric aerosol processes for climate and air quality models 2. Global sea-salt aerosol and its budgets. J. Geophys. Res. 107, 4779. http://dx.doi.org/10.1029/2001JD002004, 2003(a).

Gong, S.L., Barrie, L.A., Blanchet, J.-P., von Salzen, K., Lohmann, U., Lesins, G.,Spacek, L., Zhang, L.M., Girard, E., Lin, H., Leaitch, R., Leighton, H., Chylek, P.,Huang, P., 2003b. Canadian Aerosol Module: a size-segregated simulation of atmospheric aerosol processes for climate and air quality models. 1. Module development. J. Geophys. Res. 108, 4007. http://dx.doi.org/10.1029/2001JD002002, 2003(b)

Gong, W., A.P. Dastoor, V.S. Bouchet, S.L. Gong, P.A. Makar, M.D. Moran, B. Pabla, S. Menard, L-P. Crevier, S. Cousineau and S. Venkatesh,: Cloud processing of gases and aerosols in a regional air quality model (AURAMS), *Atmospheric Research* 82 (1-2), 248-275, 2006.

Gordon, M., Li,, S-M., Staebler, R., Darlington, A., Hayden, K., O'Brien, J., and Wolde, M., Determining air pollutant emission rates based on mass balance using airborne measurement data over the Alberta oil sands operations, Atmos. Meas. Tech., 8, 3745-3765, 2015.

Gordon, M., Makar, P.A., Staebler, R.M., Zhang, J., Akingunola, A., Gong, W., and Li, S.-M., A comparison of plume rise algorithms to stack plume measurements in the Athabasca oil sands, revised manuscript under review for *Atmos. Chem. Phys*, 2018.

Grell, G.A., Peckham, S.E., Schmitz, R., McKeen, S.A., Frost, G., Skamarock, W.C., Eder, B., Fully coupled "online" chemistry within the WRF model, Atm. Env., 39, 6957-6975, 2005.

Hazewinkel, R. R. O., Wolfe, A. P., Curtis, C., and Hadley, K.: Have atmospheric emissions from the Athabasca Oil Sands impacted lakes in northeastern Alberta, Canada?, Can. J. Fish Aquat. Sci., 65, 1554-1567, 2008.

Hengl, T., Heuvelink, G.B., and Rossiter, D.G., About regression-kriging: from equations to case studies. Computers and Geosciences, 33, 1301-1315, 2007.

Hengl, T., A practical guide to geostatistical mapping. University of Amsterdam, 2009.

Henriksen, A. and Posch.: Steady-state models for calculating critical loads of acidity for surface waters. *Water Air Soil Poll.: Focus 1*, 375-398, 2001.

~~Henriksen, A. Changes in base cation concentrations due to freshwater acidification. Verh. Internat. Verein. Limnol., 22, 692–698, 1984.~~

Hicks, B.B, Baldocchi, D.D., Meyers, T.P., Hosker, R.P. Jr, Matt, D.R., A preliminary multiple resistance routine for deriving dry deposition velocities from measured quantities, Water, Air, and Soil Poll., 36, 311-330, 1987.

Formatted: Hyperlink, Font: +Body (Times New Roman), English (U.K.)

Formatted: Font: +Body (Times New Roman)

Hosker, R.P. Jr., and Lindberg, S.E., Review: atmospheric deposition and plant assimilation of gases and particles, Atm. Env., 16, 889-910, 1982.

Im, U., Roberto Bianconi, R., Efisio Solazzo, E., Kioutsioukis, I., Badia, A., Balzarini, A., Baró, R., Bellasio, R., Brunner, D., Chemel, C., Curci, G., Flemming, J., Forkel, R., Giordano, L., Jiménez-Guerrero, P., Hirtl, M., Hodzic, A., Honzak, L., Jorba, O., Knote, C., Kuenen, J.J.P, Makar, P.A., Manders-Groot, A., Neal, L, Perez, J.L., Pirovano, G., Pouliot, G., San Jose, R., Savage, N., Schroder, W., Sokhi, R.S., Syrakov, D., Torian, A., Tuccella, P., Werhahn, J., Wolke, R., Yahya, K., Zabkar, R., Zhang, Y., Zhang, J., Hogrefe, C., Galmarini, S., Evaluation of operational on-line-coupled regional air quality models over Europe and North America in the context of AQMEII phase 2. Part I: Ozone, *Atm. Env.*, 115, 404-420, 2015(a).

Im, U., Bianconi, R., Solazzo, E., Kioutsioukis, I., Badia, A., Balzarini, A., Baró, R.., Bellasio, R., Brunner, D., Chemel, C., Curci, G., van der Gon, H.D., Flemming, J., Forkel, R., Giordano, L., Jiménez-Guerrero, P., Hirtl, M., Hodzic, A., Honzak, L, Jorba, O., Knote, C., Makar, P.A., Manders-Groot, A., Neal, L, Perez, J.L, Pirovano, G., Pouliot, G., San Jose, R., Savage, N., Schroder, W., Sokhi, R.S., Syrakov, D., Torian, A, Tuccella, P., Wang, K., Werhahn, J., Wolke, R., Zabkar, R., Zhang, Y., Zhang, J., Hogrefe, C., Galmarini, S., Evaluation of operational on-line-coupled regional air quality models over Europe and North America in the context of AQMEII phase 2. Part II: Particulate Matter, *Atm. Env.*, 115, 421-411, 2015(b).

Jacobson, M.Z., Fundamentals of Atmospheric Modelling, Cambridge U. Press, 656pp, 1999.

Jarvis, P.G., The interpretation of the variations in leaf water potential and stomatal conductance found in canopies in the field, Phil. Trans. R. Soc. Lond., B., 273, 593-610, 1976.

Jeffries, D.S. and Ouimet, R. (eds.): Chapter 8: Critical Loads – Are they being exceeded? *in* 2004 Canadian Acid Deposition Science Assessment, Environment Canada, Ottawa, Ontario, pp. 341-368, 2005.

Jeffries, D.S., Semkin, R.G., Gibson, J.J. and Wong, I.: Recently surveyed lakes in northern Manitoba and Saskatchewan, Canada: characteristics and critical loads of acidity. *J. Limnol*. 69(Suppl. 1): 45-55, 2010.

Kaste, Ø. and Dillon, P.J., Inorganic nitrogen retention in acid-sensitive lakes in southern Norway and southern Ontario, Canada - a comparison of mass balance data with an empirical N retention model. Hydrol. Process. 17, 2393–2407, 2003.

Kirk, J. L., Muir, D., Gleason, A., Wang, X., Frank, R., Lehnherr, I. , Wrona, F. Atmospheric deposition of mercury and methyl mercury to landscapes and waterbodies of the Athabasca oil sands region. Env.Sci. and Tech., 48, 7374–7383, 2014.

Kelly, C.A., Rudd, J.W.M., Hesslein, R.H., Schindler, D.W., Dillon, P.J., Driscoll, C.T., Ghereni, S.A. and Hecky, R.E. Prediction of biological acid neutralization in acid-sensitive lakes. Biogeochemistry, 3, 129–140, 1987.

Kelly, E. N., Short, J. W., Schindler, D. W., Hodson, P. V., Ma, M., Kwan, A. K., and Fortin, B. L. Oil sands development contributes polycyclic aromatic compounds to the Athabasca River and its tributaries. P. Natl. Acad. Sci.,, 106, 22346-22351, 2009.

Kelly, E. N., Schindler, D. W., Hodson, P. V., Short, J. W., Radmanovich, R., and Nielson, C. C. Oil sands development contributes elements toxic at low concentrations to the Athabasca River and its tributaries. P. Natl. Acad. Sci.,. 107, 16178-16183, 2010.

Kurek J, Kirk J.L., Muir, D.C.G., Wang X., Evans, M.S., Smol, J.P. The legacy of a half century of Athabasca oil sands development recorded by lake ecosytems. P. Natl. Acad. Sci., 110, 1761-1766, 2013.

Laird, K. R., Das, B., Kingsbury, M., Moos, M. T., Pla-Rabes, S., Ahad, J. M. E., Wiltse, B., and Cumming, B. F.: Paleolimnological assessment of limnological change in 10 lakes from northwest Saskatchewan downwind of the Athabasca oils sands based on analysis of siliceous algae and trace metals in sediment cores, Hydrobiologia, 720, 55-73, 2013.

Laird, K.R., Das, B., Hesjedal, B., Leavitt, P.R., Mushet, G.R., Scott, K. A. , Simpson, G.L., Wissel, B. , Wolfe, J. , and Cumming, B.F.. Paleolimnological assessment of nutrient enrichment on diatom assemblages in *a priori* defined nitrogen- and phosphorus-limited lakes downwind of the Athabasca Oil Sands, Canada. J. Limnol. DOI: https://doi.org/10.4081/jlimnol.2017.1598, 2017.

Li, S.-M., Leithead, A., Moussa, S. G., Liggio, J., Moran, M. D., Wang, D., Hayden, K., Darlington, A., Gordon, M., Staebler, R., Makar, P. A., Stroud, C. A., McLaren, R., Liu, P. S. K., O'Brien, J., Mittermeier, R. L., Zhang, J., Marson, G., Cober, S. G., Wolde, M., and Wentzell, J. J. B.: Differences between measured and reported volatile organic compound emissions from oil sands facilities in Alberta, Canada, Proceedings of the National Academy of Sciences of the United States of America, 114, E3756–E3765, 2017.

Liggio, J., Moussa, S.G., Wentzell, J., Darlington, A., Liu, P., Leithead, A., Hayden, K., O'Brien, J., Mittermeier, R.L., Staebler, R., Wolde, M., and Li, S.-M., Understanding the primary emissions and secondary formation of gaseous organic acids in the oil sands region of Alberta, Canada, Atmos. Chem. Phys., 17, 8411-8427, 2017.

Liggio, J., Li, S. M., Hayden, K., Taha, Y. M., Stroud, C., Darlington, A., Drollette, B. D., Gordon, M., Lee, P., Liu, P., Leithead, A., Moussa, S. G., Wang, D., O'Brien, J., Mittermeier, R. L., Brook, J. R., Lu, G., Staebler, R. M., Han, Y., Tokarek, T. W., Osthoff, H. D., Makar, P. A., Zhang, J., Plata, D. L., and Gentner, D. R.: Oil sands operations as a large source of secondary organic aerosols, Nature, 534, 91–94, https://doi.org/10.1038/nature17646, 2016.

Lurmann, F.W., Lloyd, A.C., and Atkinson, R., A chemical mechanism for use in long-range transport/acid deposition computer modeling. J. Geophys. Res., 29, 10905-10936, 1986.

Lydersen, E., Larssen, T. and Fjeld, E., The influence of total organic carbon (TOC) on the relationship between acid neutralizing capacity (ANC) and fish status in Norwegian lakes. Sci. Tot. Environ. 326, 63-69, 2004.

Makar, P.A., Bouchet, V.S., and Nenes, A., Inorganic Chemistry Calculations using HETV – A Vectorized Solver for the SO_4^{2-}-NO_3^--NH_4^+ system based on the ISORROPIA Algorithms, *Atm. Env.*, 37, 2279-2294, 2003.

Makar, P.A., Gong, W., Milbrandt, J., Hogrefe, C., Zhang, Y., Curci, G., Zabkar, R., Im, U., Balzarini, A., Baro, R., Bianconi, R., Cheung, P., Forkel, R., Gravel, S., Hirtl, H., Honzak, L., Hou, A., Jimenz-Guerrero, P., Langer, M.,

Moran, M.D., Pabla, B., Perez, J.L., Pirovano, G., San Jose, R., Tuccella, P., Werhahn, J., Zhang, J., Galmarini, S., Feedbacks between air pollution and weather, part 1: Effects on weather. *Atm. Env.*, 115, 442-469, 2015 (a).

Makar, P.A., Gong, W., Hogrefe, C., Zhang, Y., Curci, G., Zabkar, R., Milbrandt, J., Im, U., Balzarini, A., Baro, R., Bianconi, R., Cheung, P., Forkel, R., Gravel, S., Hirtl, H., Honzak, L., Hou, A., Jimenz-Guerrero, P., Langer, M., Moran, M.D., Pabla, B., Perez, J.L., Pirovano, G., San Jose, R., Tuccella, P., Werhahn, J., Zhang, J., Galmarini, S., Feedbacks between air pollution and weather, part 2: Effects on chemistry. *Atm. Env.*, 115, 499-526, 2015 (b).

Makar, P.A., Staebler, R.M., Akingunola, A., Zhang, J., McLinden, C., Kharol, S.K., Pabla, B., Cheung, P. and Zheng, Q. , The effects of forest canopy shading and turbulence on boundary layer ozone, *Nature Communications*, **8**, art. no. 15243, doi: 10.1038/ncomms15243, 2017.

Manzano, C., Muir, D., Kirk, J.L., Teixeira, C., Siu, M., Wang, X., Charland, J.P., Schindler D., and Kelly, E.. Temporal variation in the deposition of polycyclic aromatic compounds in snow in the Athabasca Oil Sands area of Alberta. Environmental Monitoring and Assessment 188: 542, 12pp, 2016.

Meyers, T.P., Finkelstein, P., Clarke, J., Ellestad, T.G., Sims, P.F., A multilayer model for inferring dry deposition using standard meteorological measurements, J. Geophs. Res., 103, 22,645-22,661, 1998.

Milbrandt, J.A., Yau, M.K., A multimoment bulk microphysics parameterization. Part I: analysis of the role of the spectral shape parameter. J. Atmos. Sci., 62, 3051-3064, 2005(a).

Milbrandt, J.A., Yau, M.K., 2005b. A multimoment bulk microphysics parameterization. Part II: a proposed three-moment closure and scheme. J. Atmos. Sci. 62, 3065-3081, 2005(b).

Mitchell, T.D., Carter, T.R., Jones, P.D., Hulme, M. and New, M., A Comprehensive Set of High-Resolution Grids of Monthly Climate for Europe and the Globe: the Observed Record (1901–2000) and 16 Scenarios (2001–2100). Tyndall Centre for Climate Change Research Working Paper 55, 30 pp., 2004.

Moran M.D., S. Ménard, D. Talbot, P. Huang, P.A. Makar, W. Gong, H. Landry, S. Gravel, S. Gong, L-P. Crevier, A. Kallaur, M. Sassi, Particulate-matter forecasting with GEM-MACH15, a new Canadian air-quality forecast model. In: Steyn DG, Rao ST (eds) *Air Pollution Modelling and Its Application XX*, Springer, Dordrecht, pp. 289-292, 2010.

Munoz-Alpizar, R., Pavlovic, R., Moran, M.D., Chen, J., Gravel, S., Henderson, S.B., Ménard, S., Racine, J., Duhamel, A., Gilbert, S., Beaulieu, P.-A., Landry, H., Davignon, D., Cousineau, S. and Bouchet, V., Multi-year (2013–2016) $PM_{2.5}$ wildfire pollution exposure over North America as determined from operational air quality forecasts. *Atmosphere*, **8**, 179, doi:10.3390/atmos8090179, 24 pp, 2017.

Mushet, G.R., Laird, K.R., Das, B., Hesjedal, B., Leavitt, P.R., Scott, K.A., Simpson, G.L., Wissel, Björn, Wolfe, J.D., and Cumming, B.F., Regional climate changes drive increased scaled-chrysophyte abundance in lakes downwind of Athabasca Oil Sands nitrogen emissions, J. Paleolimnol., DOI 10.1007/s10933-017-9987-6, 2017.

Formatted: Font: +Body (Times New Roman)

Formatted: Font: +Body (Times New Roman), 10 pt

Formatted: Font: +Body (Times New Roman)

Nasr, M. Castonguay, M., Ogilvie, J., Raymond, B.A., and Arp, P.A., Modelling and mapping critical loads and exceedances for the Georgia Basin, British Columbia, using a zero base-cation depletion criterion, J. Limnol., 69 (Suppl. 1), 181-192, 2010.

NEG-ECP 2001: Critical Load of Sulphur and Nitrogen Assessment and Mapping Protocol for Upland Forests. New England Governors and eastern Canadian Premiers Environment Task Group, Acid Rain Action Plan, Halifax, Canada, 2001.

Nenes, A., Pilinis, C., Pandis, S.N., Continued development and testing of a new thermodynamic aerosol module for urban and regional air quality models, Atm. Env., 33, 1533-1560, 1999.

Nilsson, J., and Grennfelt, P., Critical loads for sulphur and nitrogen. Report from a workshop held at Skokloster, Sweden 19-24 March 1988. Miljorapport 15, 1-418.

Ouimet R. Cartographie des Charges Critiques d'Acidité des Forêts: Deuxième Approximation. Gouvernement du Québec Ministère des Ressources naturelles et de la Faune. Direction de la recherche forestière. Rapport interne n° 487, 48pp, 2005.

Pardo, L., Robin-Abbott, M., Duarte, N. and Miller, E.K., –Tree Chemistry database (version 1.0). Tech. Rep. NE-324. USDA Forest Service, Newtown Square, PA, 45 pp., 2005.

Paré, D., Titus, B., Lafleur, B., Maynard, D., and Thiffault, E., Canadian Tree Nutrient Database. URL: apps-scf-cfs.rncan.gc.ca/calc/en/biomass-calculator, 2012.

Pavlovic, R., Chen, J., Anderson, K., Moran, M.D., Beaulieu, P.-A., Davignon, D. and Cousineau, S., The FireWork air quality forecast system with near-real-time biomass burning emissions: Recent developments and evaluation of performance for the 2015 North American wildfire season. *J. Air & Waste Manage. Assoc.*, 66, 819-841, DOI:10.1080/10962247.2016.1158214, 2016.

Posch, M., Aherne, J., Forsius, M. & Rask, M., Past, present, and future exceedance of critical loads of acidity for surface waters in Finland. Environ. Sci. Technol. 46, 4507-4514, 2012.

Pregitzer, K. S., Dickmann, D. I., Hendrick, R., H., & Nguyen, P., Whole-tree Carbon And Nitrogen Partitioning in Young Hybrid Poplars. Tree Physiology, 7, 79-93, 1990.

RAMP, 2016. Acid Sensitive Lakes Monitoring Database. Regional Aquatics Monitoring Program (RAMP). URL: www.ramp-alberta.org/ramp/data.aspx, 2016.

Robichaud, A., Cole, A., Moran, M.D., Lupu, A., Shaw, M., Roy, G., Beauchemin, M., Fortin, V., and Vet, R., Total deposition maps evaluated from measurement-model fusion in North America (ADAGIO project), In: Mensink C., Gong, W., and Hakami, A., (eds) *Air Pollution Modeling and its Application XXVI. ITM 2018*, Ottawa, Canada. *in press* Springer Proceedings in Complexity, 2018.

Scott, K. A., Wissel, B., Gibson, J. J. & Birks, J. S., Chemical characteristics and acid sensitivity of boreal headwater lakes in northwest Saskatchewan. J. Limnol. 69, 33-44, 2010.

Slinn, W.G.N., Predictions for particle deposition to vegetative surfaces. Atmospheric Environment 16, 1785-1794, 1982.

Formatted: Font: +Body (Times New Roman)

Formatted: English (U.S.)

Formatted: English (U.S.)

Formatted: English (U.S.)

Formatted: English (U.S.)

Slootweg, J., Posch, M. & Hettelingh, J.-P., Progress in the modelling of critical thresholds and dynamic modelling, including impacts on vegetation in Europe: CCE Status Report 2010. (RIVM Report No. 680359001). The Netherlands: Coordination Centre for Effects, 2010.

Sverdrup, H., de Vries, W.: Calculating critical loads for acidity with the simple mass balance method. Water Air Soil Poll. 72, 143-162, 1994.

Stockwell, W.R. and Lurmann, F.W., Intercomparison of the ADOM and RADM Gas-Phase Chemical Mechanisms, Electric Power Institute Topical Report, 3412 Hillview Avenue, Palo Alto, Ca., 1989.

USGS, 2013. The 2010 Land Cover of North America at 250 meters. URL: www.cec.org/naatlas.

~~ValMartin~~Val Martin, M., Heald, C.L., and Arnold, S.R., Coupling dry deposition to vegetation phenology in the Community Earth System Model: implications for the simulation of surface O_3, Geoph. Res. Lett., 41, 2988-2996, 2014.

Venkatram, A., and Karamchandani, P.K., Testing a comprehensive acid deposition model, Atm. Env., 22, 737-747, 1988.

Vet, R., Artz, R.S., Carou, S., Shaw, M., Ro, C-U., Aas, W., Baker, A., Bowersox, V.C., Dentener, F., Galy-Lacaux, C., Hou, A., Pienaar, J.J., Gillet, R., Forti, M.C., Gromov, S., Hara, H., Khodzher, T., Mahowald, N.M., Nickovic, S., Rao, P.S.P, Reid, N.W., A global assessment of precipitation chemistry and deposition of sulphur, nitrogen, sea salt, base cations, organic acids, acidity and pH, and phosphorus, Atm. Env., 93, 3-100, 2014.

Vogel, B., Vogel, H., Bäumer, D., Bangert, M., Lundgren, K., Rinke, R., and Stanelle, T.: The comprehensive model system COSMOART – Radiative impact of aerosol on the state of the atmosphere on the regional scale, Atmos. Chem. Phys., 9, 8661–8680, 2009.

Voldner, E.C., Barrie, L.A., and Sirois, A., A literature review of dry deposition of oxides of Sulphur and nitrogen with emphasis on long-range transport modelling in North America, Atm. Env., 20, 2101-2123, 1986.

Wang, X., Chow, J.C., Kohl, S.D., Percy, K.E., Legge, A.H., and Watson, J.G., Characterization of $PM_{2.5}$ and PM_{10} fugitive dust source profiles in the Athabasca Oil Sands Region, J. Air & Waste Management Association, 65, 1421-1433, 2015.

Watmough, S.A., Whitfield, C.J., and Fenn, M.E., The importance of atmospheric base cation deposition for preventing soil acidification in the Athabasca Oil Sands Region of Canada, Sci. Tot. Env., 493, 1-11, 2014.

Wesely, M.L., Parameterization of surface resistances to gaseous dry deposition in regional-scale numerical models, Atm. Env., 23, 1293-1304, 1989.

Wesely, M. L., Cook, D. R. and Hart, R. L. Measurements and parameterization of particulate sulfur dry deposition over grass, J. Geophys. Res., 90, 2131–2143, 1985.

Wesely, M.L.~~,~~ and Hicks, B.B., ~~A review of~~ Some factors that affect the ~~current status of knowledge on dry~~ deposition~~, Atm. Env, 34, 2261-2282, 2000.~~ rates of sulfur dioxide and similar gases on vegetation, J. Air Poll. Control Assoc., 27, 1110-1116, 1977.

Formatted: HTML Cite

Formatted: HTML Cite

Formatted: HTML Cite

Formatted: HTML Cite

Formatted: English (U.S.)

Wesely, M.L., and Hicks, B.B., A review of the current status of knowledge on dry deposition, Atm. Env, 34, 2261-2282, 2000.

Whaley, C.H., Makar, P.A., Shepherd, M.W., Zhang, L., Zhang, J., Zheng, Q., Akingunola, A., Wentworth, G.R., Murphy, J.G., Kharol, S.H., and Cady-Pereira, K.E., Contributions of natural and anthropogenic sources to ambient ammonia in the Athabasca oil sands and north-western Canada, Atmos. Chem. Phys., 18, 2011-2034, https://doi.org/10.5194/acp-18-2011-2018, 2018.

Whitfield CJ, Aherne J, Watmough SA, McDonald M. Estimating the sensitivity of forest soils to acid deposition in the Athabasca Oil Sands Region, Alberta. J Limnol, 69(1s):201–8, 2010.

WMO/GAW, 2004, 2015: Manual for the GAW Precipitation Chemistry Programme: Guidelines, Data Quality Objectives and Standard Operating Procedures., No. 160, M.A. Allen, Editor, World Meteorological Organization/Global Atmosphere Watch, Geneva, Switzerland, 170 pp., 2004, amended 2015.

Zhang, J, Moran, M.D., Zheng, Q., Makar, P.A., Baratzadeh, P., Marson, G., Liu, P., and Li, S.M, Emissions preparation and analysis for air quality modelling for the JOSM project over the Athabasca oil sands region of Alberta, Canada, ~~*submitted to ACP/ACPD special issue*, 2017~~*under review, ACP*, 2018.

Zhang, L., Gong, S., Padro, J., and Barrie, L., A size-segregated particle dry deposition scheme for an atmospheric aerosol module, Atm. Env., 35, 549-560, 2001

Zhang, L., Moran, M.D., Makar, P.A., Brook, J.R., Gong, S., Modelling gaseous dry deposition in AURAMS: a unified regional air-quality modelling system, Atm Env., 36, 537-560, 2002.

Zhang, L., Brook, J.R., and Vet, R., A revised parameterization for gaseous dry deposition in air-quality models, Atmos. Chem. Phys., 3, 2067-2082, 2003.

Formatted: Normal, Indent: Left: 0 cm, Hanging: 1.27 cm, Line spacing: single, Don't adjust space between Latin and Asian text, Don't adjust space between Asian text and numbers